CITY UNIVERSITY

DEPARTMENT OF MECHANICAL ENGINEERING AND AERONAUTICS

LONDON

Reduction of Wind Turbine Noise through Design

A Thesis Submitted for the Degree of

Doctor of Philosophy

by

Mansour Mohamed Mansour El-Bardisi

June 1992

CONTENTS

LIST OF FIGURES

LIST OF TABLES

ACKNOWLEDGEMENTS.

The author wishes to express his thanks and appreciation to his supervisor, Prof.G.T.S.Done, Head of Department, for suggesting the subject of this research, supervision of all steps achieved, many valuable discussions and his continuous encouragement throughout this project.

The author is also indebted to Dr.D.Wilson of the Cavendish Laboratory, University of Cambridge, who provided the test site for measurement, and also considerable help and encouragement in discussion.

The author would also like to thank Dr.J.Anderson for his technical advice and fruitful discussions.

The help offered by Dr.A.Garrad is also sincerely acknowledged, especially his valuable discussions.

The author remains greatly indebted to his country (Egypt) for the financial support.

ABSTRACT

The trend towards wind farms in Europe has brought with it a requirement for quieter wind turbines in order to satisfy planning constraints, and to obtain subsidy bonuses. The aim of the present work is to enable the redesign of a wind turbine for reduced noise emission whilst maintaining the same output power. This can be achieved largely by reducing the aerodynamic noise though appropriate blade redesign and establishing new procedures for the design of blades which take into consideration the specific characteristics of the wind turbine itself. Also it is important to understand the nature of such noise and the effect of various parameters on the overall noise level; thus the mechanical noise contribution may be identified and reduced through well known techniques. The noise structure of wind turbine generators has been investigated and a survey has been made to identify the major source of the noise and effect of each source on the overall noise level. This has enabled the development of a computer model that allows noise synthesis from geometric and engineering data to be predicted. A computer program entitled WTGNOISE has been written which embodies the noise model; this predicts wind turbine generator noise with acceptable agreement with measurement.

The program verification made use of detailed noise emission measurements made on the experimental downwind machine at Lords Bridge near Cambridge under a variety of conditions.

It is shown from the measurements carried out that the noise level from the machine is similar to that predicted by the mathematical model, especially the aerodynamic part. The difference between measured and predicted noise level is due mainly to mechanical noise. From use of the WTGNOISE it is seen that the reduction of peak aerodynamic pressures on the blades will have a large effect on the noise level emitted from the wind turbine. By appropriate changes to the geometry and the aerofoil design the peak pressure on the blades can be reduced leading to a reduction in the noise level. Application of the code to Garrad aerofoils GHP1, GHP2 shows that the noise level due to aerodynamic sources can be reduced while keeping the output power the same. Also upwind rotors are shown to have an advantage over downwind rotors from the noise point of view. Applying the knowledge acquired in current research in the case of a wind farm design, it has been found that a group of large machines produces a higher noise level than the equivalent number of smaller machines; thus, there are advantages from a noise point of view in using smaller rather then larger machines.

LIST OF SYMBOLS AND ABBREVIATIONS

Symbol	Definition
b	local chord
c	speed of sound
C_p	pressure coefficient
d	distance of observer from source
V	fixed volume of fluid enclosed by surface
Σ	enclosed surface.
$f(\mathbf{x},t)=0$	equation of blade surface
$g = T-t + \frac{r}{c}=0$	equation of collapsing sphere centered at observer position $\mathbf{x}$
$\partial(f)$	is one dimension delta function which is zero everywhere except when F=0.
i	indices of summation
l_i	local force per unit area on fluid in direction i
l_r	forces on the blade in the radiation direction.
L.E.	leading edge
M	Mach number
M_r	Mach number in radiation direction
$\mathbf{n}$	unit normal vector to surface
$p(\mathbf{x},t)$	acoustic pressure
R	radius
$\mathbf{r}$	radiation vector, $\mathbf{x-y}$
r	length of radiation vector, $\lvert\mathbf{x-y}\rvert$
$\mathbf{r}$	unit radiation vector

S	surface area of blade
t	observer time
V	volume of fluid enclosed by surface Σ.
$\bar{\rho}$	an overbar implies that variable is to be regarded as a generalized function
T.E	trailing edge
Vn	local normal velocity of blade surface
v	local velocity of blade surface
x	observer position fixed with respect to undisturbed medium
Y	source position
α	blade pitch angle
π	3.141592654
ρ_o	density of undisturbed medium
T	source time
T^*	emission time
C_L	lift coefficient of an aerofoil
$C_L max$	maximum lift coefficient of an aerofoil
LS-1	type of an aerofoil designed by wind energy group
θ	represents the angle between the normal to the surface of the blade and the radiation vector
U_N, U_T	are air velocity components relative to blade section.
ϕ	inflow angle which is the angle between the wind velocity vector and the blade chord line.
a	axial induction factor.

a' tangential induction factor.

L, D lift and drag forces on the blade.

T_{ij} Lighthill stress tensor.

Laplacian operator

$$\nabla^2 = \frac{\partial^2}{\partial y_1^2} + \frac{\partial^2}{\partial y_2^2} + \frac{\partial^2}{\partial y_3^2}$$

$\frac{\partial^2 T_{ij}}{\partial y_i \partial y_j}$ is so-called quadrupole noise due to turbulence.

R is rotor radius

r is local rotor radius

X is tip speed ratio,

x is local speed ratio,

V_∞ free stream wind velocity

u Axial flow velocity at the rotor

A is the axial interference factor=$1-u/V_\alpha$

A' is the tangential interference factor at the rotor $A' = \frac{\omega}{2N}$

ω is the fluid angular velocity downwind of the rotor.

B is the number of blades.

c is the mean chord.

N is the rotational speed.

C_L is a mean lift coefficient.

Pa sound pressure in pascals.

dB(A)	noise level [A-weight]
dB	sound pressure level linear.
dT	is the incremental thrust.
dQ	is the incremental torque.
W	is the resultant velocity relative to the rotor

Abbreviations used

FORCE	a computer programme for the calculation of the pressure on wind turbine.
WEG ML-1	a type of machines using an LS-1 type of aerofoil.
GHP1	new type of an aerofoil designed by Garrad Hassan and Partners Bristol England.
GHP2	new type of an aerofoil designed by Garrad Hassan and Partners Bristol England.
ML-1	Wind turbine machine designed by Wind Energy Group.
OASPL	overall sound pressure level, dB(A) (re 20 upa)
SPL	sound pressure level dB (re 20 upa)
WTGNOISE	The computer programme for prediction of noise level from wind turbine rotor.

Subscripts

f	frame fixed with respect to undisturbed medium.
r	radiation direction
ref	reference position
ret	retarded time evaluated at $T=T^*$

Vectors are denoted by bold lettering.

CHAPTER

1

INTRODUCTION

1 INTRODUCTION

Wind energy has been successfully harnessed for well over a thousand years, and for many centuries the traditional windmill has been a major source of energy. Wind energy has long been recognized as benign because it is safe, non-polluting and does not deplete the world's energy resources.

In 1973 the increase in the price of oil, and other fossil fuels, such as coal and gas, led to a new interest in wind energy by major consumer countries; for example, since 1980 the U.S.A. has spent more then 3 billion dollars on wind energy [1]. In the U.K studies have shown that 10 percent of its electricity needs could be obtained from the wind [2]. In 1988 the Department of Energy-CEGB collaborative programme on wind farms, announced by the Parliamentary Under Secretary of State for Energy, Mr.Michael Spicer, brought the commercialisation of wind generated electricity in Britain a step nearer reality. Lord Marshall of Goring, Chairman of the CEGB, followed the Minister by amplifying the Board's plans for three wind farms on suitable sites around the country and the construction of an offshore wind turbine installation. The proposed wind farm programme would place great emphasis on the social and environmental acceptability of such installation and include studies of noise, communication interference and the use of land.

The establishment of a market leading to deployment, together with further research and development, are necessary steps in reducing costs. Hence The Non Fossil Fuel Obligation (NFFO) stated that 11p/kWh should be paid to the Regional Electricity Companies for generating capacity from wind [3].

As the wind energy industry develops, the low generation costs will be achievable on a widespread basis at moderate wind speed sites [4].

The environmental aspects of wind energy are important in populated Europe. The most important aspects are noise, visual intrusion, safety and interference of electromagnetic transmissions, and damage to birds. Studies have shown that noise is considered to be the most single important factor affecting the population's attitude towards large scale wind energy projects. The occurrence of noise depends on two factors; firstly on the level of acoustic emissions of the turbine and secondly on the distance between the turbine and the nearest residence. A ten dB(A) reduction in wind turbine noise would allow the wind turbine machine to be three times closer to the building. To achieve such a reduction the noise sources of a wind turbine would need to be carefully studied and reduced without changing the output of the machine. Mechanical noise arising from moving parts and the gearbox are judged able to be tackled by well known techniques and

methods. However aerodynamic noise associated with the motion of blades relative to the air is considered to be more difficult to address, and investigations into its characteristics are urgently needed to find methods for reducing it. The dimensions and shapes of the blades are known to have an effect on the noise level. The need to establish criteria and desirable features for these shapes and dimensions is a fairly new requirement in the study of wind turbine noise. Using a computer code which relates such dimensions and shapes to noise generation could be an important contribution. Analysis of the sources have shown that for smaller turbines, with a rotor diameter of up to 20 m, the mechanical component is the most important factor, where as for larger turbines with diameter of 50 m or more, it is the the aerodynamical component which is more important [5].

The aim of the present work is to enable the redesign of a wind turbine such that it is quieter whilst maintaining the same output power. This can be achieved by reducing the aerodynamic noise though blade redesign and establishing new procedures for the ab initio design of blades which take into consideration the specific characteristics of the wind turbine itself. To do this it is important to understand the nature of the noise emissions and the effect of each aerodynamic parameter on the noise level; thus mechanical noise, for example may be identified and

reduced through well known techniques. In this thesis, the noise structure of wind turbine generators has been investigated and a survey made to identify the major sources of noise and the contribution of each source to the overall noise level.

This has enabled the development of a computer model that allows noise synthesis from geometric and engineering data to be predicted. A computer programme has been written entitled WTGNOISE which embodies the noise model, and this is shown, through a verification exercise, to predict wind turbine generator noise with an acceptable degree of accuracy.

Chapter 2 outlines the noise problems, the characteristics of wind turbine noise, and the sources of wind turbine noise. A review of existing noise prediction computer codes for wind turbines is presented in Chapter 3. Chapter 4 provides the background theory of the numerical model employed in the computer programme WTGNOISE. This makes use of two forms of the solution of the important Ffowcs-Williams and Hawkings wave equation which is used in deriving the formulations of the numerical model. WTGNOISE is capable of predicting the noise level of a machine at any wind speed taking into account the geometric and engineering data of the aerofoils, distribution of the aerodynamic pressure on the blade, and the position of the observer relative to the machine. In order to verify the

computer programme and check its results, measurement of the noise emission from a suitable wind turbine is necessary.

An experimental wind turbine situated at Lords Bridge near Cambridge has been used for validation measurements, and the details are described in Chapter 5, and the results presented and discussed in Chapter 6. The validation results showed that the computer code may be reasonably relied upon to estimate the noise level from horizontal wind turbine machines.

By applying the computer code it is possible to determine the effect of changing certain geometric and engineering data, and to decide which changes are more acceptable from the noise point of view. Comparisons of designs are also possible on the basis of keeping the output power the same. The differences may be highlighted between upwind and downwind wind generators.

The achievement of quieter wind turbines by design is discussed in Chapter 7, and this includes comments on whether or not a smaller number of large machines is better than a larger number of smaller machines on a wind farm of required power output.

CHAPTER

2

THE NOISE PROBLEM IN WIND TURBINES

2.1 INTRODUCTION

Whilst the level of technology associated with the production of energy through wind turbines has matured, the environmental aspects continue to present problems. In the populated countries of Europe environmental constraints could seriously limit the use of wind turbines, which is why attention should be concentrated on this aspect.

2.2 ENVIRONMENTAL PROBLEMS

Wind turbines can cause environmental problems such as interference of electromagnetic transmission and reception due to reflection, scattering and diffraction of electromagnetic waves. When the wind turbine is operating there will be periodic disturbance due to the movement of the rotor blades. The impact of this disturbance depends on the type of telecommunication service (e.g.radio broadcast, TV broadcast, radar) being affected. The geographical location of a wind turbine is generally governed by economic factors, but the machine must be visually acceptable to the public at large. Safety is also an environmental issue, but is ranked less severe because safety standards can always be assumed through appropriate engineering design and operation. However one of the most important environmental problems is the noise from wind turbines [6-7]. For example, the operation of large wind turbines has led to complaints from residents living up to

3km from a machine, and in one particular case, a local resident has written a paper describing the form of noise and providing measurements [8]. The wind turbine may produce both impulsive and broadband noise. Impulsive noise is a characteristic of downwind machines. Broadband noise is generated by all types of machines. These noise components are affected by the atmospheric absorption, propagation, and distance to receiver. The receiver may be influenced by the background noise level, location of receiver, and any vibration induced by the noise. The factors which are important in evaluating human exposure to wind turbine noise are illustrated diagrammatically in Fig 2.1 which is taken from reference [9].

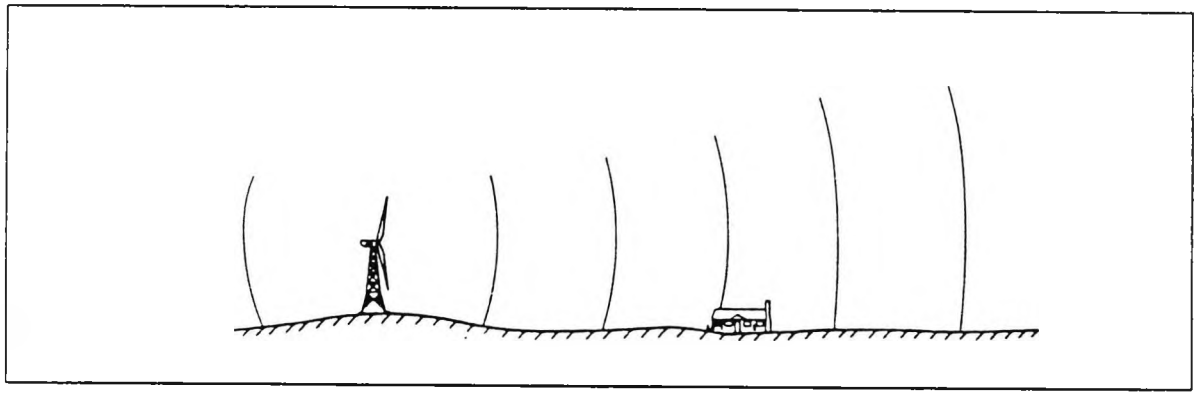

SOURCE	PATH	RECEIVER	CRITERIA
. IMPULSIVE	. DISTANCE	. BACKGROUND NOISE	. PERCEPTION
. BROADBAND	. WIND GRADIENT	. INDOOR/OUTDOOR	. ANNOYANCE
		. VIBRATION	

Fig 2.1 Wind turbine noise assessment factors.

2.3 The noise problem in wind turbines

Environmental constraints could seriously limit the use of wind turbines, and noise is one of these environmental constraints and therefore particularly important for land based machines. In deciding to proceed with a consent application to develop a particular site for a wind turbine or wind farm, interested parties will need to know that a realistic noise specification can be placed on the machine to ensure that the development will not lead to complaints from the community nearby. Although there are standard procedures for doing this in the case of general industrial noise, wind turbines have a number of special features which make these difficult to apply. This means that there is a need to develop a wind turbine noise prediction scheme in order to develop procedures that avoid complaints from nearby residents. To this end a computer synthesis of wind turbine noise needs to be developed to investigate the variation in signal at positions around the machine and to identify the key parameters affecting the noise level from wind turbines. An area surrounding the turbine may be divided into two regions, the near field and the far field. It is unlikely that there will be anyone living in the near field and so the region of interest is the far field. The level of noise in the far field will however be affected by climatic conditions, topography and other local effects.

2.3.1 Noise induced building vibration

The operation the of the MOD-1 wind turbine resulted in reports of building vibration induced by low frequency impulsive noise. This was also found in a recent review of data derived from several sources including vibration caused by subsonic jet and propeller aircraft and helicopters [9]. Wall or floor vibration can result in the shaking of wall or floor mounted objects such as pictures and china cabinets; audible sound may thus be generated.

2.4 Characteristics of wind turbine noise

Wind turbines operate continuously in a very "dirty" part of the earth's boundary layer as well as in open space, and are subject to special features like propagation phenomena, radiation patterns and absorption from the atmosphere as well as noise from the wind itself. Operational experience of wind turbines has shown that there is a need to establish criteria for the noise emitted from a machine and a standard technique of measurement with better understanding of the special characteristics of wind turbine noise.

2.4.1 Propagation phenomena

Sound propagating through air is attenuated by the conversion from sound energy to heat (absorption or dissipation). The attenuation of sound as it propagates from a source to an observer is influenced by various phenomena, including geometric spreading, air and ground absorption, refraction, diffraction, scattering and distance from source to the observer [10-18]. Attenuation is dependent on frequency, temperature, air pressure and relative humidity. The reduction is proportional to the length of the sound path between source and receiver, i.e, is quoted as dB per metre. The attenuation is strongly dependent on frequency and is negligible at low frequencies. Absorption due to the presence of the wind gradient on turbine noise is shown in Fig 2.2 which is a schematic illustration of the effect of distance and wind direction on the sound propagation from wind turbine generators assuming a high fixed frequency [9].

The low frequency components suffer small atmospheric losses and thus might be expected to propagate downwind as a function of distance according to the inverse distance law. It is believed that this low frequency component is responsible for the complaints of nearby residents and is more difficult to tackle. For the higher frequency components the atmospheric absorption is greater [10-18]. On the other hand, for upwind conditions the sound is

refracted upwards, resulting in the formation of an acoustic shadow zone. The distance from the wind turbine to the shadow zone depends upon the wind velocity and the height of the noise source above the ground.

2.4.2 Ground Effect

Fig 2.3 shows a simple model of the way that sound travels above a ground surface along a direct and a reflected propagation path. The direction of propagation is represented by a ray which is a line normal to the wavefront surfaces [10]. This is a convenient way of representing sound propagation. The interaction between the direct and reflected waves gives rise to the ground interference effect. This effect causes an attenuation of sound, particularly at frequencies around 200 to 800 Hz, in excess of that caused by spherical spreading and atmospheric absorption (termed "excess attenuation"). Figs 2.3 and 2.4 show an example of the excess attenuation calculated using an established theory of sound propagation across a ground surface which indicate that ground surfaces have a wide range of acoustic impedance or effective flow resistivity, [19-21]. The excess attenuation effect is caused by the direct and reflected waves arriving completely or partially out of phase with each other and therefore cancelling out the fluctuations in the sound wave, (so-called "destructive interference").

At certain frequencies the predicted excess attenuation

could be -6 dB, i.e, a 6 dB higher level than would be expected in the free-field situation with no ground surface. This is due to constructive interference i.e, the summation of the energy, in phase, from the two transmission paths. The extent to which the direct and reflected waves interfere depends on the difference in the relative length of the direct and reflected ray paths and on the acoustic impedance. Fig 2.4 shows the change in excess attenuation spectrum caused by different ground surfaces, calculated using accepted acoustic theory. The parameter which is varied in Fig 2.4, the effective flow resistivity or acoustic impedance, is used within the theory to calculate a spectrum of acoustic impedance over various types of ground surface. Table 2.1 lists the values for some common ground surfaces; a higher value indicates an acoustically harder surface, i.e the reflected wave has virtually the same strength as the incident wave. In this case the transmitted wave carries negligible energy since the velocity transmission coefficient is effectively very small **[10], [19-21].**

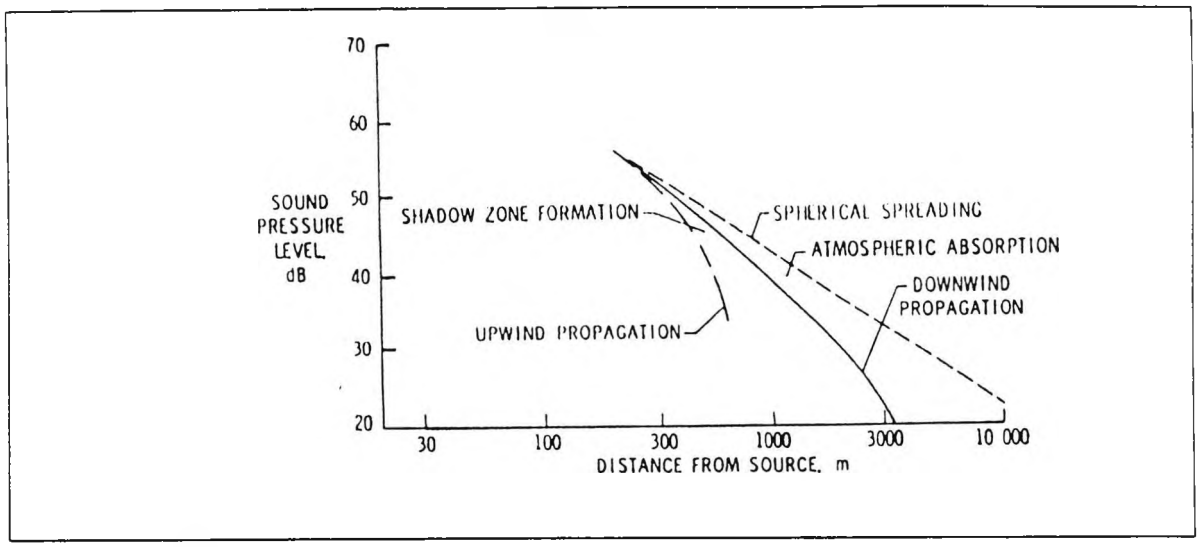

Fig 2.2 Schematic illustration of the effects of distance and wind direction on the sound propagation from a wind turbine generator. Extracted from Ref [9], specific frequency not quoted.

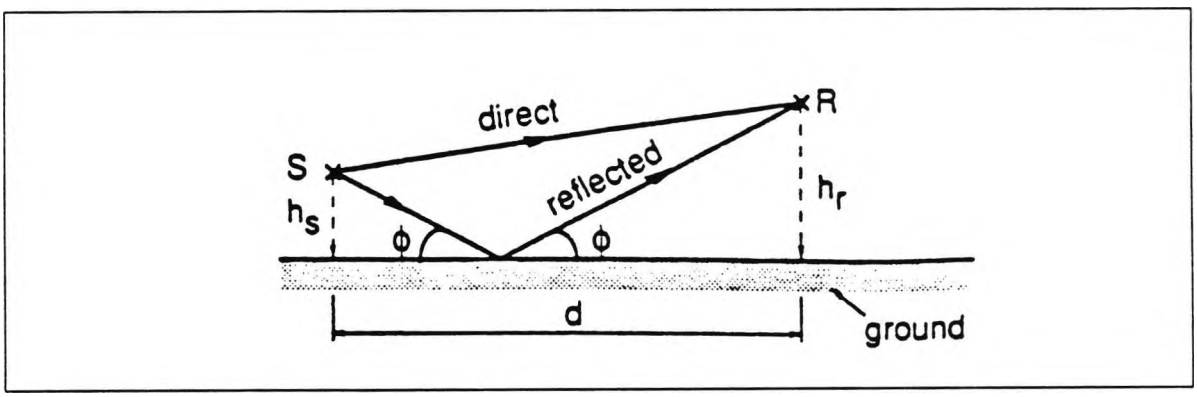

h_s=source height h_r=receiver height

d= horizontal distance between source and receiver

Fig 2.3 A simple model of sound propagation above a ground surface. Extracted from Ref [19].

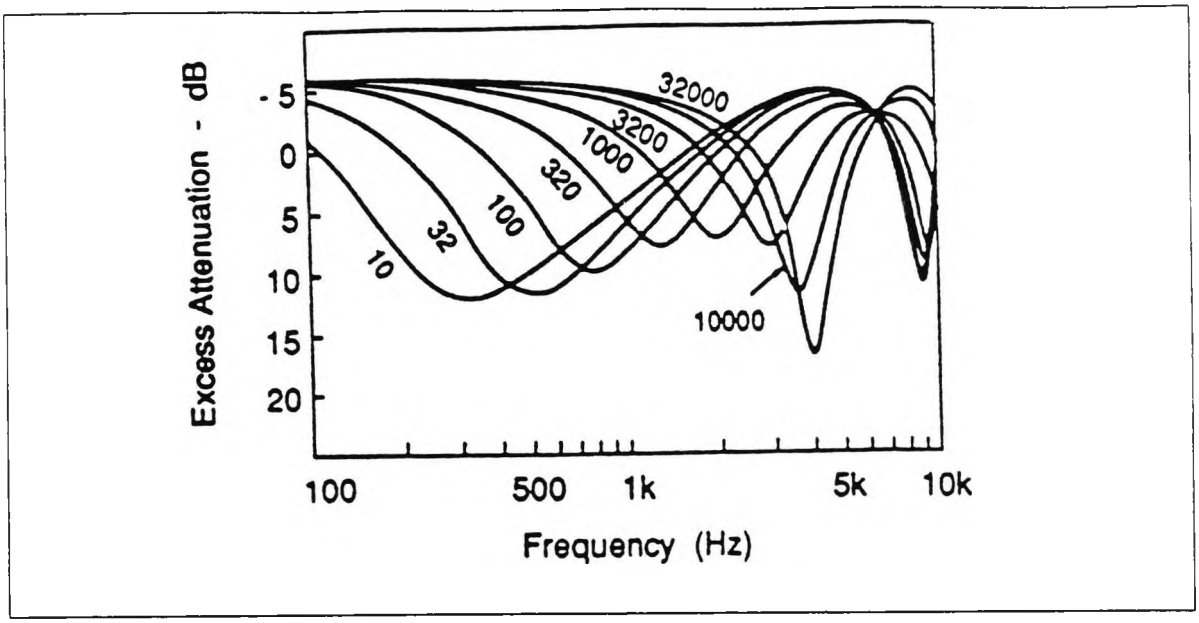

Fig 2.4 Effect of ground surface type on excess attenuation (Extracted from Ref [19]) h_s=0.31 m h_r=0.46 m, d= 7.62 m, SEFR is the Surface Effective Flow Resistivity, (rayls x 10^{-3} using mks measurement system) values of which for different surfaces are provided in Table 2.1 below

Table 2.1

Surface Effective Flow Resistivity (mks rayls) [19]

Snow	10,000 to 30,000
Pine forest floor	20,000 to 80,000
Grassland	150,000 to 300,000
Asphalt	20,000,000

The speed at which sound waves travel over the ground depends on both temperature and wind. The sound velocity, c, increases with increasing temperature, t, according to the approximate relationship: $c = 331 + 0.6\ t$ (m/s) **[19-22]**. Air temperature varies with height above the ground, therefore the speed of sound varies with height. Wind speed increases with height above the ground in the lower atmosphere. The result of the wind and temperature profiles is thus to create a sound velocity profile. Ray tracing is a useful aid in defining the refraction effect of a velocity profile on sound propagation. The effect of refraction is indicated by ray paths being curved rather than straight.

The temperature distribution above the earth's surface is complex and difficult to determine except by careful measurement but a general pattern can be defined which is useful in assessing outdoor sound propagation. The sound velocity profiles caused by the combination of wind and temperature gradients cause refraction of sound waves, i.e, different parts of the wave front are travelling at different speeds, and the resulting ray propagation path is curved. The refraction effects of wind and temperature are illustrated in Figs 2.5 and 2.6. These show a phenomenon which occurs upwind and under normal atmospheric lapse rate conditions, the shadow zone. In this zone there is an increase in excess attenuation, which is, however, not the

same for all frequencies. The shadow is more effective at higher frequencies [19].

2.4.3 Turbulence

Wind blowing across a rough ground surface and convection due to temperature causes the lower atmosphere to be more turbulent. Turbulence affects sound propagation outdoors by scattering the sound field, and scattering causes sound penetration into the shadow zone, variability in received signals, attenuation of propagating sound waves and disruption of interference patterns caused by ground reflections. High frequency sound is affected more by turbulence than lower frequency sound.

2.4.4 Topography

The data available for hilly sites is much less extensive than that for flat ground and present knowledge is therefore sketchy. An extreme case which has been investigated shows that hilltop to hilltop propagation approximates well to spherical spreading and atmospheric absorption. Recent studies suggest that propagation over curved ground surfaces is analogous to propagation in a wind or temperature gradient. Fig 2.7 [taken from Reference [19]] shows that a concave slope has multiple ray arrivals, as in an inversion, while a convex slope can result in a shadow zone.

2.4.5 Radiation patterns

Observed radiation patterns are influenced by the characteristics of the noise sources and by refraction due to wind speed gradients. The latter effect is most evident at large distances from the wind turbine [10-18].

Measurements made within 1 to 2 rotor diameters of wind turbines indicate that the low frequency loading noise, a characteristic of downwind machines, is highly directional and radiates predominantly in the upwind and downwind directions.

The radiation pattern of the broadband noise can be approximated as non-directional for these close-in measurement locations but is affected by the wind at larger distances. Measurements at large distances are fragmentary and are not sufficient to describe the shapes of the distance radiation patterns. Fig 2.8 shows the ray path diagrams downwind and upwind of a distributed source, indicating the refraction effect of a mean wind gradient.

Fig 2.9 shows ray path diagrams upwind and downwind from two different heights, indicating that for the higher source the noise travels larger distances.

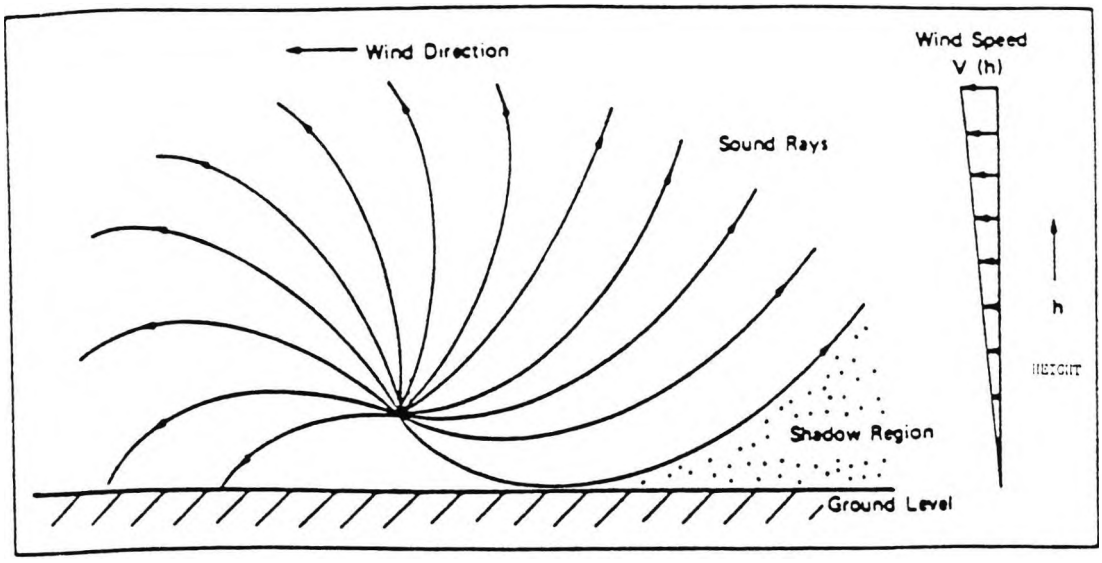

Fig 2.5 Refraction of sound rays by wind, extracted from Ref [19].

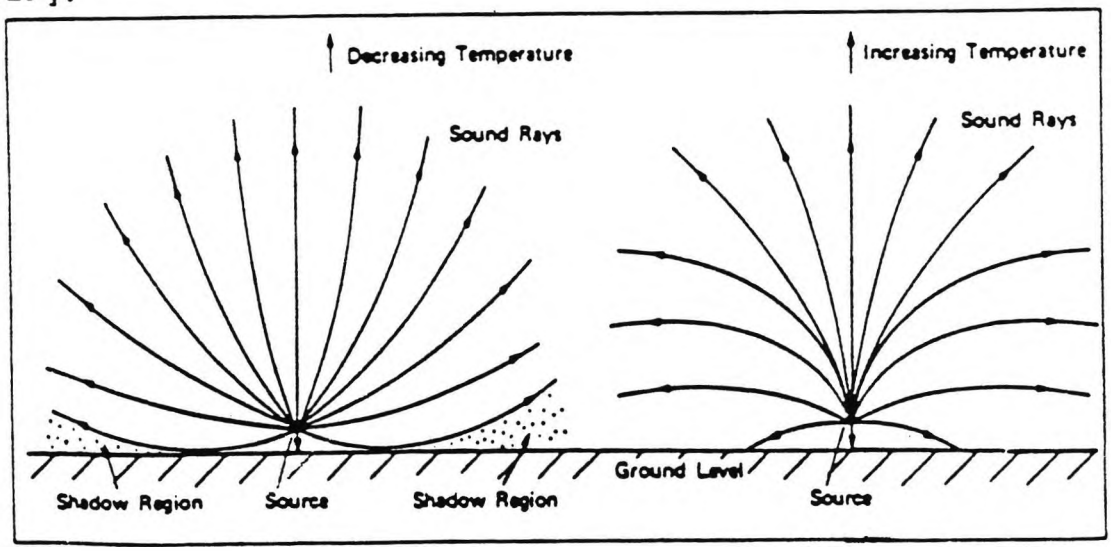

Fig 2.6 Refraction of sound rays for decreasing (normal atmospheric lapse rate) and increasing (atmospheric inversion) temperature with height, extracted from Ref [19].

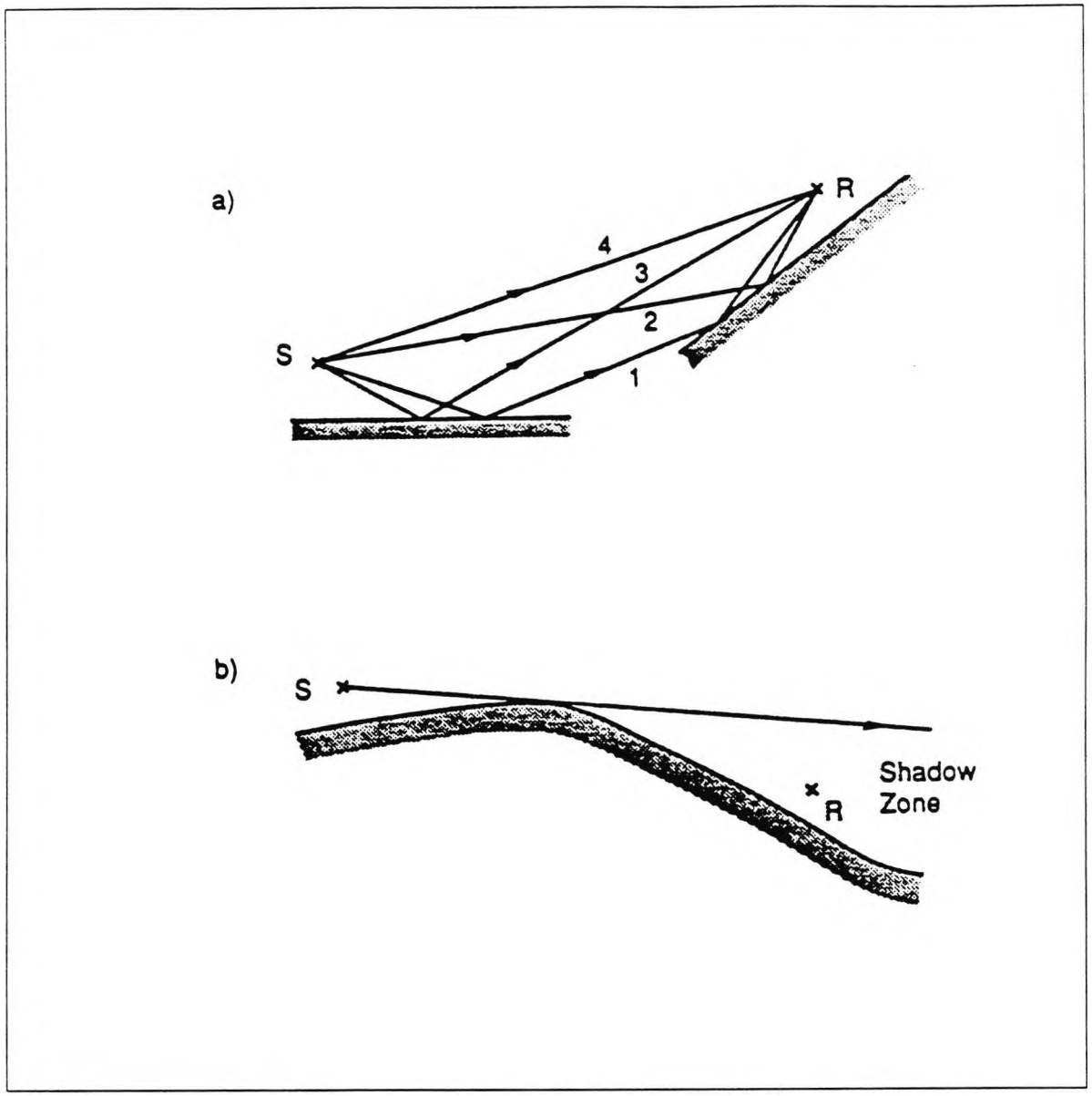

Fig 2.7 Simple-path ray diagrams for a neutral atmosphere for ground with (a) concave and (b) convex slopes. Extracted from Ref [19].

2.4.6 Screening

Walls, earth banks, buildings or any other acoustically solid objects may act as a means of noise reduction by blocking the direct transmission path between source and observer. A barrier is most effective if placed either close to the source or close to the receiver.

2.4.7 Interactions

The effects described above do not operate in isolation; there are complex interactions between them. For example, the attenuation of a barrier can be reduced by refraction of sound due to an inversion, or, downwind, refraction effects and turbulence will influence ground interference effects. Turbulence, topographical effects and scattering by obstacles can degrade meteorological shadow zones.

2.4.8 Impulsive noise

The impulsive noise generated consists largely of a fundamental (blade passing) frequency. Although the impulse resulting from a blade passing through the wake of the tower is uniquely defined by the time history of the pressure pulse, it is more common to define the noise by a frequency spectrum which, with information on the phase relationship between harmonic components, completely describes the noise signature [9].

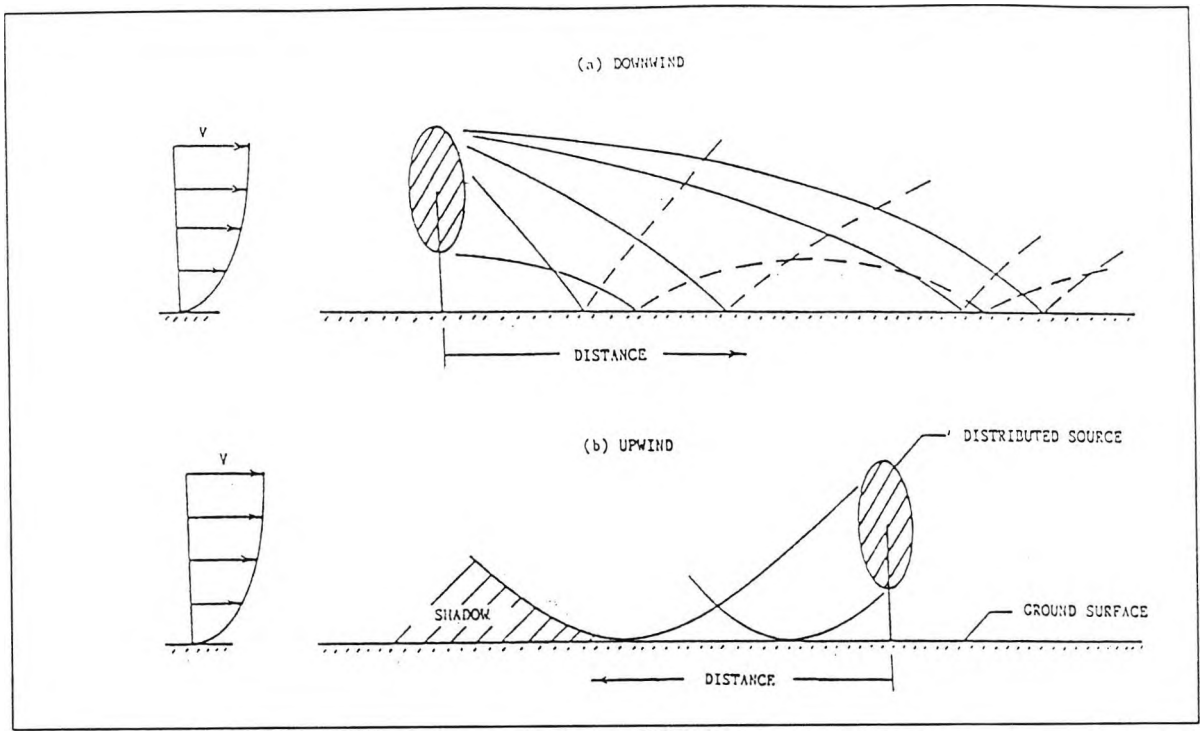

Fig 2.8 Ray path diagrams downwind and upwind of a distributed source, indicating the refraction effects of a mean wind gradient. (Extracted from Ref [23]).

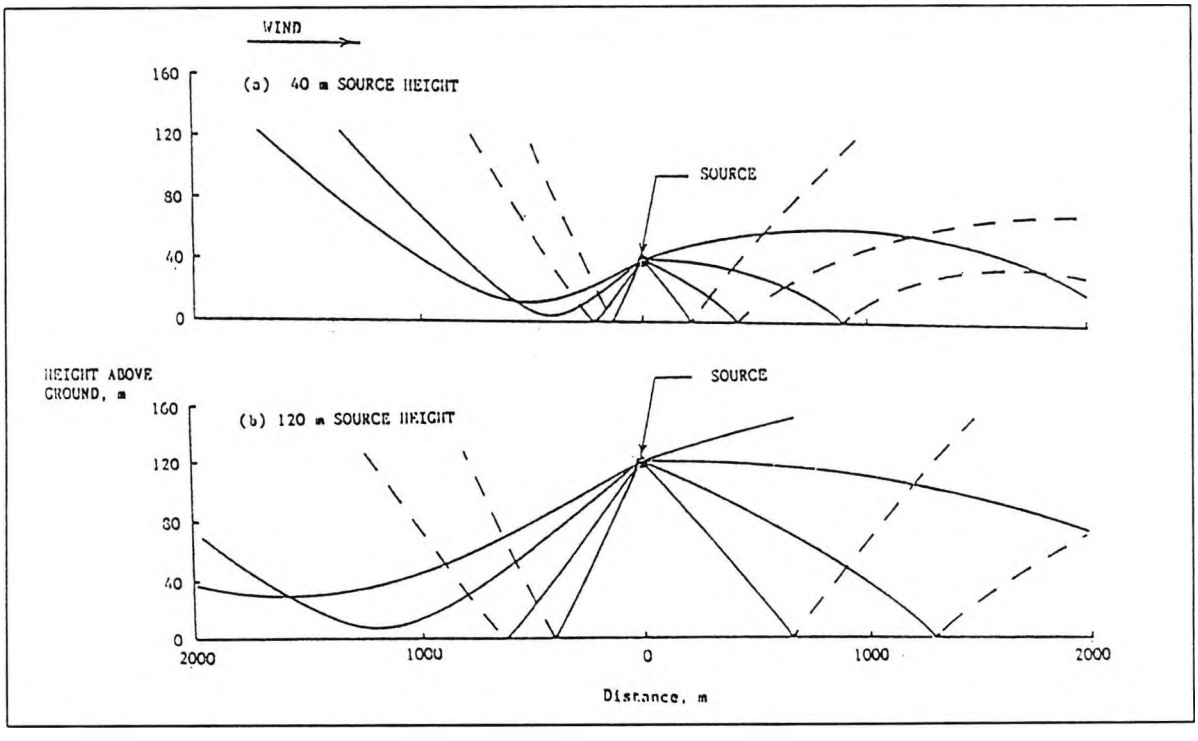

Fig 2.9 Ray path diagram upwind and downwind from two different heights. (Extracted from Ref [23]).

2.4.9 Broadband noise

With the growing trend towards large wind turbines, and the commissioning of the wind farms in Europe, experience indicates that for large wind turbines, broadband noise is of most importance in the frequency range 500-2000 Hz where, in addition, ambient noise levels tend to be relatively low [9].

2.5 Sources of wind turbine noise

In order to analyse and get a better understanding of the noise of wind turbines as well as seeking ways to reduce that noise it is necessary to identify the main sources.

2.5.1 Mechanical noise

The mechanical noise associated with wind turbines is that arising from the gearbox, the mechanical transmission and similar parts. A gearbox that is generating excessive noise can be clearly distinguished by its characteristics. The noise originates from the meshing action of the gears. The vibration produced by the gear teeth is transmitted to the gear casing, then through the supporting structure leading to secondary vibration and radiation [24].

Some of the important factors that influence noise generation and its characteristics from this source are the type of gear tooth, its profile, pressure angle, accuracy of machining, wear profile, load, speed, imbalance of the rotor and lubrication. Brakes and yaw movement can also

generate noise and vibration. For small wind turbine machines with a rotor diameter of up to 20 m, the mechanical component is believed to be the most important factor, whereas for larger turbines, the aerodynamical component is more important [9]. Mechanical noise is able to be effectively controlled by well known techniques, the main question being the cost of treatment.

2.5.2 Aerodynamic noise

The aerodynamic sources are associated with the motion of the blades relative to the air; a typical spectrum, Fig 2.10, shows the different type of noise. When an airflow is disturbed, turbulent pressure and density fluctuations can be created that, under the right conditions, combine to produce a propagating pressure wave (sound) in the atmosphere. The problems of mathematically describing such a flow and of determining the sound field have been studied extensively over the last 30 years in connection with the sound of rotating blades and jet engines. Early work on the noise produced by propellers and on the description of turbulent flows was done by Lighthill [25] in the early 1950's which led to the first full theoretical treatment of how a turbulent airflow can result in a sound field. Subsequently this work has been extended and experimentally verified as a general theory of aerodynamic noise generation.

Three types of aerodynamic sound sources have been identified. The first results from local additions of fluid into the atmosphere and is called a fluctuating mass source. The second type of source is due to the effect of fluctuating pressures on surfaces. This is called a fluctuating force source. The final source mechanism is that produced by the stresses in an unbounded turbulent airflow and this is called a fluctuating stress source. Keast and Potter [26] have determined the properties of the three types of aerodynamic sound. The identification of sources was accomplished through dimensional analysis, but as this analysis was limited to an ordinary rotor it could not be used for advanced blade geometry.

Since regular operation of the MOD-1 wind turbine began, there have been complaints from households nearby, and so efforts have been directed to identifying the cause of the noise and towards finding methods of reducing it. To this end NASA (Lewis Research Center) developed computer prediction codes and obtained experimental data to verify these codes; see Kelley [27]. A computer program was developed for calculating the intensity and frequency characteristics of sound generated by a wind turbine in a non-uniform wind flow field. However, propagation effects due to terrain and atmospheric conditions complicated the amplitude correlation with MOD-1 data to cause an amplification of 6 dB or more. The code has been used to

determine the source of the noise generation from MOD-1 as well as to identify operation conditions associated with the highest noise levels. Modelling of wind turbine flow field characteristics showed that the predominant source of noise from MOD-1 was the wind velocity deficit in the wake of the tower. Because the rotor plane was downwind of the tower this deficit produced changes in the aerodynamic forces on the blades resulting in sound pressure variation in the acoustic field. The level of the sound pressure variation is most strongly a function of rotor speed and wind speed. The approach used in developing this wind turbine sound prediction code, was to apply an available theory used for calculating noise from conventional aircraft propellers.

The development of this and similar theories goes back to 1937 when Gutin [28] first successfully calculated the noise from a propeller in a uniform flow.

The effect of the shape and geometry of the blades however on the noise level was inconclusive.

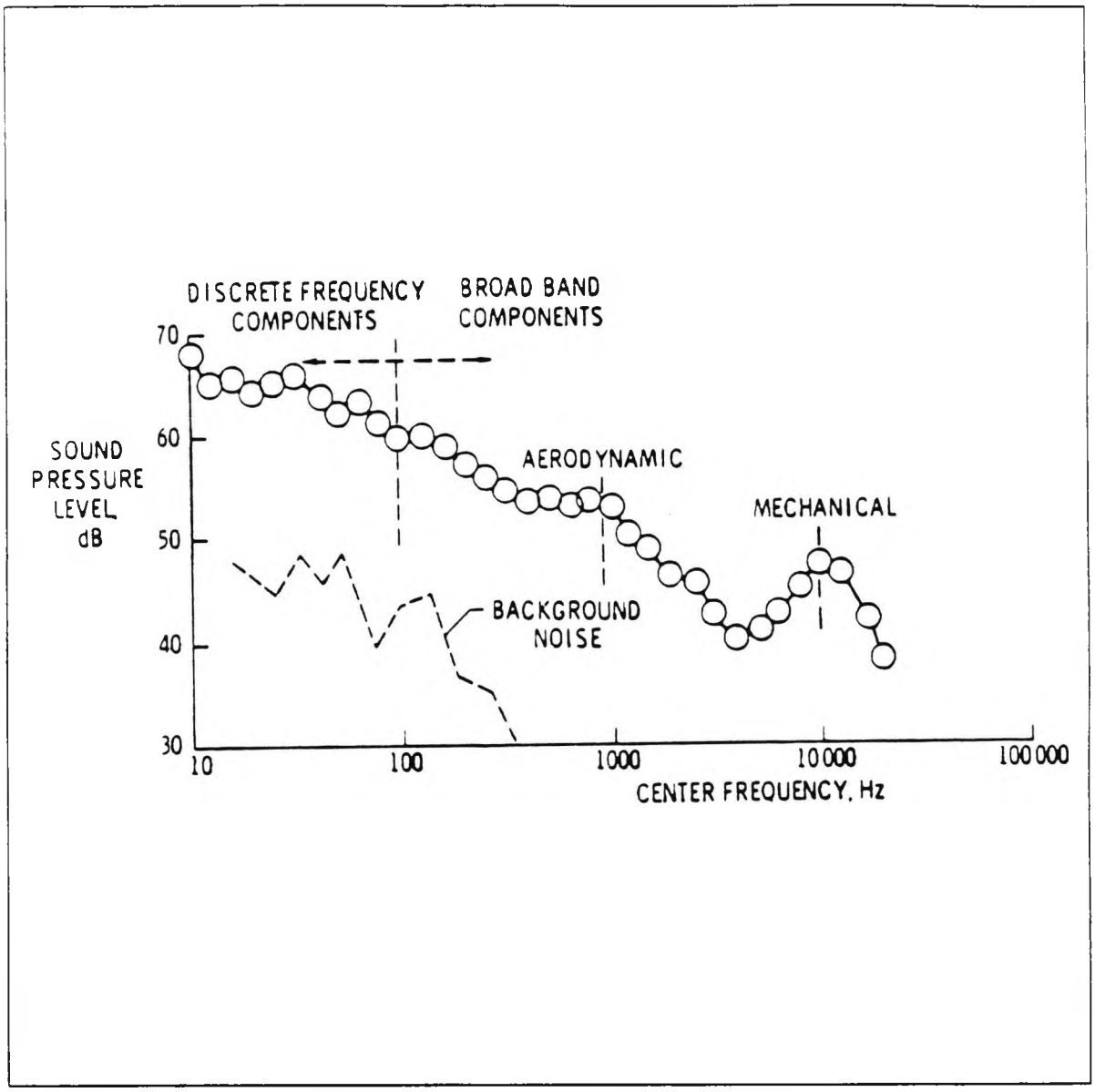

Fig 2.10 One third octave band spectrum of noise from the MOD-OA Wind Turbine Generator. Data were measured at a distance of 61 m directly downstream, and wind velocity of 5 m/s. (Extracted from Ref [9]).

2.6 Acoustic measurement of wind turbine noise.

To monitor the low-frequency acoustic emission associated with a wind turbine whilst its rotor operates normally, measurements need to be taken. Etter and others [29-35] measured the noise from the MOD-0 wind turbine, when the machine was operating at 35 rpm in a wind speed of 4-7m/s. There was some evidence of impulses with tones between 10 Hz and 25 Hz. The discrete machine peaks were present, but there was no evidence of any broadband noise and it was concluded that there was evidence of impulsive behaviour in the downwind configuration at 35 rpm, but no such evidence at the other nominal rotor speed of 23 rpm in either the downwind or the upwind configuration. It was established, based on this work on the MOD-1 wind turbine, that impulsive amplitudes generated by blade-tower wake interaction are not electrical output power dependent.

In a different study, Shepherd and Hubbard [23] measured the noise from a wind turbine at distances up to 1050 m, over a range of frequencies from 8 Hz to 2000 Hz, and for a wind turbine noise source in windy conditions (wind speed from 9.4 to 13.0 m/s), and showed that the assumption of a distributed noise source leads to better noise estimates in the upwind direction.

CHAPTER

3

REVIEW OF EXISTING NOISE PREDICTION COMPUTER CODES FOR WIND TURBINES.

3.1 Introduction

The generation of sound from moving bodies, such as a rotating propeller, helicopter rotor, or wind turbine rotor is an undesirable byproduct. The estimation of the sound level emitted by such bodies is, therefore, essential in achieving the design of quiet machines. The theory for the estimation of this sound has been developed to a high level in recent years for the helicopter rotor and rotating propeller, but in the case of the wind turbine there is still some way to go [36], [37]. One of the main purposes of this work is to make a step in this direction through determining the acoustic pressure signature for a typical wind turbine machine. The starting point of the most available prediction codes is the equation developed by Ffowcs Williams and Hawkings, denoted the FW-H equation [38], and its solution [39].

3.2 Prediction computer codes

There have been developments in recent years in the prediction codes available to estimate the emission of noise from a wind turbine. These codes have been developed mostly in the U.S.A, with one computer code from the U.K derived from the work done at the University of Southampton. Only the Southampton code was obtainable for evaluation. In this chapter there is a brief description of some of these codes with analyses of their bases and limitations in addition to the advantages and disadvantages

of each one.

3.2.1 Hamilton Standard Division Technologies Corporation computer code [40].

In order to predict the noise of a wind turbine Metzger and Klatte [40] have adapted a theoretically based methodology used for predicting propeller noise. This method uses an extension of the theory contained in [38].The methodology calculates tone noise due to steady loading associated with the volume of the blade, and unsteady loading caused by the wind shear and tower wake defect. Broadband noise due to turbulence at the blade with inflow turbulence is also calculated. The method is capable of evaluating the influence of ground reflection on measured noise, but this feature has not yet been considered necessary for wind turbine predictions. The method is computerised and is a far-field time domain method, i,e., it will calculate noise only at locations which are a minimum of several rotor diameters from the wind turbine, and the output of the calculation is a frequency spectrum. In order to run cases, the performance of the rotor is calculated, and the characteristics of wake velocity defect and wind shear are used to calculate unsteady blade loads. These two sets of input information are used to calculate the tone noise components of the noise spectrum. The impulse character of the noise due to the wake defect is calculated by the tone noise program. For the present annoyance studies, broadband

noise due to trailing edge or inflow turbulence has not been considered. The problem with this computer code is that it does not include the dimension and shape of the blade and it is not clear whether or not it is capable of handling large machines. The wake calculation in the code is not clearly defined which raises doubt about its accuracy.

3.2.2 NASA,Langley Research Center computer code [41]

Greene and Hubbard [41] produced noise calculations for far field conditions around a wind turbine which is a modified version of the Nystrom and Farassat propeller noise prediction program described in Reference [42]. The program properly accounts for the significant geometry features of the rotor, its operating condition, and the non uniform distribution of aerodynamic loading over the rotor disc. It is particularly useful for the studies of the evaluation of the effects of ingestion by the rotor of the tower wake which contains velocity deficiencies. The authors are not aware of any validations of the code applied to large wind turbines to date, apart from MOD-1. The MOD-1 "thump" is the result of the interaction of the turbine rotor and the complex tower wake. Detailed calculations of the noise would require a detailed description of the rotor loading as it passes through the complex tower wake and would be difficult to make with certainty. However, average noise calculations using

average wake characteristics are in general agreement with average noise measurements. It was not clear in the code if the calculations of forces on the blade described in Reference [42] were sufficiently accurate enough or not to predict the noise level from a machine.

3.2.3 NASA Langley Research Center computer code [43]

This computer code is based on the calculation of the periodic and nonperiodic components of the aerodynamic noise, whereas the code presented previously in (3.2.2) is based on the modified version of the Nystrom and Farassat propeller noise prediction program as described in Reference [42].

Greene [43] showed from calculations and model tests that placing the rotor upwind of the support tower minimizes the noise risk. It is difficult in his view to extrapolate model results for the downwind configuration to full scale since all the parameters which affect the wake affect the generated noise. The inherent unsteadiness of wake flows may produce noise which is louder than would be expected from average measurements or calculations based on average wake characteristics. Prediction of the nonperiodic sources of rotor noise on the other hand is less exact. For example, the spectrum, scale length and intensity of random atmospheric turbulence is not known nor have pressure fluctuations in the boundary layer been thoroughly documented. Detailed knowledge of the structure of the wake

of the rotor is required to estimate tip vortex and trailing edge noise and this information is not available. As a result, estimation of the noise due to viscous shear effects has been predominantly empirical. It can be seen from his analysis that his code is based on empirical formulae which are difficult to generalise.

3.2.4 The Boeing Vertol Company computer code [44]

Spencer[44] suggested that sources of noise in wind turbine generator systems may be classified into two categories with respect to the position of the rotor relative to its support tower structure: (1) rotors which operate upwind and (2) those which operate downwind of the support structure. Rotors which are positioned closely downstream of the tower experience air load fluctuations as the blade passes through the disturbed wake of the structural members.

Spencer suggested that upwind rotor wind turbines, which tend to produce mainly nonperiodic sources of noise such as those generated by random atmospheric turbulence, a turbulent boundary layer, or the formation of a trailed tip vortex filament, produce a nonimpulsive acoustic signature that is characterized by a swishing, rather than a thumping sound. These sources of noise tend to have low radiation efficiencies and broadband spectra which are more acceptable than discrete tonal noise components. Any device which reduces the disturbed wake behind the tower structure

of a downwind rotor will also improve the acoustical signature of a downwind rotor.

Upwind rotors appear to have an advantage over downwind rotors in his view from an acoustical standpoint. Predictions for the MOD-2 turbine indicate that the noise signature will be of a broadband nature. Although noise measurements had not been made on the MOD-2 turbine, comments from observers indicate that the predominant noise is a swishing sound characteristic of a broadband noise source. Levels between 60-65 dBA have been predicted for MOD-2 at a distance of 200 ft, similar to those near a freeway with moderate traffic at an equivalent distance. Spencer suggested that improved prediction methods for broadband, nonperiodic sources of noise were required in order to estimate the acoustic signature of new turbine generators with confidence. The existing empirical broadband methodology lacked a rigorous analytical understanding which would have to be developed from an adequate data base in order to accurately quantify these sources. Additional measurements should be made to verify the unsteady loading noise theory as it is developed.

There is a lack of a fully theoretical description of the noise emission from a machine.

3.2.5 Massachusetts Institute of Technology computer code [45]

In this computer code Martinez, Widnall, and Harris[45] have developed theoretical models to predict the radiation of low frequency and impulsive sound from horizontal-axis wind turbines due to three sources; (1) steady blade loads; (2) unsteady blade loads due to operation in a ground shear; (3) unsteady loads felt by the blades as they cross the tower wake. These models are then used to predict the acoustic output of MOD-1. Predicted acoustic time signals are compared to those actually measured near MOD-1 and good agreement is obtained.

Based on the predictions of the models, they conclude that neither steady blade loads nor loads due to operation in ground shear contribute substantially to the acoustic signal from a wind turbine such as MOD-1. Also, comparison of the theoretically predicted signal for noise from interaction with the mean wake for a 35 rpm rotational speed, and the measured one indicates a close resemblance, both quantitatively and qualitatively. The conclusion to be drawn from this is that high level impulsive sound could radiate from MOD-1 due to the interaction of its blades and tower wake. However in the prediction code description there is no mention of the aerofoil specification and it is not clear whether this code can be applied on an upwind rotor with the same accuracy.

3.2.6 The NASA wind turbine sound prediction code (WTSOUND) [46]

Viterna embodied in his wind turbine noise prediction code, WTSOUND, available theory used for calculating noise from conventional aircraft propellers. The development of such theories goes back to 1937, when Gutin [28] first successfully calculated the noise from a propeller in a uniform flow field. Since then, Gutin's theory has been extended to include the effects of non-uniform flow fields and applied to helicopters and turbo-machinery as well as propellers. The WTSOUND code was written using this theory to provide a means of calculating sound intensity and frequency characteristics specifically for wind turbines in non-uniform flow fields.

The predominant sound produced by a wind turbine is associated directly with the aerodynamic pressures on the blades. These pressures can be related for convenience to the thrust and torque forces on the rotor. The thrust and torque forces have components that are both steady and unsteady in time. The steady forces produce sound called rotational noise, which consists of pressure variations in the acoustic field at the blade passing frequency with harmonics of rapidly decreasing magnitude. The unsteady forces may be either periodic (i.e. from tower shadow and wind shear) or random (i.e. gusts). Noise due to periodic unsteady forces may be dominant over rotational noise and

generate higher harmonics of amplitude comparable to that of the fundamental.

The procedure used in the code can be summarized as follows:

(1) calculation of the steady aerodynamic blade forces,

(2) variation in these forces due to unsteady aerodynamics,

(3) Fourier analysis of the force variation, and

(4) calculation of sound pressure levels in the acoustic field.

The total thrust force and torque on a rotor in uniform flow is determined from blade element-momentum theory.

Viterna claims that the WTSOUND computer code shows generally good agreement with sound spectra measured in the vicinity of a wind turbine. In the far field, however, correlation of the absolute amplitude of the sound level is complicated by propagation effects. For the case in this study, terrain and meteorological conditions caused an increase of about 6 dBA.

3.2.7 University of Southampton computer code [47]

The computer code from the University of Southampton [47], predicts noise emitted from three aerodynamic source mechanisms associated with wind turbine generators. These are trailing edge noise, drag noise and inflow noise. It uses an analytical method for the prediction, also it

assumes that the observer is in the geometric far field of the rotor. The model includes the effects of observer distance, atmospheric attenuation and ground reflection. The effect of wind on noise propagation is not included. Furthermore the computer code does not allow the effect of geometry and shape of the blade on the emitted noise level from a machine, to be determined.

3.3.Conclusion

The above computer codes can be summarised in the following table which gives brief features and application description of each computer code for easy comparison.

Table 3.1 comparison of different computer code

Computer code	Feature	Application
3.3.1 Hamilton Standard Division	Theoretically based; used for prediction of propeller noise. Calculation of noise is due to steady, unsteady load broadband turbulence noise.	Performance of the rotor is calculated, wake velocity defect and wind shear calculated. The wake defect calculation may not be very accurate.
3.2.2.NASA	Modified version of Farassat and Nystrom propeller noise prediction code.	The program properly accounts for the significant geometry features of the rotor and its operating condition. No validations of the code applied to large wind turbines, apart from MOD-1.

Computer code	Feature	Application
3.2.3.NASA	Based on empirical formulae. Model test found to be average measurement based on average wake characteristics.	Prediction of the nonperiodic sources of is not exact. Estimation of the wake of the rotor is not accurate this code is based on empirical formulae which are difficult to generalise.
3.2.4. The Boeing Vertol Company	Classified into two categories periodic(thrust, drag, radial), and nonperiodic(inflow turbulence viscous shere), estimate of viscous shear is empirical.	Prediction of nonperiodic sources is less exact then the periodic sources, the later being empirical which means that it can't be generalised.

Computer code	Feature	Application
4.2.5. Massachusetts Institute of Technology	Based on prediction of different noise sources; such as steady and unsteady load and load caused by the blade as it passes the supporting tower.	It is not clear whether this code can be applied to an upwind rotor with acceptable accuracy or not.
3.2.6. THE NASA-LERC	Based on theory used for calculating noise from conventional aircraft propellers. Calculation of steady aerodynamic forces, estimate of unsteady aerodynamic forces.	In the far field but the meteorological conditions are not included.
3.2.7. University of Southampton	Includes trailing edge noise, drag noise and inflow turbulence. The model includes the effect of observer distance, atmospheric attenuation.	Noise propagation is not included.

Study of the above computer codes shows that none of them significantly includes the geometry and shape of the blade. Also some cannot be generalised due to use of empirical formulae. The University of Southampton computer code was not capable of handling panels on the blade, nor of handling aerofoil geometry [47], which implied that it would be difficult to adapt to the requirements of the current research.

The lack of an ideal noise prediction computer program led to the decision to write a new computer code which included the detailed specification of the aerofoils such that the aerodynamic forces on the wind turbine blades could be computed. Furthermore, ground effect, observer position and height, and the height of the wind turbine itself would be included. A significant advantage would be the ability to modify the program when necessary. The proposed computer program should be able to perform the following tasks.

1 Estimation of noise levels from different types of aerofoil in order to effect comparisons.

2 Whilst keeping the output power the same, the changing of parameters such as blade chord, number of blades, rotational speed etc. in order to minimise noise levels.

CHAPTER

4

THEORETICAL FORMULATION

The formulations which take into account the above factors rely on two forms of the solution of the Ffowcs-Williams and Hawkings (FW-H) wave equation [38], [39], [42].

The theory of aerodynamic sound is built upon the equations of mass and momentum conservation of a compressible fluid. Consider a fixed volume of fluid V enclosed by surface Σ. Suppose V is divided into regions 1 and 2 by a surface of discontinuity S encroaching on region 2 with velocity **v**. Let $\mathbf{l}_i$ be the outward normal from V, and **n** be normal to surface S going from region 1 to region 2. The superscripts 1 and 2 refer to the two regions, and an overbar implies that variable is to be regarded as a generalized function valid throughout V, e.g. $\bar{\rho}$ is equal to ρ^1 in V^1 and ρ^2 in V^2. If ρ represents the fluid density, then the rate of change of mass within V is

$$\frac{\partial}{\partial t}\int_V \bar{\rho}\, dV = \frac{\partial}{\partial t}\int_{V^1} \rho^1\, dV + \frac{\partial}{\partial t}\int_{V^2} \rho^2\, dV \qquad (4.1)$$

The two regions have a moving boundary S, so that for each region

$$\frac{\partial}{\partial t} \int_{V^1} \rho^1 \, d\,V = -\int_{\Sigma^1} (\rho u_i)^1 \, l_i \, d\Sigma$$

$$-\int_S \left[\rho \, (u_i - v_i) \right]^1 n_i \, dS \qquad (4.2)$$

where u_i is the component of the fluid velocity in the direction x_i (i=1,2,3), and the repeated suffix implies a summation over these values. Hence the rate of change of the total mass within V is

$$\int_V \bar{\rho} \, dV = -\int_\Sigma (\overline{\rho u_i}) \, l_i d\Sigma$$

$$+ \int_S \left[\rho (u_i - v_i) \right]_1^2 n_i dS \qquad (4.3)$$

the symbol $\left[\quad \right]_1^2$ meaning the difference of the contents between regions 2 and 1.

Equation (4.3) leads to the generalised mass equation (4.4)

approximations, it is difficult to compute. An important approximation is introduced by assuming that the body does not disturb the medium appreciably and thus the nonlinearities may have negligible effects. The governing equation for the acoustic pressure is then a wave equation with some inhomogeneous source terms depending on the net local force of the body on the fluid and the normal velocity of the surface of the body. One of the common assumptions in treating the problem of acoustic radiation is the compactness of the sources. A stationary source is compact if its dimension is much smaller than the wave length of radiation. This definition needs to be modified for moving sources. Effectively a compact source may be treated as a point source and considerable simplification is introduced in the acoustic analysis.

The main result from Farassat [39] is the development of a theory for the calculation of the acoustic pressure signature for bodies in arbitrary motion in the ground fixed coordinate system where the observer is not limited to fixed location, and no compactness assumption is made.

The starting point of the Farassat [39] development is the Ffowcs-Williams and Hawkings equations (4.4), (4.5), with a view towards application to wind turbines.

The developments of Farassat depend upon a mathematical technique called embedding. The purpose of the embedding technique is to convert a problem with a restricted domain

into a problem with an unbounded domain. The procedure is employed to drive the Ffowcs-William and Hawkings equation into a form of expression valid for horizontal axis wind turbines. The advantages of using the Farassat expression are that there are fewer limitations, in particular no compactness limitation, and more suitability for wind turbine application.

4.2 Embedding Procedure

A brief description is provided below; full details may be found in Reference [39]. This technique is used to unbound the original equation which was restricted to the domain outside the moving body, and also required compactness of the source to unbounded space. The technique is illustrated by using an ordinary differential equation.

Consider the differential equation

$$y - y'' = f(x) \qquad \begin{bmatrix} x \text{ in } [a,\infty\,] \\ f(x) \longrightarrow 0 \text{ as } x \longrightarrow \infty \end{bmatrix} \qquad (4.6)$$

with the boundary conditions

$$y(a) = y_a$$
$$y \longrightarrow 0 \quad \text{as } x \longrightarrow \infty$$

This problem can be solved by finding the solution of the following equations:

where H(x) is the Heaviside unit function defined by

$$\left.\begin{aligned} H(x) &= 1 \qquad \text{for } x > 1 \\ &= 0 \qquad \text{for } x < 1 \end{aligned}\right\} \tag{4.10}$$

The solution for y is then the following:

$$y(x) = \left[G(x,\xi)\ f(\xi) \right] + y_2(x)$$

$$= \int_a^{\infty} G\ (x,\xi)\ f(\xi)\ d\xi + y_2(x)$$

$$= e^{a-x} \int_a^{x} \sinh(a - \xi)\ f(\xi)\ d\xi + \sinh(a - x)$$

$$+ \int_x^{\infty} e^{a - \xi}\ f(\xi)\ d\ \xi + y_a\ e^{a-x} \tag{4.11}$$

The solution of equation (4.8) which is

$$y_2 = y_a\ e^{a-x}$$

has been utilised in the above equation.

This technique, which extends the domain of the definition of a differential equation, is called the embedding procedure, and has been used to derive the Ffowcs-Williams and Hawkings equation to a form suitable for wind turbines. The equations (4.4), (4.5) are valid in the region exterior to any closed internal surfaces that may be present, and

can be combined to give an inhomogeneous wave equation governing the generation and propagation of sound waves in that region. Such a situation is essentially inhomogeneous in space.

The governing wave equation for the determination of the acoustic pressure p (**x**,t) , using the embedding procedure described in full detail in Reference [39], is

$$\frac{1}{c^2}\frac{\partial^2 p}{\partial t^2} - \nabla^2 p = \frac{\partial}{\partial t}\left[\rho_o v_n |\nabla f| \delta(f)\right] - \frac{\partial}{\partial x_i}\left[l_i |\nabla f| \delta(f)\right] + \frac{\partial^2 T_{ij}}{\partial y_i \partial y_j} \qquad (4.12)$$

where the Laplacian operator

$$\nabla^2 = \frac{\partial^2}{\partial y_1^2} + \frac{\partial^2}{\partial y_2^2} + \frac{\partial^2}{\partial y_3^2}$$

and $\frac{\partial^2 T_{ij}}{\partial y_i \partial y_j}$ is the so-called quadrupole noise due to turbulence.

The acoustic pressure is p, c and ρ_o are the speed of sound and the density in the undisturbed medium respectively, and v_n is the magnitude of the normal velocity on the blade surface. The component in the i^{th} direction of the local aerodynamic pressure on the blade surface is denoted by l_i, the observer position is given by **x**, and the source position

given by **y** with F being the frame fixed with respect to undisturbed medium so it has a fixed position with respect to fixed ground coordinates allows full description of the blade geometry. The function $\partial(f)$ is the one-dimensional delta function which is zero everywhere except when F=0 i.e at the frame position relative to the coordinates.

The first term on the right hand side in the above equation arises as a result of the component of motion of the surface in a direction normal to its surface. The second term comes from the local surface stress. Physically, this term is the contribution of the net force acting on the fluid due to the pressure distribution on the blade surface.

In order to solve the equation, the required parameters are the body geometry, time history of motion and its surface pressure distribution. The flow parameters on the moving surface are known and obtained by computation of the aerodynamics using the computer code FORCE [50] which has been demonstrated by validation exercises to be accurate and reliable.

Since the case of interest is a wind turbine blade, the region of turbulent flow is small and of relatively low intensity. Therefore it is assumed that the term involving T_{ij} in equation (4.12) may be neglected, following Lighthill [25] who stated "that turbulence is a very inefficient noise producing mechanism"

blade. The vector **r= x - y** where **y** is the source position and **x** is the observer position. In equation (4.13) $M_r = \mathbf{v}.\hat{\mathbf{r}}/c$ where **v** is the local velocity on the blade surface and $\hat{\mathbf{r}} = \mathbf{r}/r$ the unit vector in the radiation direction, while M_r is the Mach number in the radiation direction, l_r is the magnitude of the local pressure component on the blade in the radiation direction and F=0 represents frame fixed with respect to undisturbed medium. Subscript r indicates the radiation direction, see Fig 4.1. Fig 4.2 is a diagrammatic sketch showing the observer position relative to the path of an acoustic source on a rotor blade.

For a supersonic case

$$4\pi p\,(\mathbf{x},t) = \frac{\partial}{\partial t}\int_{\substack{f=0\\g=0}} \frac{\rho_o\, cv_n + l_r}{r \sin\theta}\,.\,dR\,dt$$

$$+\int_{\substack{f=0\\g=0}} \frac{c\, l_r}{r^2 \sin\theta}\,.\,dR\,dt \qquad (4.14)$$

where g (T,t) = T - t + r (T,t)/c, when g = 0 that imply g = T -t + r/c = 0. dR is an element of length of the curve of intersection for the surfaces f = 0 and g = 0. The symbol θ in equation (4.14) represents the angle between the normal to the surface and the radiation vector.

Equation (4.14) applies to supersonic sound generating surfaces, and since wind turbine generators operate at rotational speeds for which the tips are subsonic then equation (4.13) is appropriate.

4.4 The numerical approach to noise calculations

This section is concerned with the method of implementing equation (4.13) on a computer for wind turbine noise calculation. Each blade is first divided into panels and the contribution of each panel to the acoustic pressure (denoted by p_i) using equation (4.13) may be written as

$$4\pi p_i(\mathbf{x},t) = \frac{1}{c}\frac{\partial}{\partial t}\left[\left\{\frac{\rho_o c v_n + l_r}{r|1-M_r|}\right\}\right]_{ret,i} \partial s_i + \left[\left\{\frac{l_r}{r^2|1-M_r|}\right\}\right]_{ret,i} \partial s_i \qquad (4.15)$$

where l_r is a vector of the force on the blade in the radiation direction and v_n is the local normal velocity of the blade surface (i.e l_r and v_n are magnitudes, respectively). The contributions of all panels from all blades are summed to obtain the acoustic pressure signature, $p(\mathbf{x},t)$, at a specific observer position and instant of time, thus :

$$p(\mathbf{x},t)=\sum p_i(\mathbf{x},t), \quad i: \text{ all panels.}$$

The differentiation with respect to time in equation (4.15) is performed numerically after the summation on all panels is performed.

Although the concept behind the application of this equation is simple, past experience has indicated that acoustic calculations based on the above equation are sensitive to errors. Both the specification of the blade geometry and the emission time calculation must be done as precisely as possible [42], [48], [49].

WTGNOISE calls the following subroutines to perform the noise pressure calculations.

1 FORCE. This calculates the pressure distribution along the blade using strip theory to obtain the instantaneous aerodynamic force components acting on a section of blade, as shown in Fig 4.3.

2 LMN. (Local Mach number) This calculates the instantaneous emission time and the value of M_r.

3 INTEG1. This calculates that part of the pressure on the blade which derives from the first term on the RHS of equation (4.15).

4 INTEG2. This calculates that part of the pressure on the blade that derives from the second term on the RHS of equation (4.15).

Fig 4.4 shows the flow chart for the computer code developed to predict the noise level at the design stage and will be explained in greater detail in Chapter 7.

4.5 Blade coordinate and description

Because of the chord length, aerofoil section, and coning angle, the blade sources should not be assumed to lie in a plane. To describe the blade, the chord, aerofoil section and thickness ratio of the blade are specified.

4.6 Calculation of the emission time

If T is the time measured at the source, t is that measured at the observer, and the distance between the observer and the source is r, the emission time $T = T^*$ is calculated from the relation

$$c(T^*-t) + r = 0 \qquad (4.16)$$

The emission time is the time when a source on a panel emits sound which arrives at the observer at time t. The source position **y** is a function of T, so r itself is a function of T.

A numerical method to solve equation (4.16) can be used. Assuming that the observer time and position are fixed, which is normally the case for wind turbines, one can show that for a given source in motion

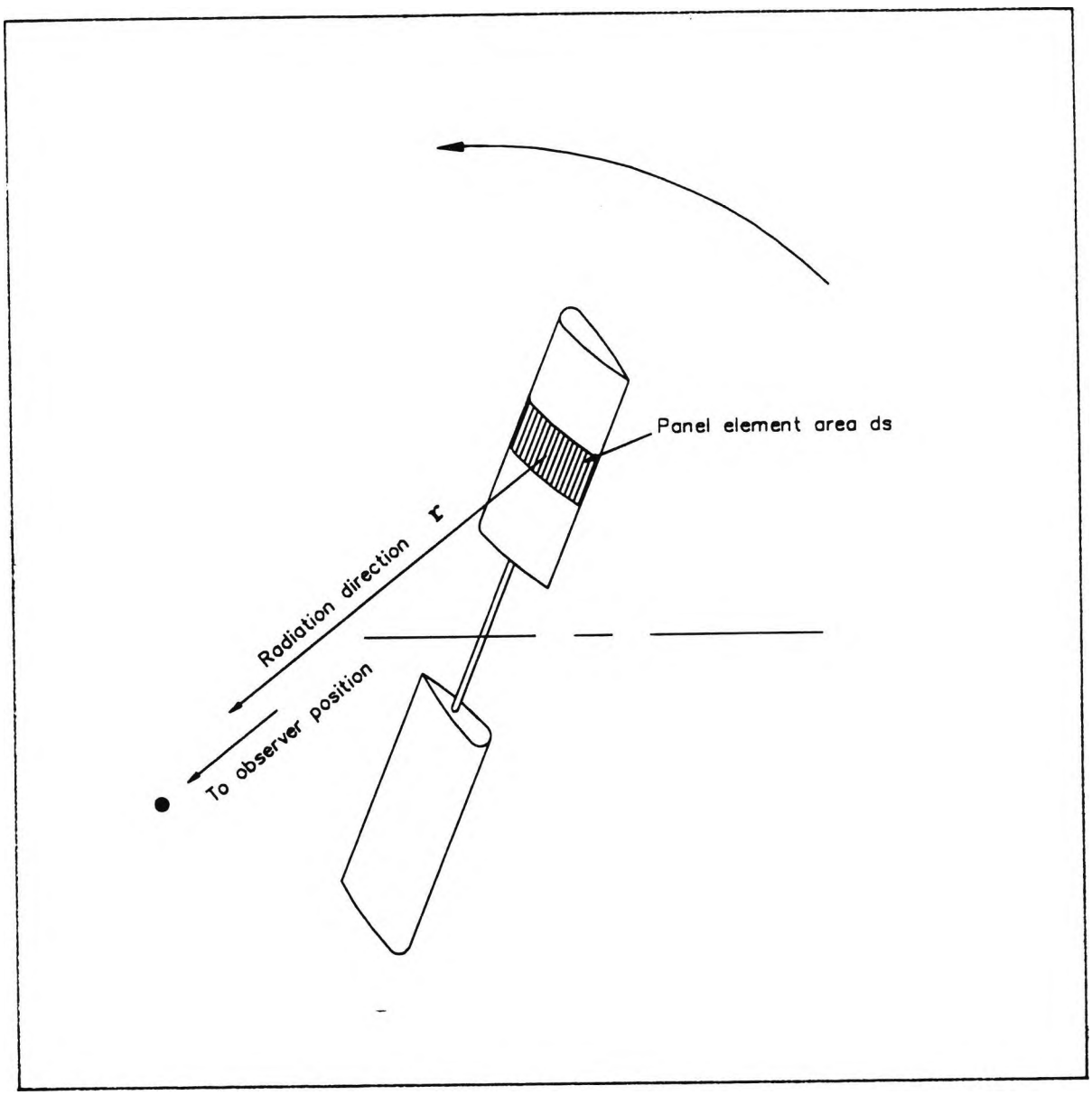

Fig 4.1 Rotor blade element source (panel) on the rotor disc.

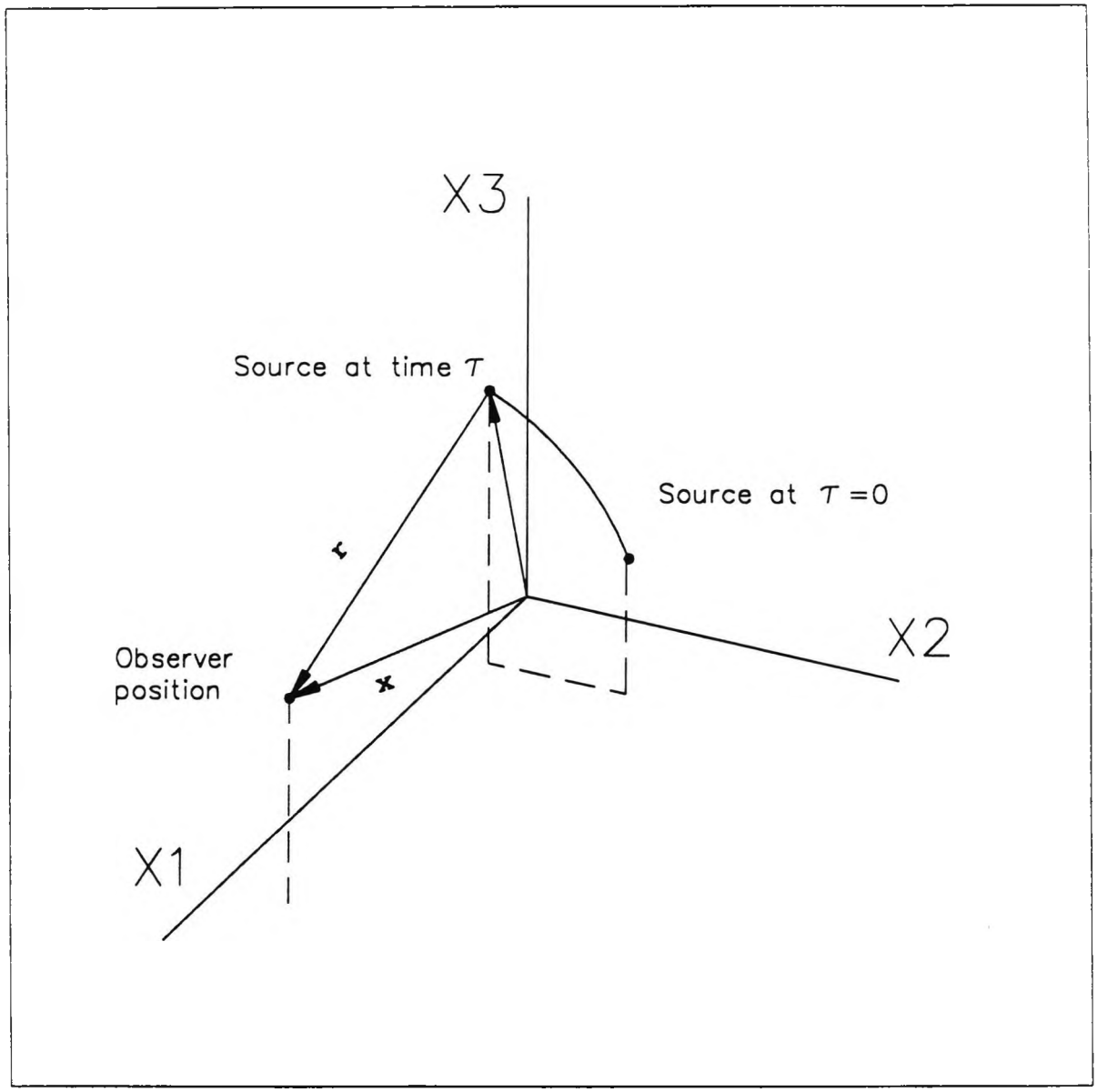

Fig 4.2 Rotor Blade Element source relative to the observer position

$$\frac{\partial g}{\partial t} = 1 - M_r$$

where $M_r(T) = \frac{\partial\, r(t,T)}{\partial\, t}$ is the Mach number corresponding to the rate of change of distance between the source and observer, and where $g(T,t) = T - t + r(T,t)/c$. Equation (4.16) demonstrates that, viewed as a function of a single variable T, the emission times of a source in motion are the zeros of function g. For sources in subsonic motion $M_r < 1$ and therefore $\frac{\partial g}{\partial t} > 0$. This means that the function g is strictly an increasing function of T and thus can have only one zero. Newton's iterative method [48], [49] is used to obtain the emission time for each panel on the blade. To speed up the convergence of iteration, the known emission time of a nearby panel is used as the initial guess for the emission time of the next panel.

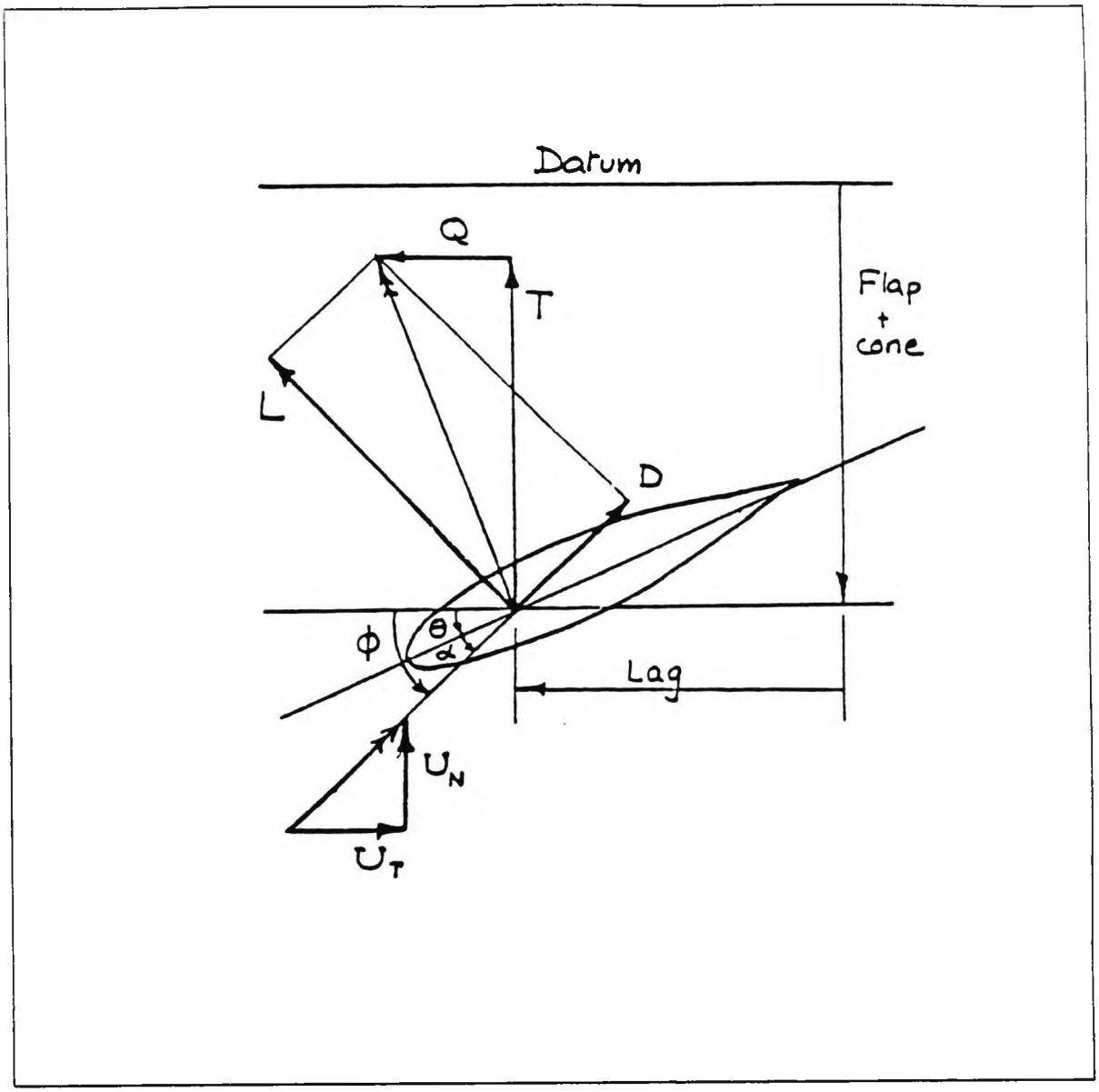

Fig 4.3 Aerodynamic force acting on a blade section where T is thrust force, Q is the tangential force, L and D are lift and drag forces on the blade. U_N,U_T are air velocity components relative to blade section.(Extracted from Ref [50].)

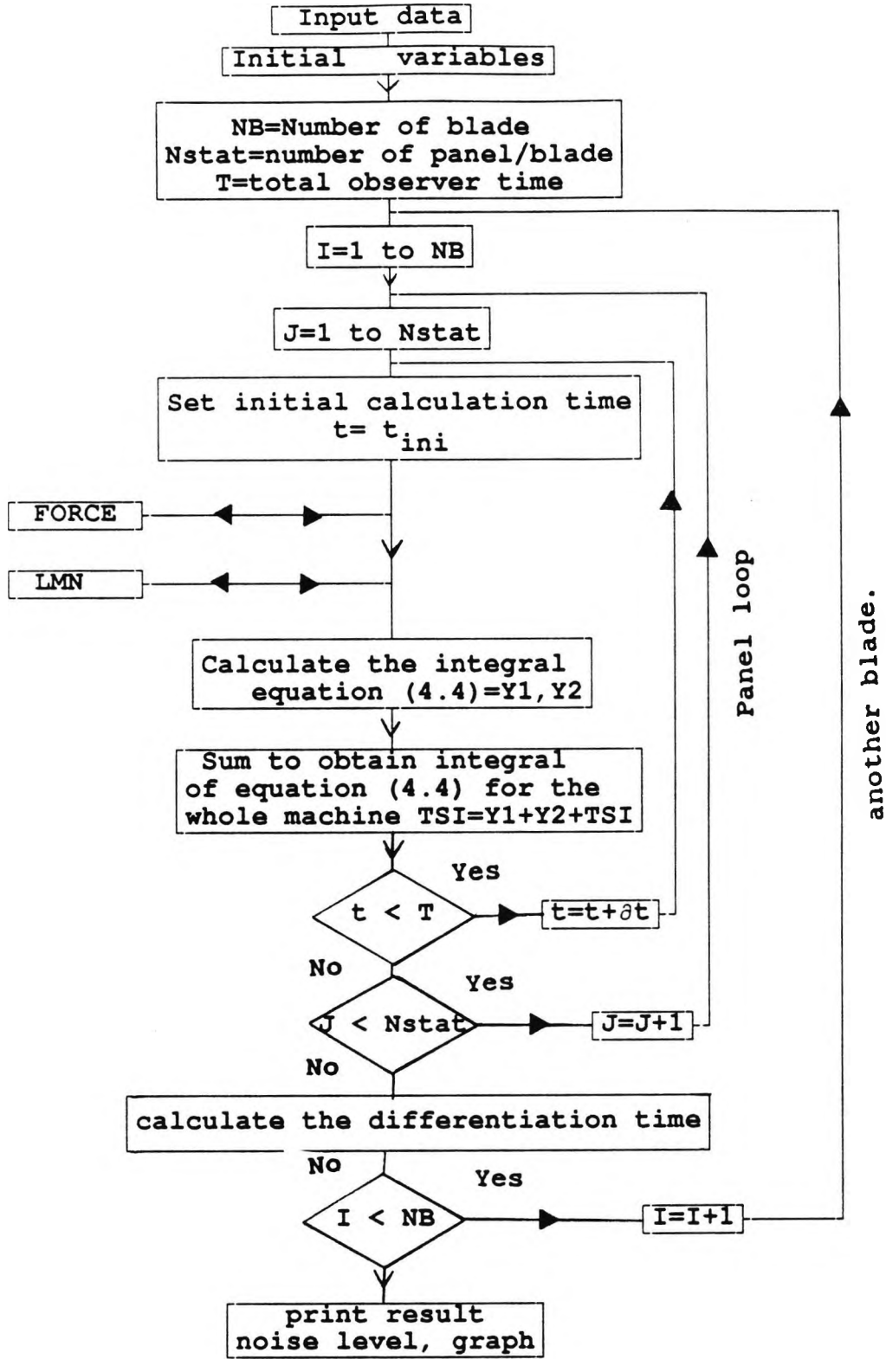

Fig 4.4 Flow chart for computation of noise for a wind turbine generator.

4.7 Application of the Numerical Technique

The term l_r in equation 4.14 is calculated using the computer program FORCE [50] written by J.Kawadri, a postgraduate student of the Department of Mechanical and Aeronautics engaged in wind turbine dynamics (see Appendix [2]). FORCE calculates the pressure on a wind turbine blade given the geometric data of the aerofoil, the blade dimensions and aerodynamic properties. Other parameters provided are rotational speed, ambient wind speed, hub height, tower radius, overhang, angle of yaw, angle of tilt, angle of cone and blade pitch angle.

FORCE employs strip theory to determine the instantaneous aerodynamic forces (i.e. at a particular blade azimuth angle) acting on a section of blade taking the following factors into account:

(i) Tip loss factor which allows for the reduction in the force coefficients near the blade tip.

(ii) Wind shear (using a power law distribution) since wind turbines are constructed high above the ground and subject to the atmospheric boundary layer. The wind speed increases with height across the rotor diameter which causes changes to the blade loading as it proceeds around its path.

(iii) Tower shadow (using the potential flow field around a cylinder). For downwind rotors, the blade traverses through the wake of the tower once every revolution.

The region behind the tower is turbulent and has a reduced velocity field where the blade experiences a sharp reduction in force. In the case of an upwind rotor there is a similar altered velocity field in the region of the tower which again affects blade forces.

The dynamic model in FORCE has been verified using data for the WEG MS-1 machine; results from this code have been compared with those from another validated code. The agreement between the two sets of results was found to be generally acceptable.

Fig 4.5 shows the flow chart for the aerodynamic computer program FORCE in which the following subroutines are called.

WNDSHR. Calculates the changes in wind velocity at a particular station on the blade due to wind shear.

TWRSHD. Calculates the changes in wind velocity at a particular station on the blade in the vicinity of the tower.

TIPLOS. Calculates the tip loss factor.

It should be mentioned here that it is generally difficult to obtain the aerodynamic blade data required by WTGNOISE. The only data that were sufficiently detailed and which were readily available for use in the wind turbine area was that which applied to the Wind Energy Group MS-1 [51], (NACA 4415), together with that for the Garrad Hassan and Partners aerofoils GH1 and GH2.

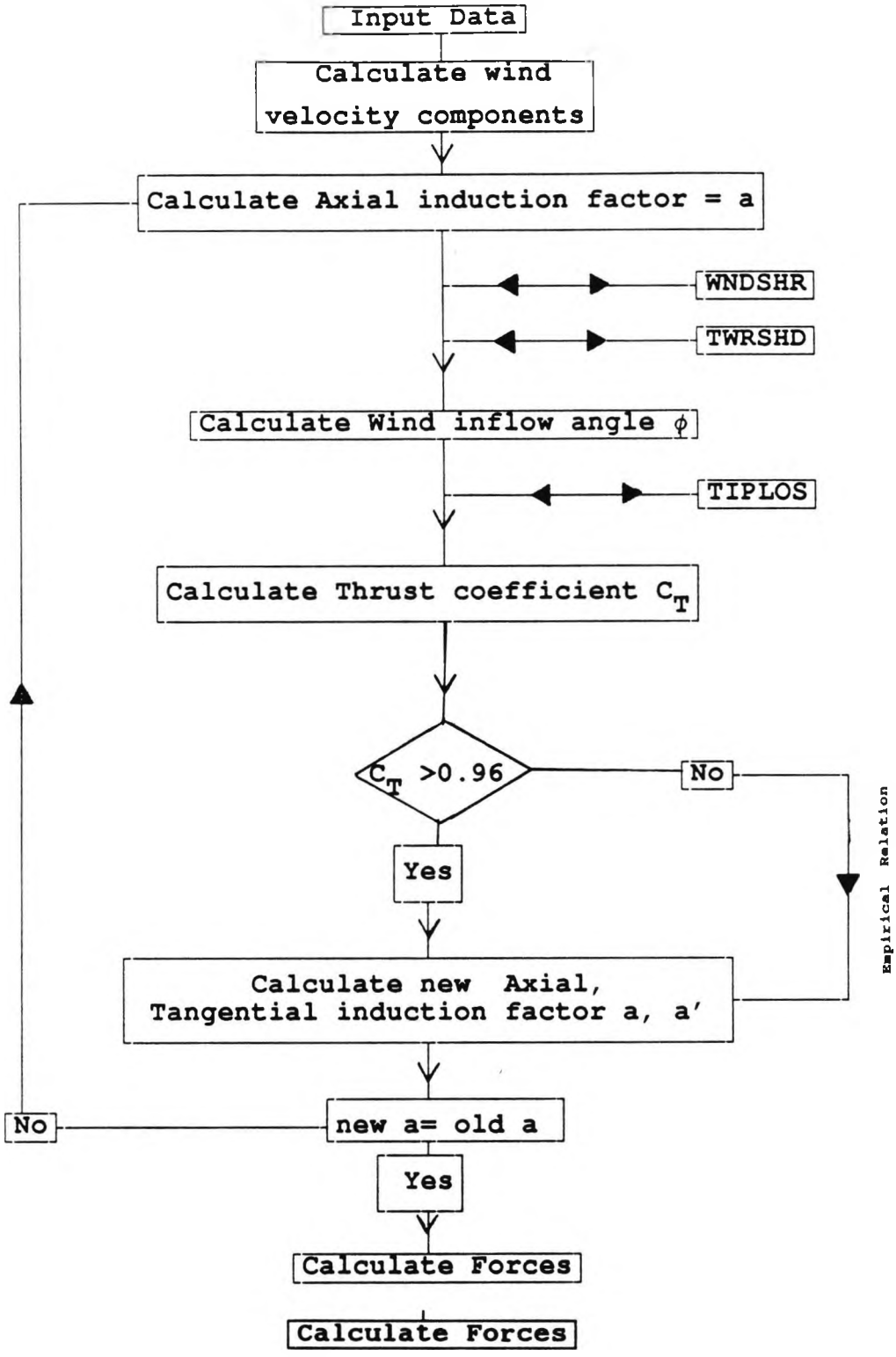

Fig 4.5 Flow chart for computation of Aerodynamic computer program FORCE [50].

CHAPTER

5

MEASUREMENT OF WIND TURBINE NOISE

5.1 Introduction

It was decided that a suitable way to verify the computer program was to attempt to obtain actual noise measurements from an operating wind turbine in the field.

Resulting from enquires in the wind turbine community, an offer to provide the experimental machine situated at Lords Bridge near Cambridge was kindly made by Dr. D.Wilson of the Cavendish Laboratory, University of Cambridge. Although this machine was a downwind model and based on relatively old technology, it had two major, and in the event over-riding, advantages.

These were that it was freely available for use and accessible, and that it was near to London. The latter led to minimal accommodation and transport costs (including transport of equipment) which were important factors in view of the unpredictability of the wind and weather.

The main implication in using a downwind rather then upwind machine for verification of WTGNOISE is that although that part of the tower shadow effect due to the flow directions changing in the vicinity of the tower is accounted for in the noise prediction programme, that part due to turbulence from the tower of a downwind machine is absent.

This Chapter contains a description of the measurement methods and the study required to make the comparisons with the prediction code.

5.2 The field site

The site lies towards the southern side of the Mullard Radio Astronomy Observatory at Lords Bridge approximately 5 miles south-west of Cambridge. Fig 5.1 shows the field site taken from an Ordnance survey 1:5000 map of the observatory area, the hatched rectangle illustrating the field site. The site is 17 m above sea level and it is generally flat. Fig 5.1 shows some of the larger structures present at the observatory site, which includes a group of buildings and the large radio telescope base lines. A disused radio telescope track runs along the side of the wind turbine site, with an old aerial to the South-East. The Northern and Western sides are bounded by fields under cultivation, with rows of trees about 10 m high, 250 m away from the edge of the turbine site. No comprehensive data on wind at the site were available; the nearest available meteorological station is at Cardington, approximately 19 miles to the East [52]. The position of the wind turbine and anemometers at the site is shown in Fig 5.2.

5.3 Outline description of the wind turbine

The machine is a downwind two-bladed horizontal-axis turbine of 5 m rotor diameter, operating in free yaw. The blades are independently and freely flap-hinged at the hub, with a hinge offset from the shaft of roughly 6% of the blade radius. The rotor drives an electrical generator in

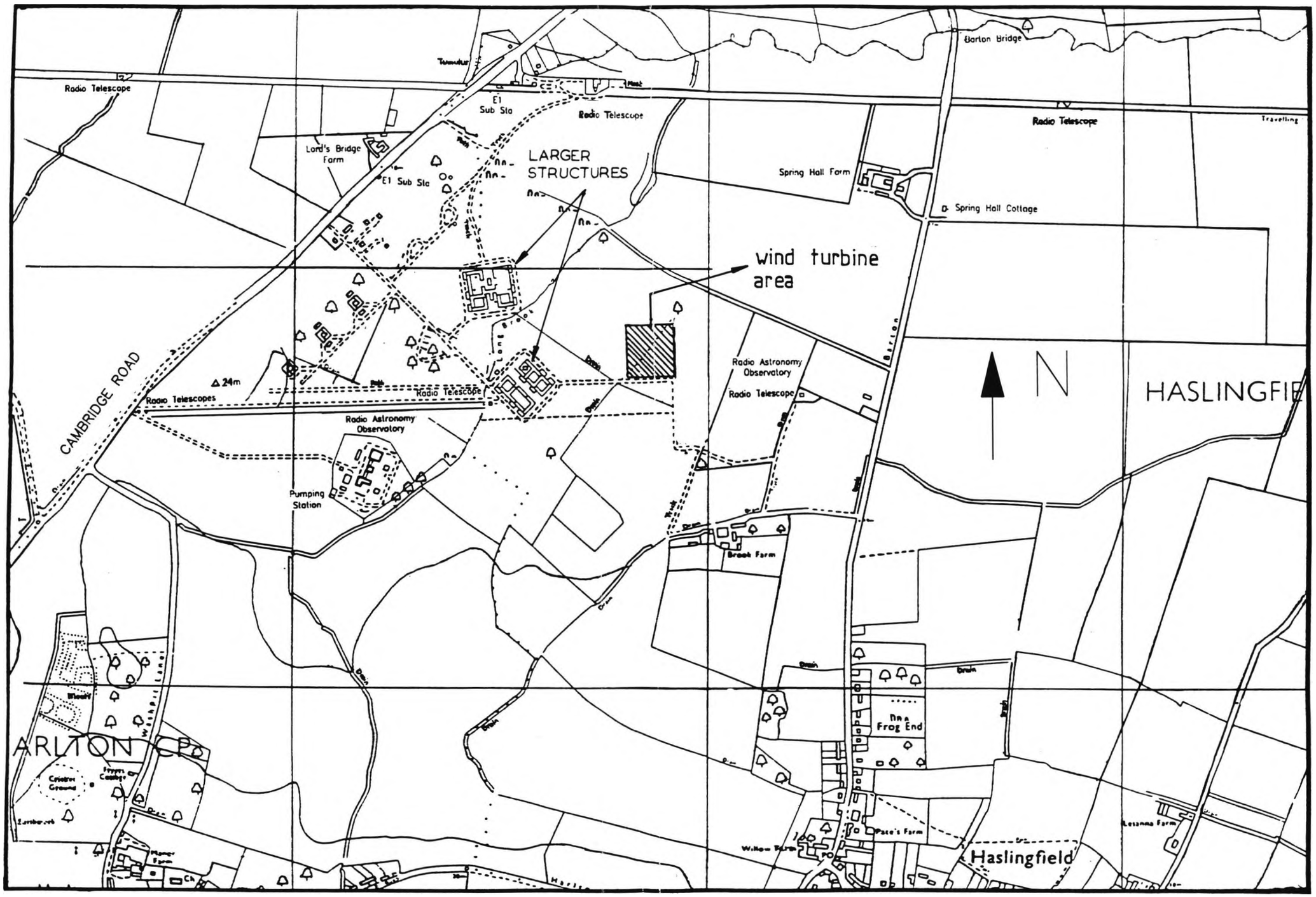

Fig 5.1 Reproduction from the 1982 Ordnance Survey 1:5000

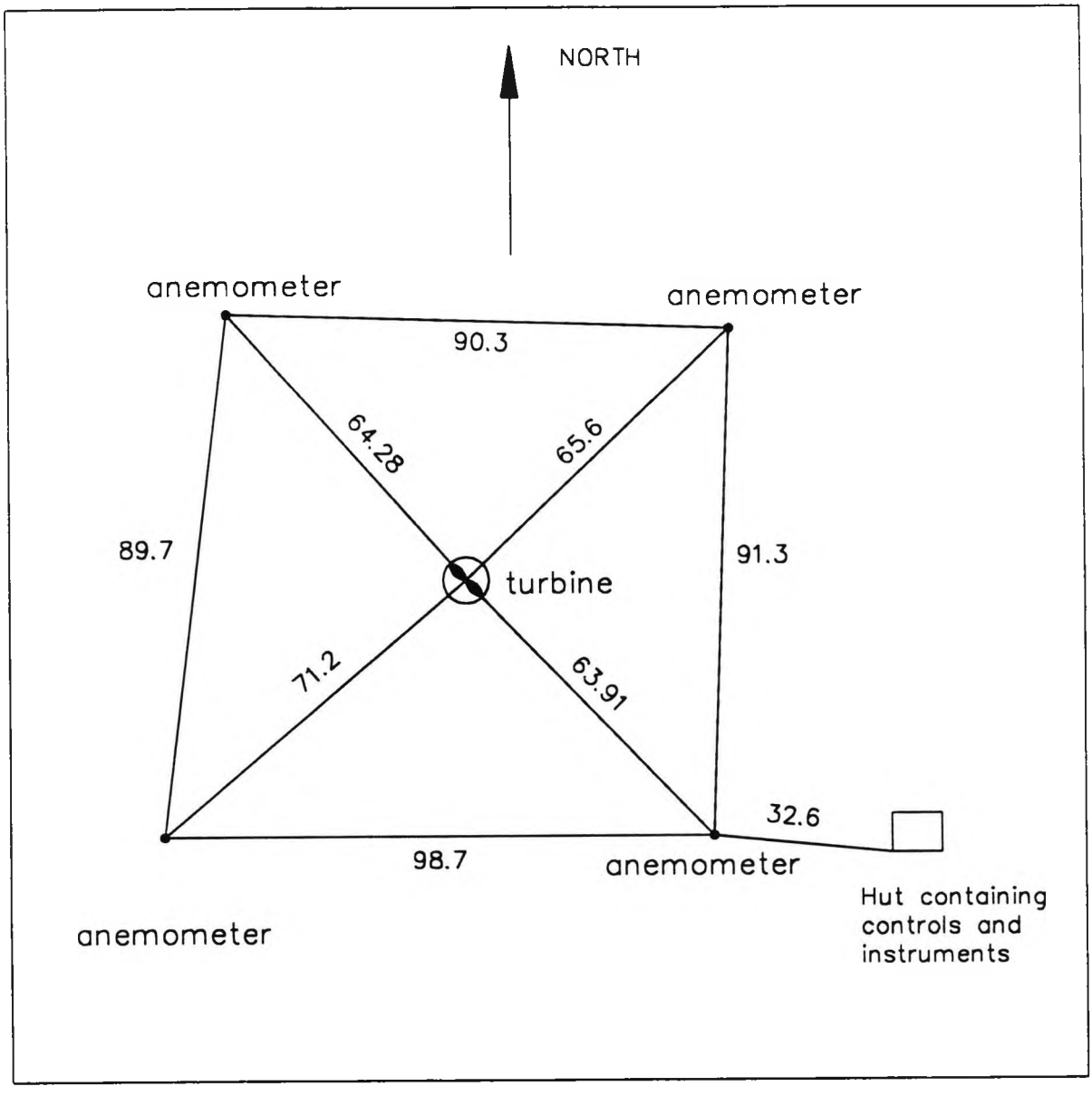

Fig 5.2 Layout of Lords Bridge field site, (dimensions in meters).

the nacelle. The tower is a tubular steel mast tapering slightly and of octagonal section. The tower is mounted on a cross-frame of very heavy steel girders standing directly on the ground. The hub height is 9.5 m above the ground.

For access to the machinery and instrumentation in the nacelle, the tower is mounted on pivots and the nacelle can be lowered nearly to the ground level by a winch and pulley arrangement. A list of important machine parameters is given in Table 5.1; these have been described previously by Fordham [52]. Fig 5.3 shows the wind turbine major machine dimensions.

5.3.1 The turbine rotor blades

These have been described in detail previously by Fordham [52] and Anderson [53]. but a brief description follows.

The blades (see Fig 5.4, 5.5) were manufactured for the Cambridge Wind Energy Group by Wave Power Ltd. (later Gifford Technology Ltd.) of Southampton.

The blade is untwisted, with a chord tapering linearly from 205 mm at 0.375 m radius to 65 mm at the blade tip. The blade pitch angle is constant at 1.47 degrees (see Fig 5.6). The aerofoil section is N.A.C.A. 4415, which has lift and drag characteristics provided from the work of Abbott and Doenhoft [54].

The Wood Epoxy Saturation Technique was used in construction (W.E.S.T), a method developed in U.S.A for boat building;it involves building up the structure from

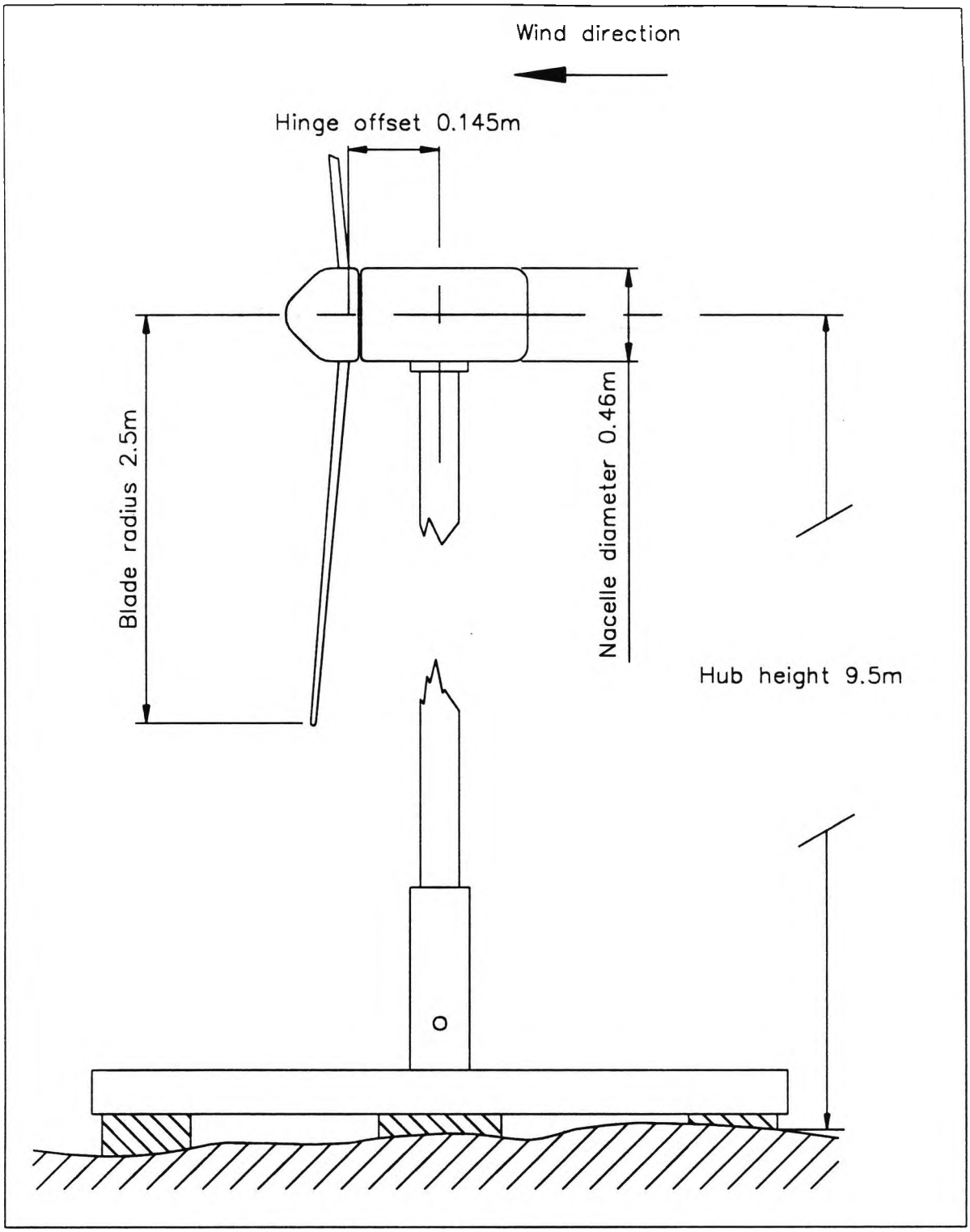

Fig 5.3 Diagram of the wind turbine showing major machine dimensions.

thin wood laminations. Each lamination is thoroughly soaked in epoxy resin, which then becomes glue, matrix, filler and sealer for the timber. This method seals the wood completely against the spread of moisture and variations in moisture content, leaving a stable structure based on wood, and protected against warping. A blade section is illustrated in Fig 5.4 in this Chapter; the main blade surfaces are layers of thin veneers with a beech main spar and leading edge. The interior contains only a foamed plastic former around which the blade is built. The resulting blade is very light, flexible, with the centres of gravity and torsion well forward, and believed to be aeroelastically stable. No flutter problems have been actually encountered in operation [52], [53].

Vibration frequencies quoted by Fordham are 4.7 Hz[52] for the first flapping mode, 22 Hz for the first lead-lag mode and 85 Hz for the first torsional mode. These frequencies are for vibrations on the bench; centrifugal stiffening in operation will increase the vibration frequencies of the flapping and lead-lag modes when the blade is rotating.

The blade root, with bearing bushes for freely hinged mounting, is illustrated in Fig 5.7.

5.3.2 Rotor hub

The hub of the turbine carries the electronics for the rotating shaft telemetry system.

Before assembling the turbine in the field the rotor assem-

bly was carefully balanced statically in the laboratory, adding counterweights where necessary to the hub. The moment of inertia of the rotor was determined by the pendulum method after static balancing [52].

5.3.3 Electrical machines and control mechanisms

The turbine uses a specially-designed permanent magnet 3 - phase alternator which is directly driven by the rotor. Because the system is designed to protect the magnet from the effect of overloads it is necessary that all three phases are loaded equally and with a leading power factor. Consequently the load control is either full on or off, the fraction of the total time switched to 'ON' being varied to control the machine. The load is switched by 3 solid state relays driven in parallel by a comparator circuit with variable time constant and hysteresis.

Depending on the input to the comparator the machine can be run at constant speed, or constant tip-speed ratio or in other modes. Normally it is run at constant speed, with zero time constant and little hysteresis. This gives very accurate speed control at the expense of some small magnetic noise and vibration of the machine because of the rapid load cycling.

In addition to the electrical control system an entirely mechanical over speed brake is fitted ;this consists of a torque limiting clutch preset to a suitable level, which is engaged by a pawl triggered by a centrifugal weight on the

rotor shaft. This brake operates automatically if the machine speed exceeds 450 r.p.m.

5.3.4 Tower and yaw axis mounting

The generator unit is mounted on a base plate which pivots freely on the axis of yaw, and the centre of mass of the nacelle unit and rotor combination was originally placed directly above the yaw axis bearing to avoid coupling between yaw motion and tower bending movement. The nacelle has since been moved slightly downwind to allow a fairing to be fitted to the tower in order to reduce tower shadow effects [52]. Cabling for power or for instrumentation, is taken to the ground via a slack loop allowing about two complete revolutions of the nacelle about the yaw axis.

5.3.5 Turbine base

This is a cross-frame of heavy steel girders, which carries the tower supports and heavy pivots, and is sufficient in mass for the turbine to be lowered to a horizontal position without the nacelle touching the ground.

5.4 Instrumentation

A brief description follows.

5.4.1 Noise measurement equipment

1) Portable analogue cassette recorder mini-log 4 channel (Philips) to record noise signals, wind speed, power and rotational speed. Cut off frequency is 5 KHz.

2) Precision sound level meter (B&K Type 2204) to measure

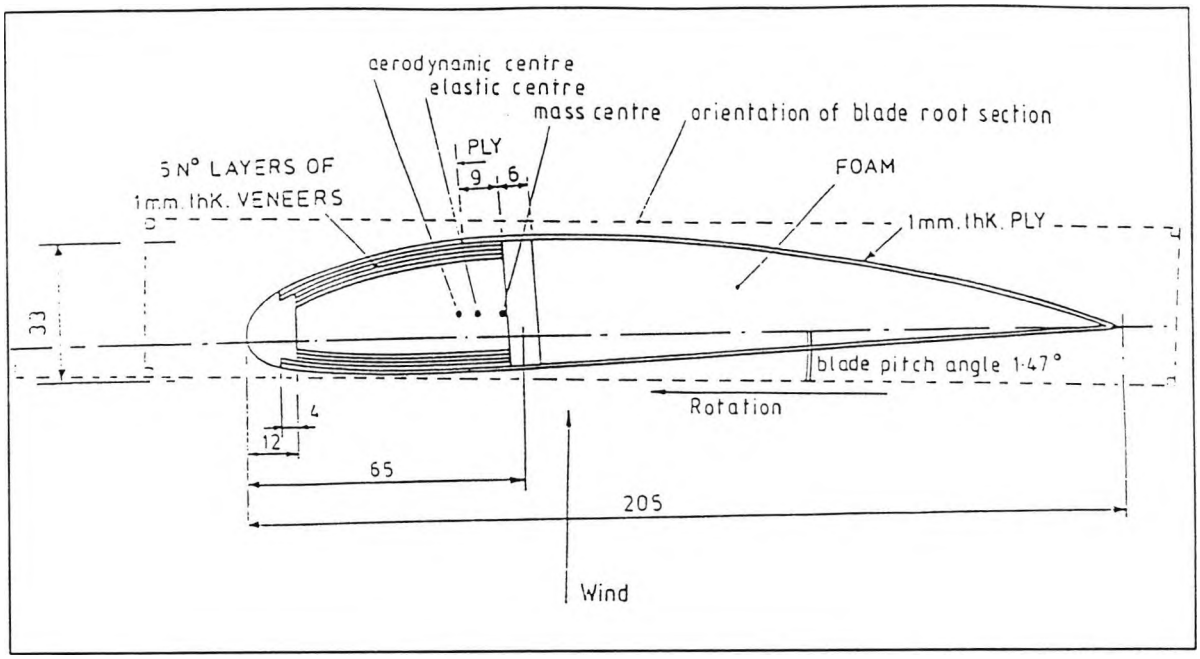

Fig 5.4 Cross section of a turbine blade,illustrating the method of construction from spars and wood veneers.Dimensions in mm for section of the blade root.The aerofoil section is N.A.C.A.4415.

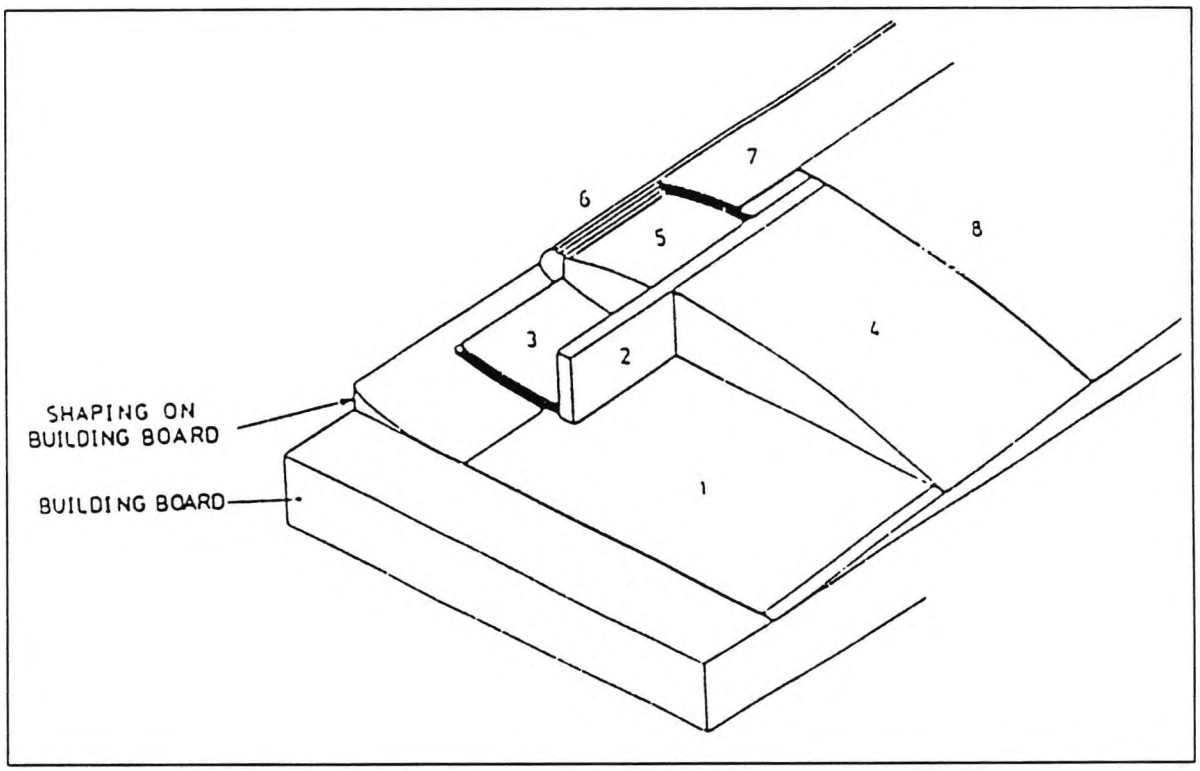

Fig 5.5 Order of construction.

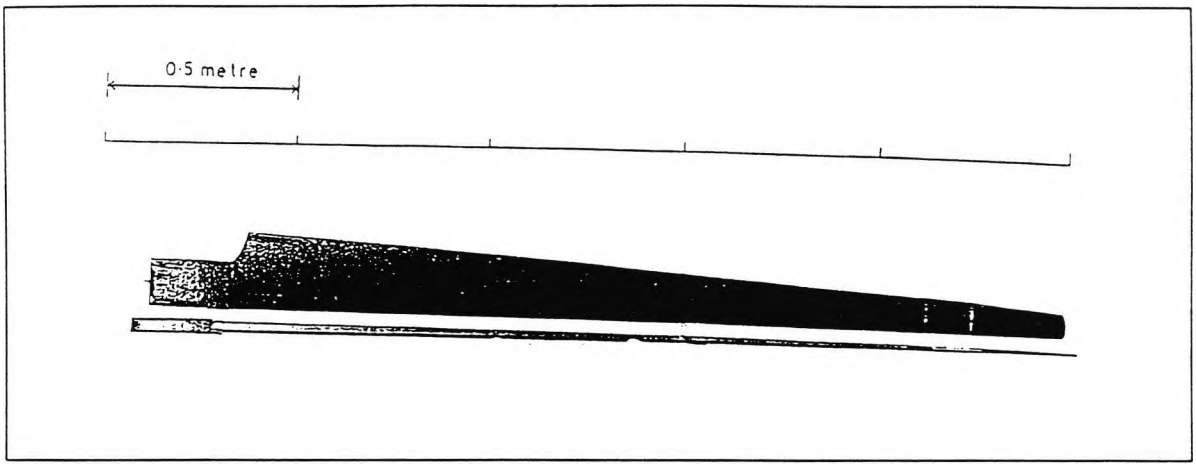

Fig 5.6 One of two blades of the turbine

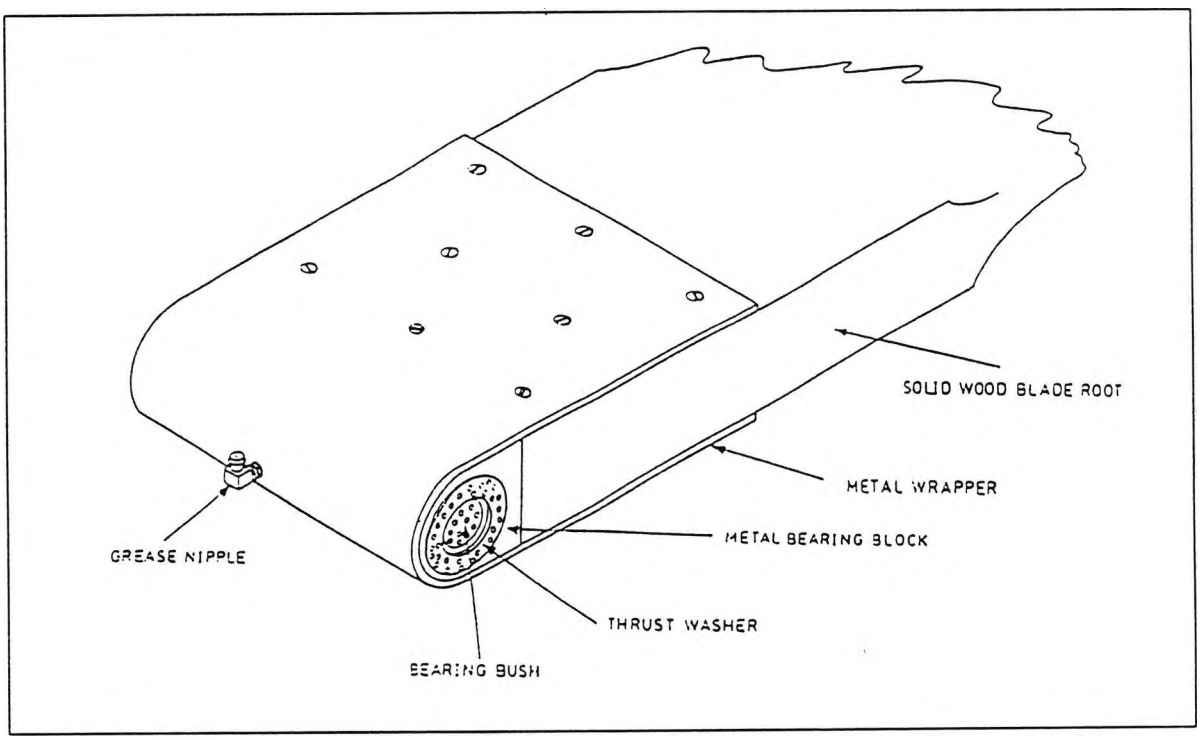

Fig 5.7 Construction of the blade root, showing the metal outer wrapper and the hinge bearing and thrust bearing bushes.

noise level.

3) Condenser microphone (B&K Type 4133) for outdoor measurement.

4) Sound level calibrator for calibration of sound level meter(B&K type 4230).

5) Dual channel signal analyser(B&K type 2032)

6) Graphic recorder(B&K Type 2313)

7) Shielded cable for the noise signal RG59 B/U.

8) To ensure the best transmutability BNC connectors were used.

5.4.2 Wind speed and direction measurement

Wind speed and direction can be found using four cup rotor anemometers, at the positions shown in Fig 5.2 in this Chapter. These give analogue output signals, after electronic frequency to voltage conversion.

5.4.3 Electrical power measurement

Delivered electrical power is measured as the mean of the instantaneous product of load current and voltage, using integrated circuit analogue multipliers.

5.4.4 Starting,stopping,loading,and control

All the electric and electronic systems for starting, braking and control of the turbine are located in the instrument cabin. The main load for dissipating the turbine power is a bank of standard electric fire elements contained in heat resistant boxes in the instrumentation cabin.

5.4.5 Cabling

A considerable quantity of cable was necessary in laying out the field site. In addition to the heavy duty four-core power cables a considerable number of light current cable cores were necessary for connections to all sensors and starting and braking systems described before.

All cabling was suspended about 0.7 m above the ground from steel wires running between posts a few metres apart.

The noise signal cable was very carefully suspended the same way.

A photograph of the equipment used for measurement and recording at the hut for Cambridge test site is shown in Fig 5.8.

5.4.6 Microphone position, distance and height

It has been recommended by National Engineering Laboratory, in a report [55], and others [56], [57] that noise measurements should be made at ground level on a plywood board of at least 1.5 X 1.8 m in area and 16 mm minimum thickness. The microphone should be positioned 15 cm from the centre of the board in the opposite direction from the turbine (see Figs 5.9, 5.10, and 5.11).

5.5 Recommissioning work

The machine had not been in use for a considerable period of time and required recommissioning. Details of the wiring system of the machine and cables had to be investigated and

checked. Although re-connection of some wires had been done, the cable for the cups was not fully working because of damage caused by wild animals. This was completely re-connected and checked to enable better measurement of the wind speed to be obtained and to allow an acceptable average value to be determined.

On some occasions when gusts of wind occurred the machine would stop automatically and could not be re-started due to the brake locking, and in such cases the machine had to be lowered to unlock the brake. This fault was remedied. Two of the anemometers were not in working condition and these were repaired. In the hut, the connection of cables to the data logging computer was changed to accommodate a tape recorder and allow the sound level meter signal to be recorded, together with the wind speed signal and the rotational speed and power signals. The recordings enabled further analysis to take place away from the site.

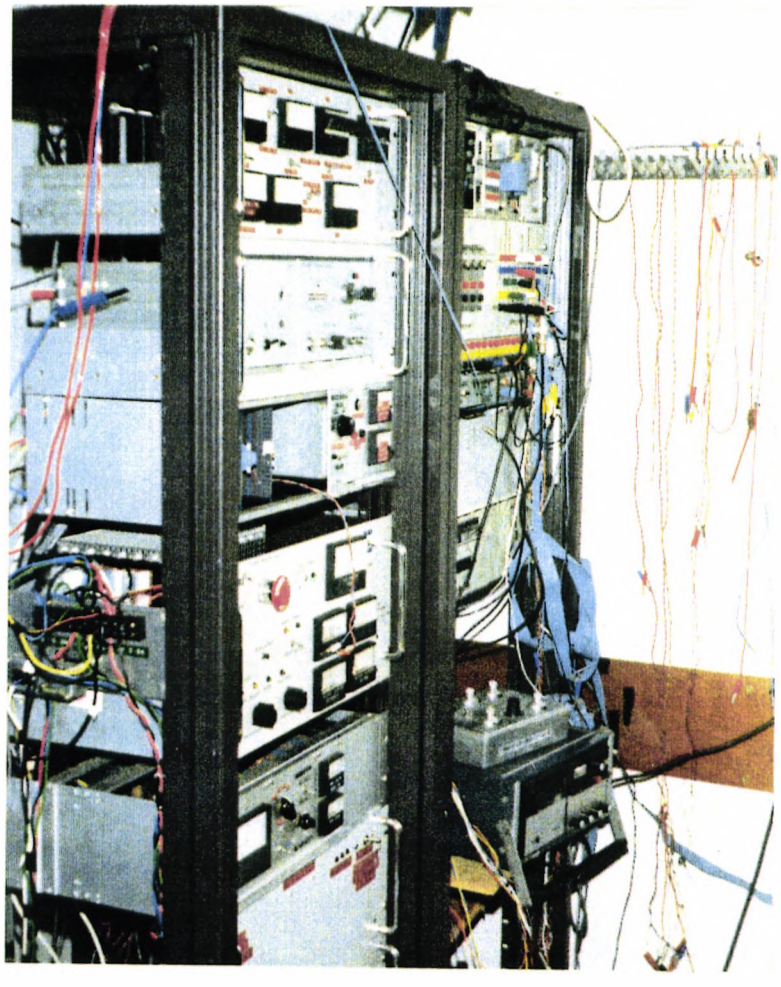

Fig 5.8 Photograph of the equipment used for measurement and recording at the hut for Cambridge test site.

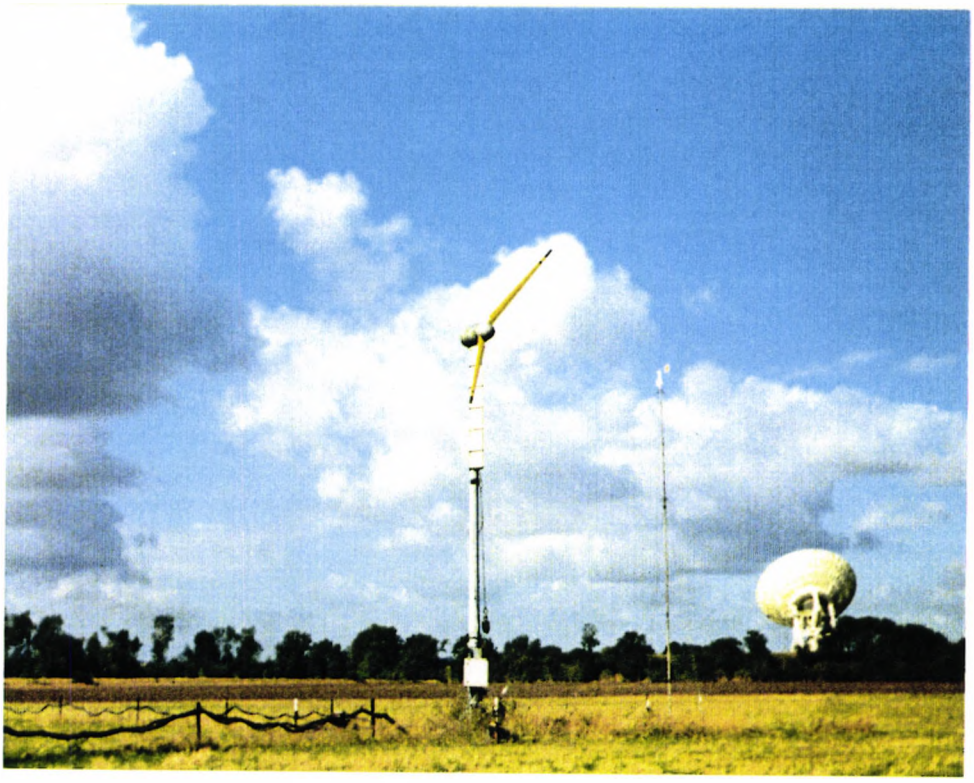

Fig 5.9 Photograph of the wind turbine machine in Cambridge

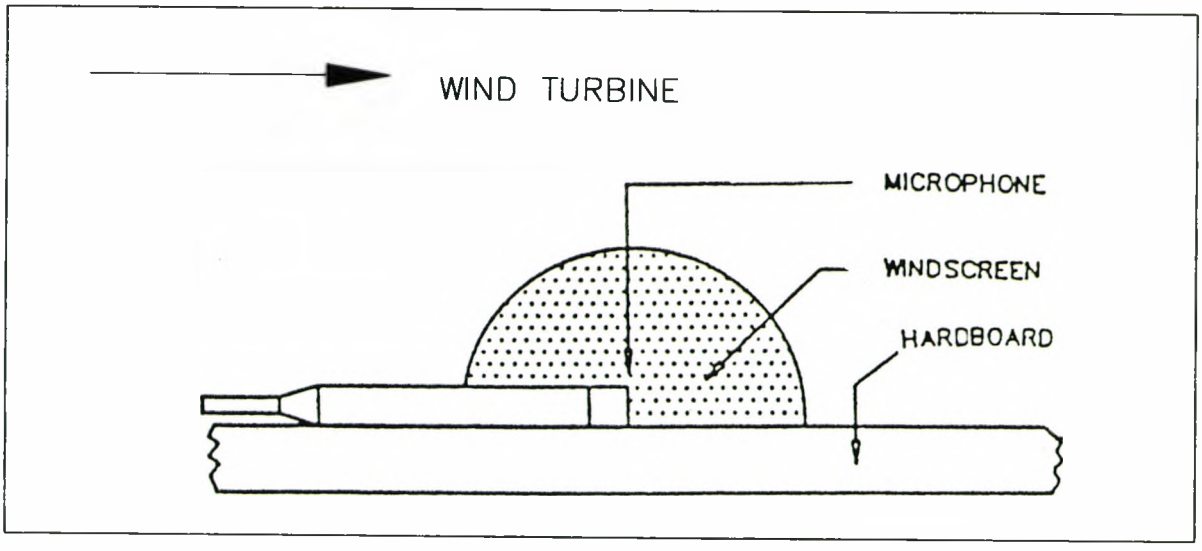

Fig 5.10 Microphone mounting arrangements

5.6 Wind turbine parameters

Table 5.1

Main wind turbine dimensions and parameters.

No of blades	2
Orientation	downwind,free yaw
Rotor blade mounting	freely hinged
Rotation sense	anti-clockwise
Hub height	9.5 m
Blade radius(zero cone angle)	2.5 m
Blade hinge offset	0.145 m
Nacelle diameter	0.46 m
Veer axis moment arm	0.31 m
Cone angle limit(approx.,at first contact with bump stop)	7 to 28 degrees
Alternator unit mass	180 kg
Cross frame base mass	>1 tonne
Max brake torque	165 Nm
Brake trip speed	425 rpm

5.7 Experimental measurement requirements

5.7.1 Effect of rotational speed on the noise level

The noise level was measured at rotational speeds of 100, 150, 200, 300 rpm, using the noise measurement equipment for a number of different wind speeds at the positions around the machine shown in Fig 5.11.

5.8 Calibration of the measuring equipment

Calibration of the sound level meter using a standard pistonphone was done. The sound level meter was also calibrated.

5.9 Results and Analysis

All records were analysed using a B&K 2032 Analyser from which narrow band, broad-band, 1/3 octave, 1/1 octave and line spectra were obtained. Fig 5.12 shows a Photograph of the dual channel signal analyzer(B&K type 2032) used for analysis of the noise signal in the laboratory. A detailed investigation of the signals with time has been studied and is described in Chapter 6 .

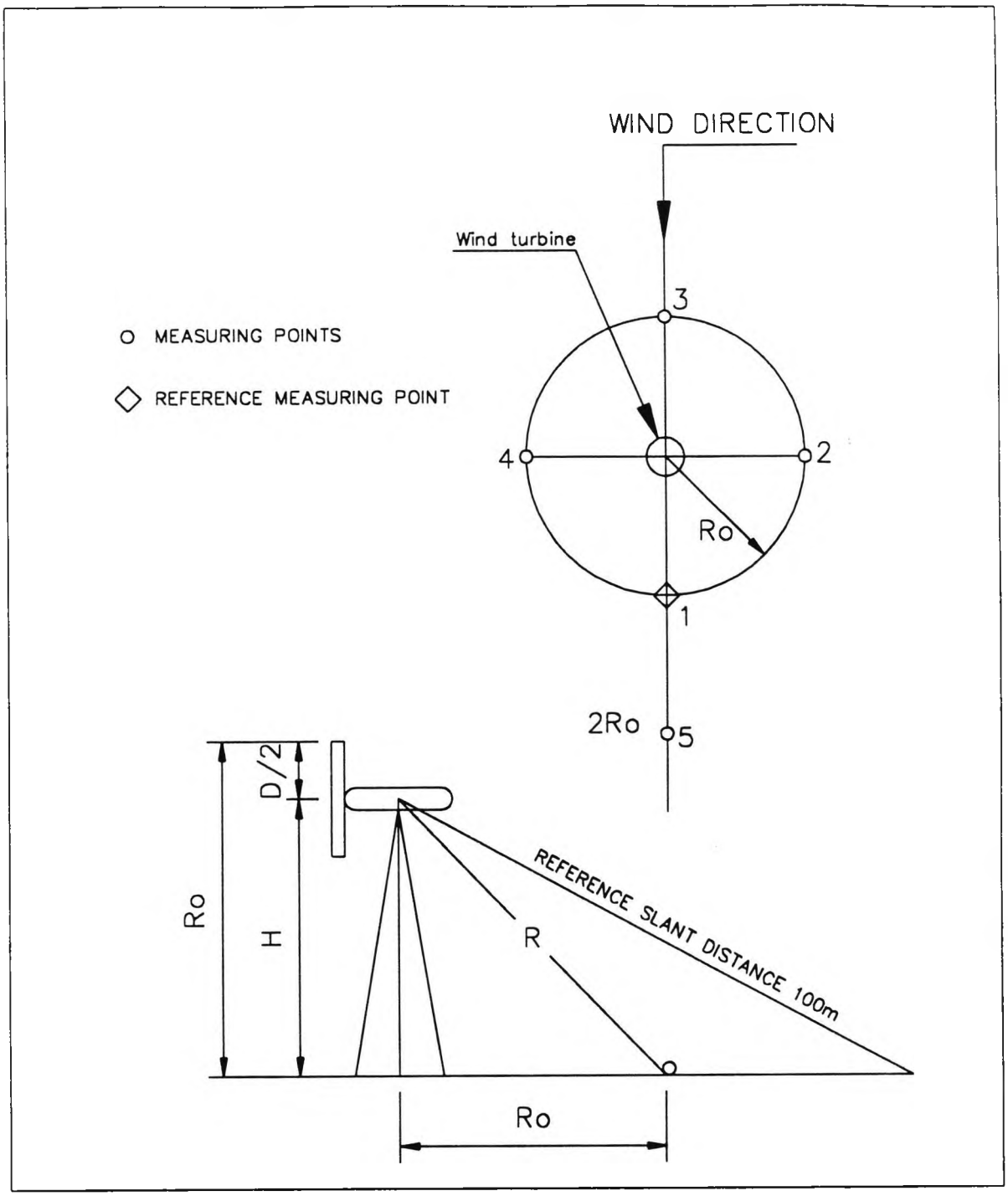

2Ro=(H+D/2)=2x(9.5+2.5)=24 m

Fig 5.11 Recommended five measurement points

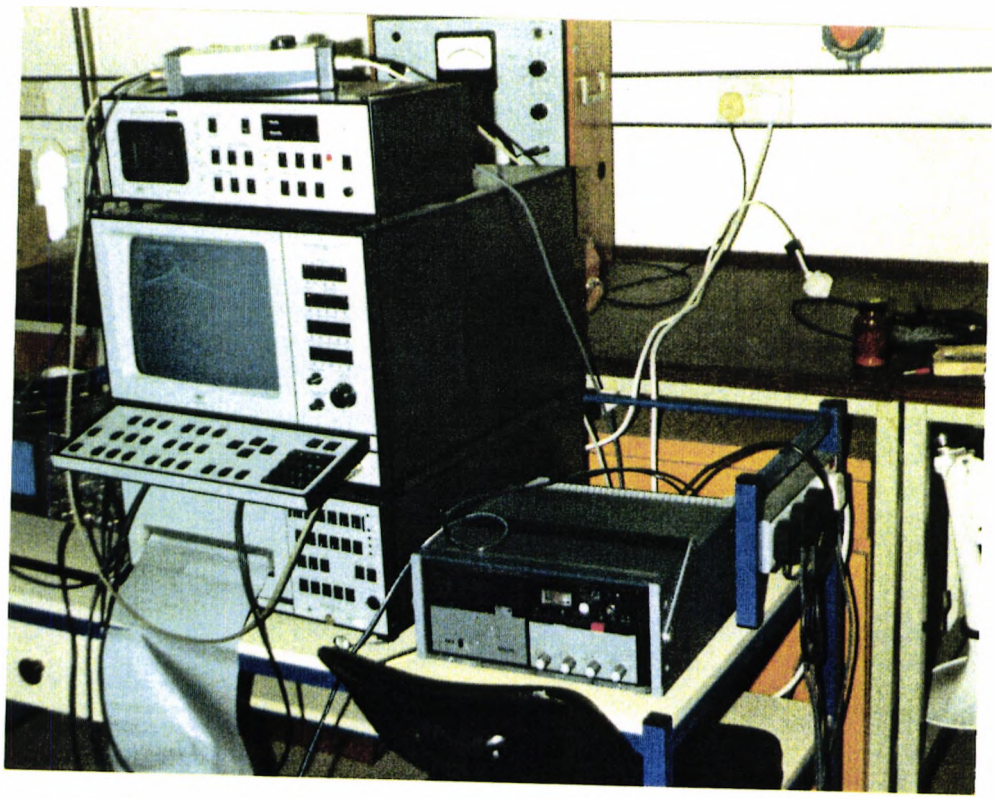

Fig 5.12 Photograph of the dual channel signal analyzer(B&K type 2032) used for analysis of the noise signal in the laboratory.

CHAPTER

6

RESULTS AND DISCUSSION

6.1 Introduction

In this Chapter the results are summarised of the measurements made on the Cambridge machine, at different positions around it, at a variety of wind speeds and rotational speeds. These show from the measurements carried out that the noise level from the machine is similar to that predicted by the mathematical model, especially that part of aerodynamic origin. Figs 6.1(a) and 6.1(b) provide a comparison between measured and predicted noise levels downstream of the machine at 100 rpm and 200 rpm, and it can be seen that there is acceptable agreement. The measurement positions are shown in Fig 6.2, and further details are provided in this Chapter.

6.2 Subjective impression of wind turbine noise

The characteristic noise emitted by the machine was different for each test. At high rotational speeds the noise emitted seemed to be much more impulsive and sounded similar to the noise of a helicopter main rotor, but at low speeds it was better described as a swishing noise.

It was also easy to recognise the mechanical noise, especially that caused by rubbing between the nacelle and the tower when the wind, and consequently the nacelle, changed its direction.

6.3 Quality of recorded data

The aim of the measurement exercises was to verify the computer program described in Chapter 4, but there were four factors which affected the perfect execution of this.

1-Noise produced by wind on the microphone itself.

2-The tape recorder frequency range which was limited to 5 kHz.

3-Other background noises.

4-Low frequency limitation of the sound level meter for signals measured below 10 Hz.

It was possible to take these factors into account and limit their effects as will be explained later in this Chapter.

6.4 The preliminary results

Preliminary results of the wind turbine noise measurements showed that the overall noise level was 56 dB(A) at a wind speed of 7 m/sec and rotational speed of 200 rpm at reference point [5] (see Fig 6.3), and at reference points [1], [2], [3] and [4] for the same condition the noise levels were 62, 58, 57 and 56 dB(A). The machine at the above condition was operating on its power curve.

By analysing the noise signal using the B&K 2032 dual channel FFT analyser, significant mechanical noise from the machine at high frequencies was identified.

The measurement data show that the impulsive character of

the noise is composed of harmonics of the blade passing frequency. While some of these harmonics exist below the audible frequency range(about 20 to 20,000 Hz) many are above the nominal audible threshold of 20 Hz. Loading noise components due to tower wake-blade interaction are a characteristic of downwind machines which may be perceived as a thumping noise. The wake velocity deficit downwind of a tower leg causes a sharp and sudden fluctuating lift on a rotor blade which is radiated as impulsive noise and contributes to the overall noise level.

Noise components of both aerodynamic and mechanical origin have been identified, but although the aerodynamic noise was judged to be dominant, it was quite easy to recognize mechanical noise due to the rubbing caused by yawing movement of the nacelle yawing following a wind direction change.

6.5 Effect of the background noise on wind turbine

Fig 6.4(a) shows a typical noise signal from the wind turbine and from the wind by itself, and Fig 6.4(b) shows the related 1/3 octave band spectra. By comparing the two figures it can be seen that the wind turbine noise level is above the background noise for all frequencies, and that the spectra achieves high level of about 166 Hz representing the swishing sound generated by the blade at a rotational speed of 200 rpm.

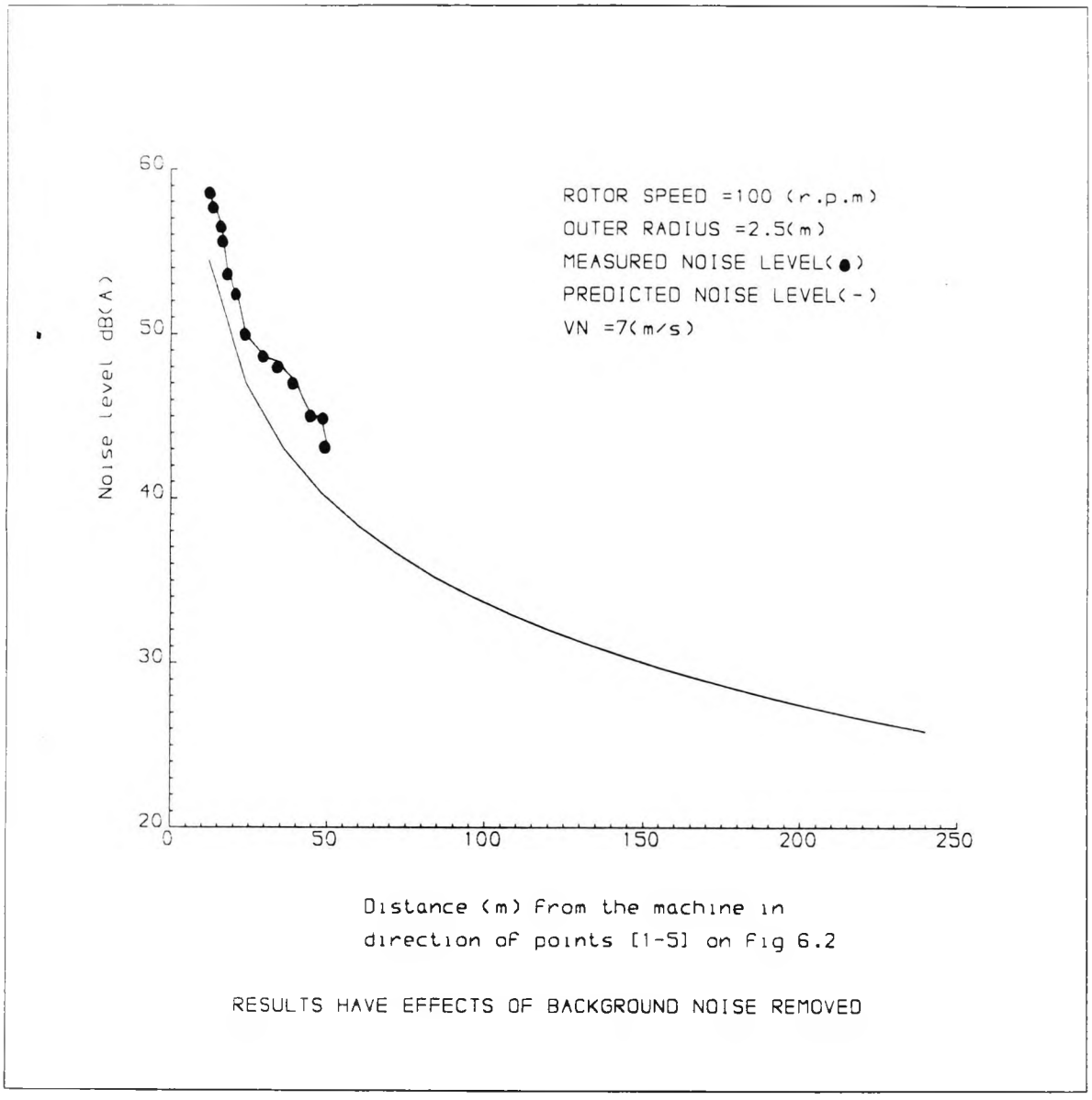

Fig 6.1 (a) Comparison between measured and predicted noise level emitted downstream from Cambridge test site machine. The output power ≅ .45 kW.

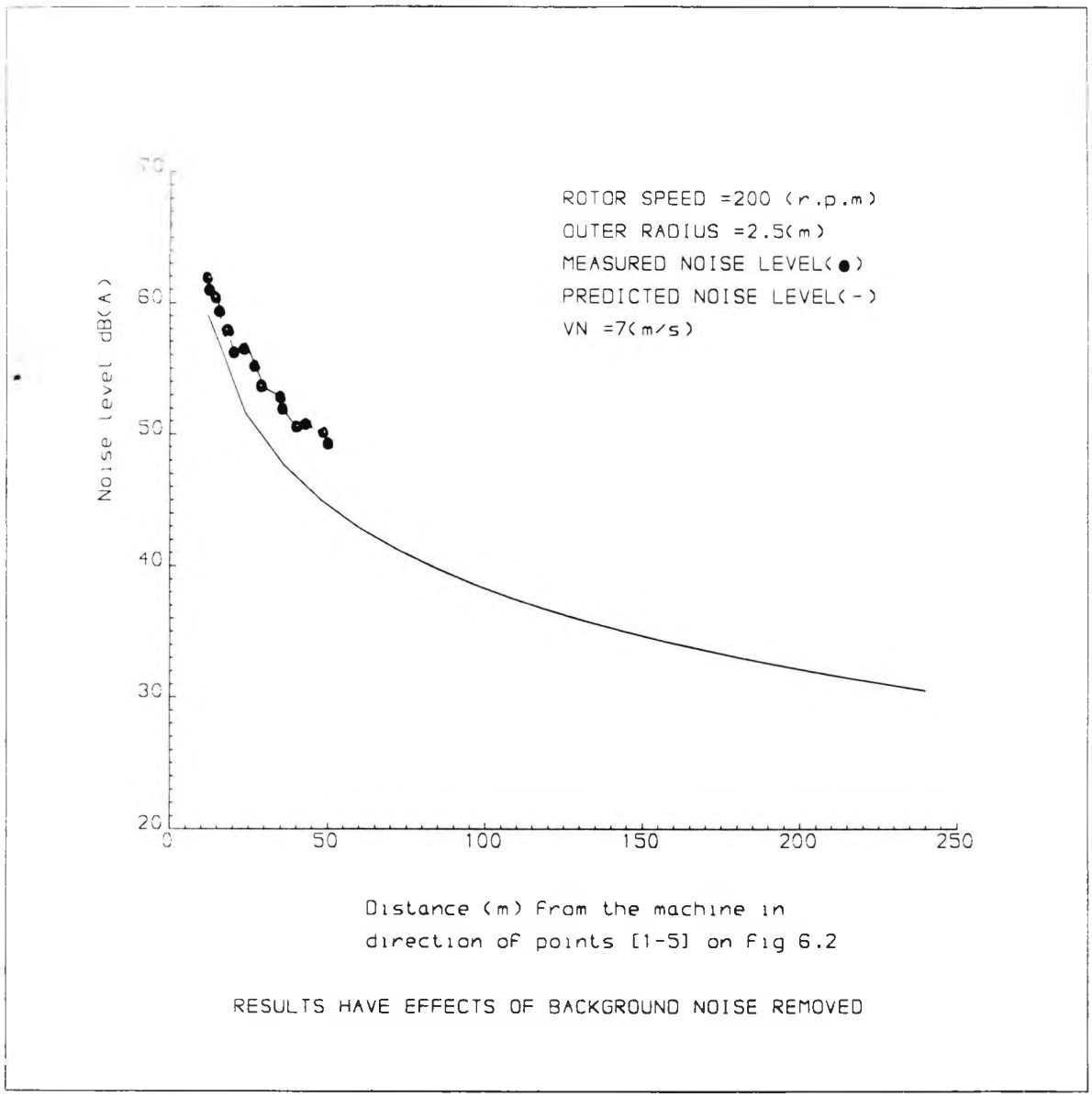

Fig 6.1 (b) Comparison between measured and predicted noise level emitted downstream from Cambridge test site machine. The output power ≅ .8 kW, machine on its power curve.

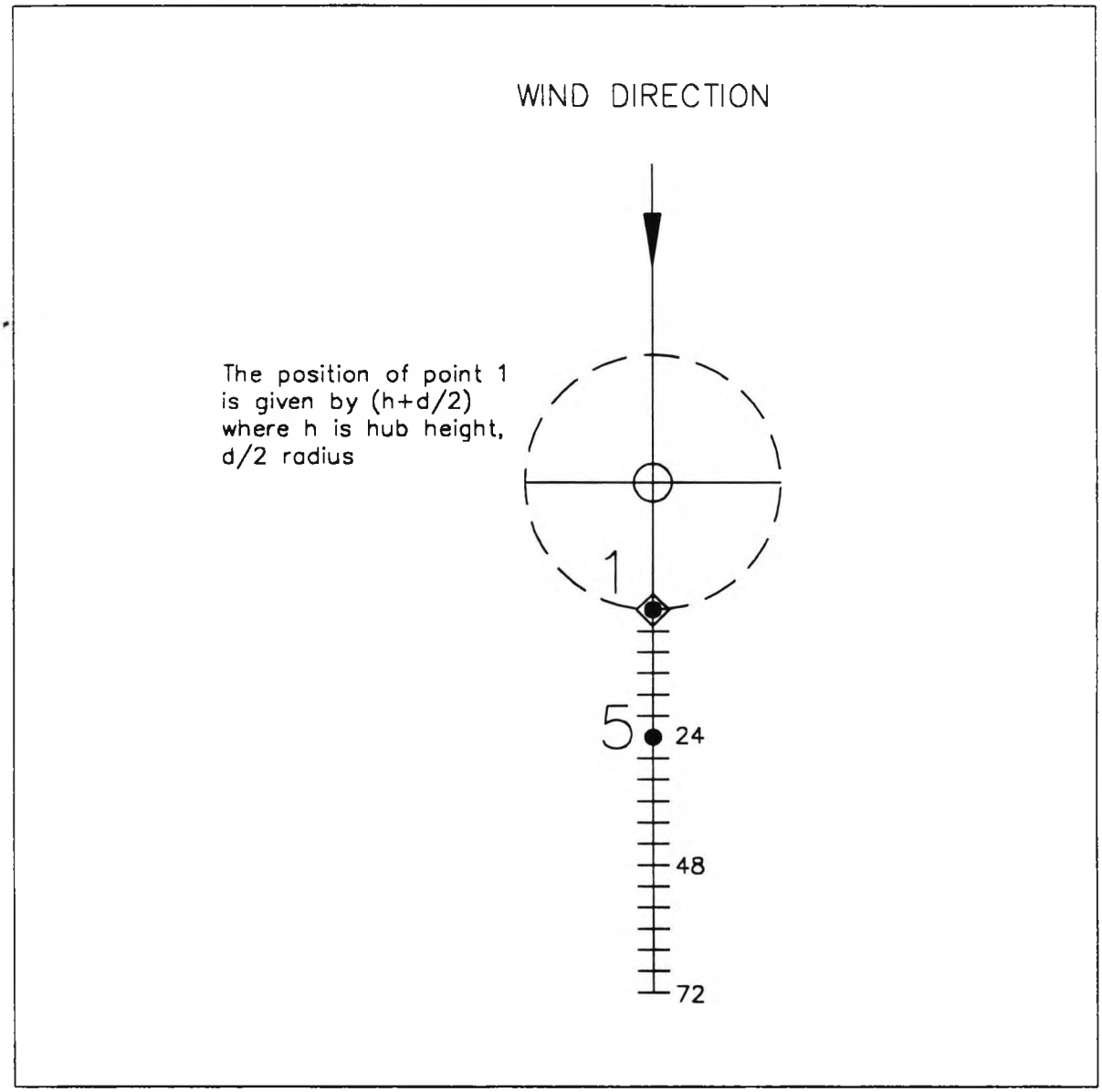

—— points of measurements used for Figs 6.1(a) and (b).

Fig 6.2 Position of measurement and direction (dimensions in (m)).

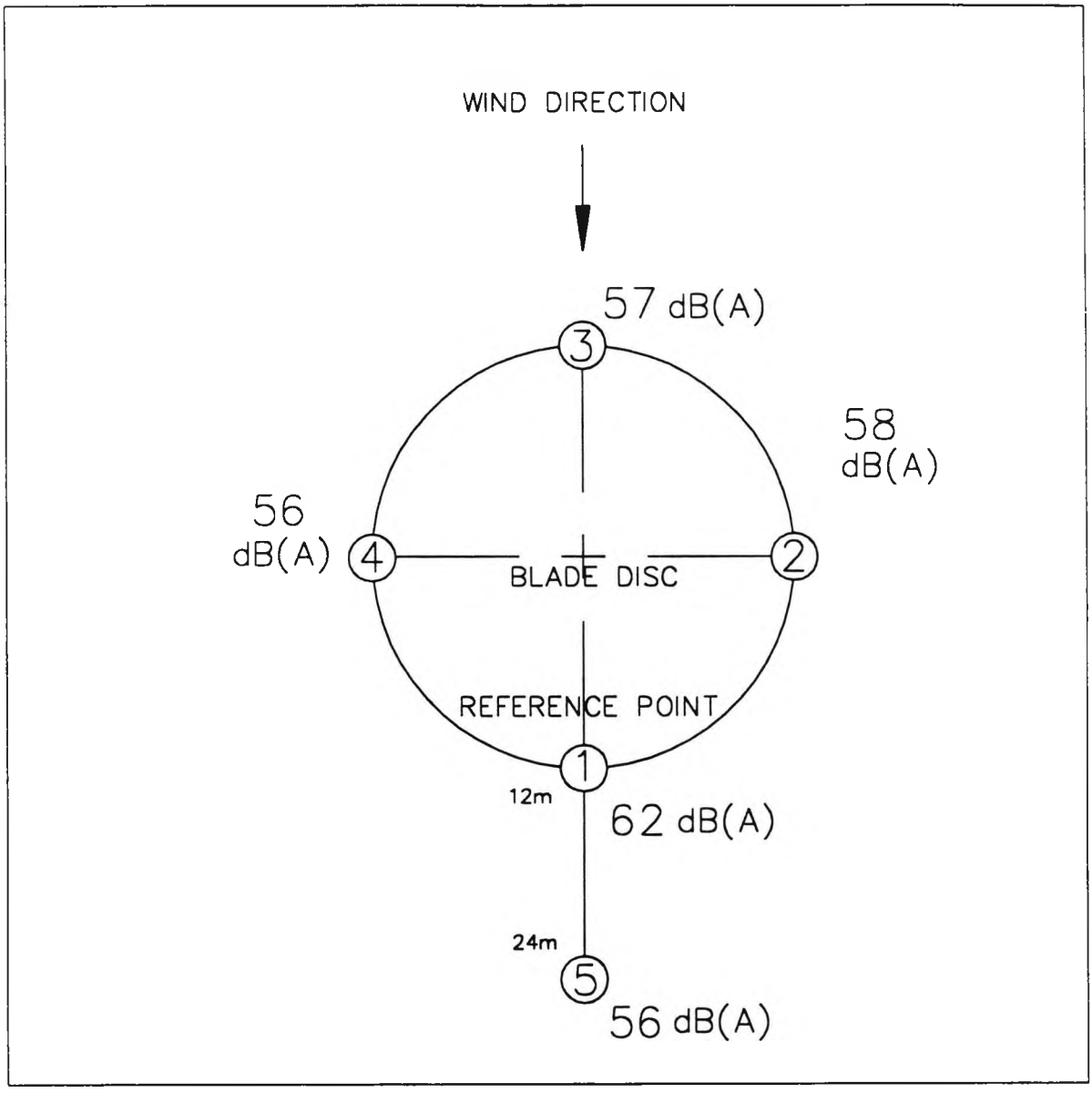

Fig 6.3 Noise levels measured at reference points [1]-[5] at the Cambridge test site. Ambient noise level =45 dB(A), wind speed of 7 m/sec and rotational speed=200 rpm.

Noise levels due to wind blowing over the microphone are highest at higher frequencies and decrease rapidly as the frequency decreases. Frequencies of lower than about 50 Hz do not appear on the spectra due to analyser limitations.

As an objective of these measurements is to check the validity of the computer programme, it was considered appropriate to rely on standard techniques for measurements in line with the view of Hubbard, Ferdinand, and Kevin [18]. Other background sources arising from windy conditions were produced from trees, electricity and signals cables, plus additional background noise produced by road vehicles on the Cambridge road and by aircraft. It was possible to avoid intermittent background sources by excluding the measurements when they occurred. The overall background noise level varied during measurement days from around 41 dB(A)) to 45 dB(A), excluding aircraft noise.

Figs 6.4(a) and 6.4(b) show that the noise level at reference point [1] is noticeably higher when the turbine is operating than the noise level of the wind by itself, when the turbine is not operating. As the distance of the measurement point increases away from the wind turbine the noise level decreases, due to spherical spreading, atmospheric absorption, and attenuation of the ground surface. However, because the noise of the wind is random whilst the wind turbine noise is periodic and therefore different in character, discrimination is possible in the latter

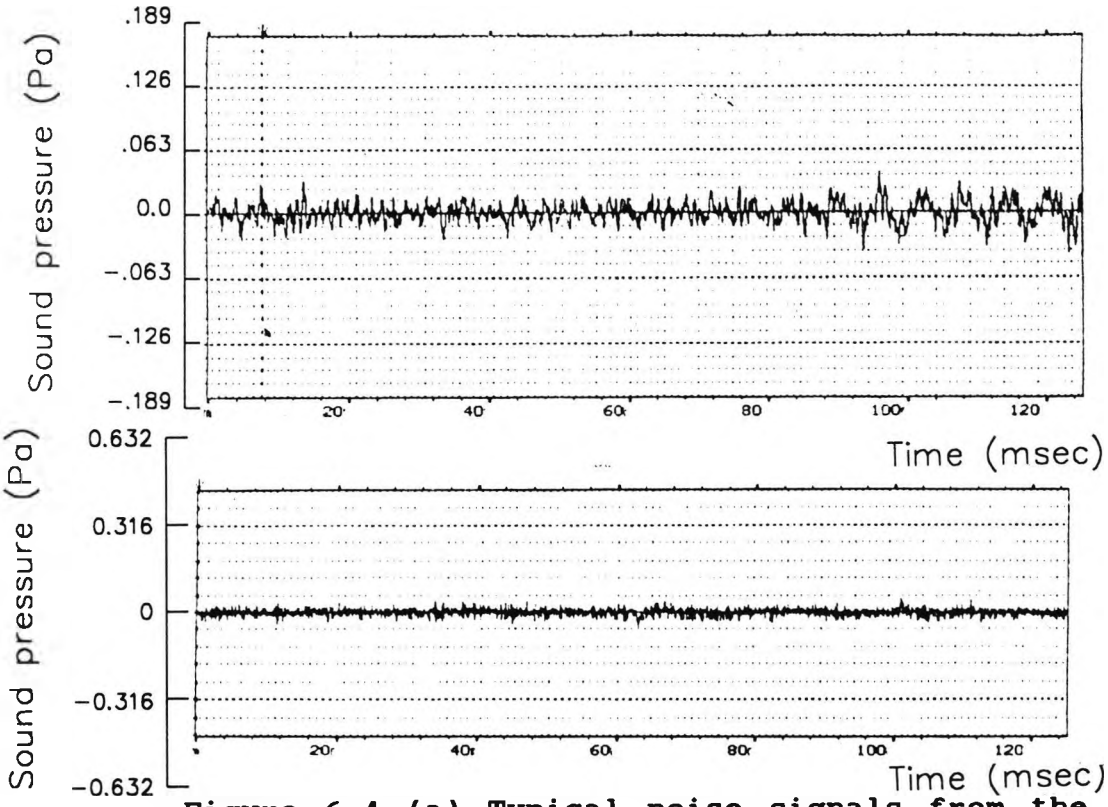

Figure 6.4 (a) Typical noise signals from the wind turbine (upper graph) and from the wind by itself (lower graph).
Rotational speed =200 rpm, reference position [1] Average wind speed = 6.8 m/s

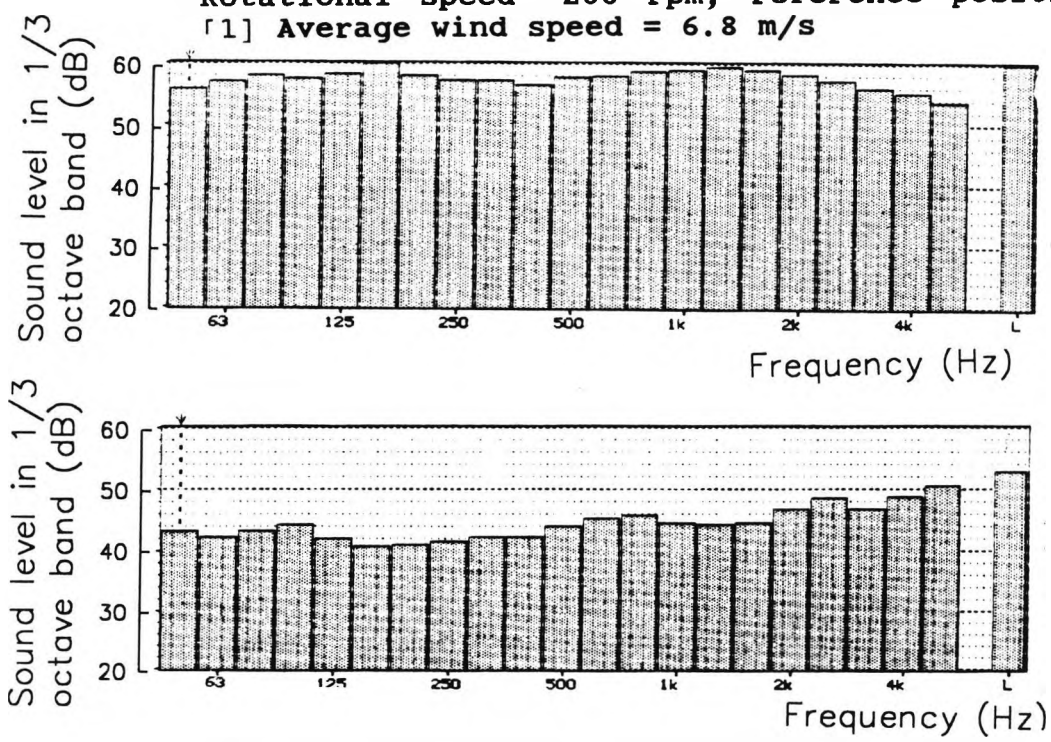

Fig 6.4 (b) Typical 1/3 oct band spectrum of the wind turbine noise (upper graph) and of the wind by itself (lower graph) for the conditions corresponding to Fig 6.4 (a)

situation.

6.6 Effect of the rotational speed of wind turbine

Fig 6.5 clearly shows that an increase in rotational speed results in an increase in the noise level perceived at a given position. This is in agreement with previous investigations [31], [58], [59], [60], [61] and confirms the conclusion that decreasing the rotational speed in the absence of other changes makes a significant decrease in noise level. However, the problem here is that by doing so the output power also decreases. Figs 6.1(a) and 6.1(b) show the relationship between predicted noise level and measured noise level for two different rotational speeds. The trend between measured and predicted noise level is similar, and the difference in magnitude is considered to be due to mechanical noise which will be discussed later in this Chapter in Section 6.13. The results shown in Figs 6.6 and 6.7 are for rotational speeds of 200 and 150 rpm, respectively, and refer to reference point [5], and a wind speed of 7 m/sec. In each case there is a peak at about 166 Hz, shown clearly on Figs 6.6 (d) . The effect is also seen in the 1/1 and 1/3 octave band spectra. This occurrence is independent of the rotation speed of the turbine, and is considered to be associated largely with the characteristic aerodynamic swishing sound heard.

Figs 6.6(a) and 6.7(a) show the signature of noise versus

time for rotational speeds of 200 and 150 rpm respectively. The diminution of the aerodynamic contribution (the periodic part causing the swishing noise) is clearly seen at the slower rotational speed. Fig (6.8) shows the evidence of periodicity at a rotational speed of about 200 rpm and there is a discernable peak at 5 Hz, the approximate blade passing frequency. Below this frequency range the measurement fails due to the equipment limitation.

It is self evident that rotational speed is a very important factor in determining the noise level emitted from a machine, as indicated in Fig 6.5.

6.7 Discrete frequency noise .

Figs 6.6(d) and 6.7(d) show that the discrete frequency noise appears as discernable peaks at harmonics of the blade passing frequency. Below 33 Hz (i.e.the fifth harmonic based on 200 rpm and two blades) the level falls due to the poor low frequency response of the sound level meter. The fact that there are harmonics in the spectra is probably due to the impulsive loading effect of the blade passing through the tower wake.

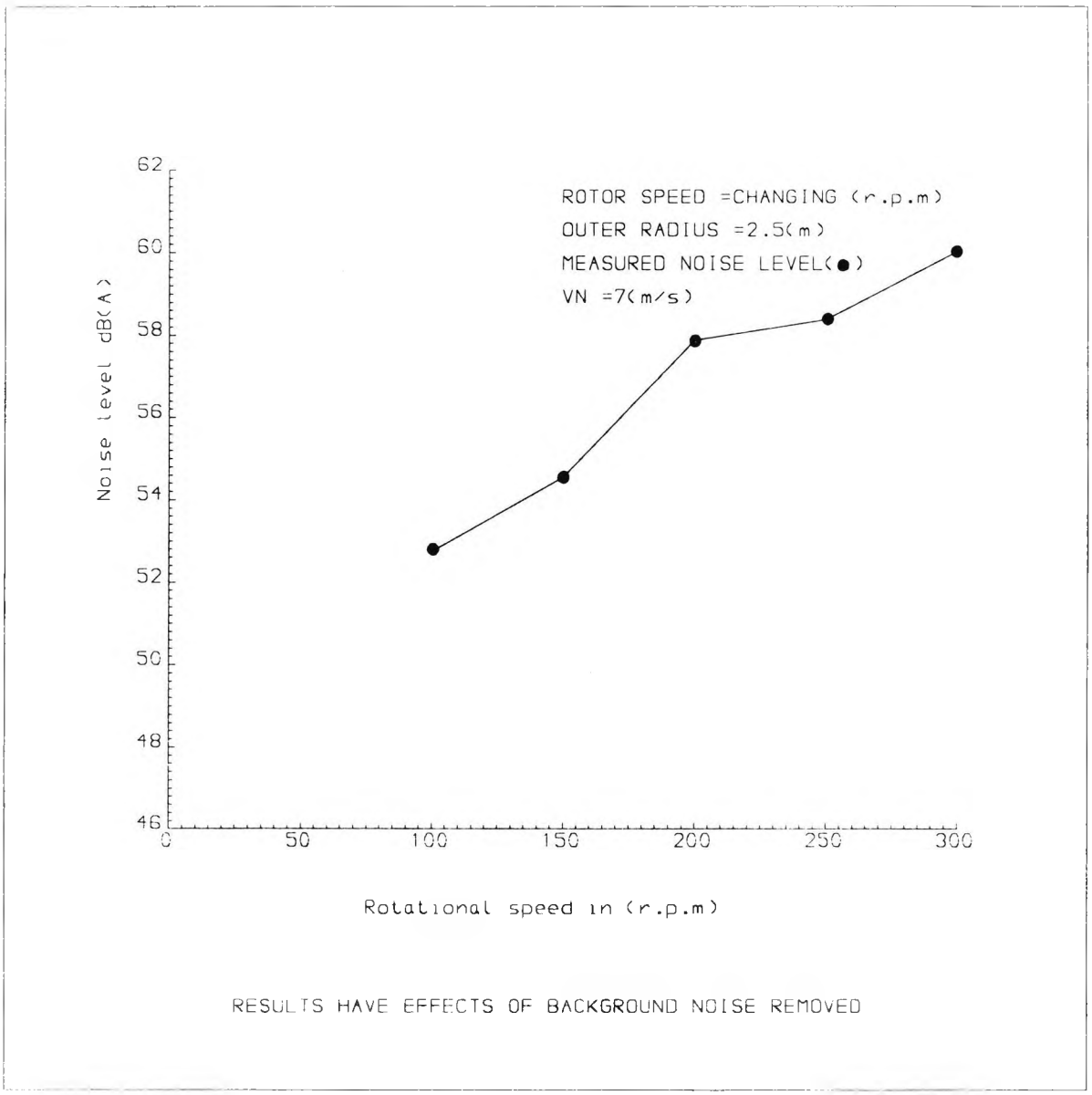

Fig 6.5 Effect of rotational speed on measured noise level at Cambridge test site reference position [5].

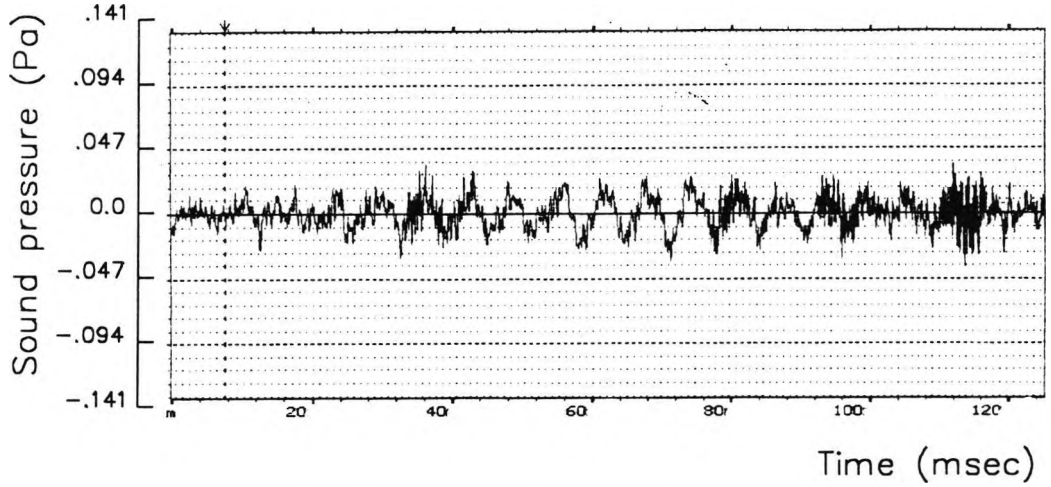

Fig 6.6 (a) Typical noise signal verses time at reference position [5], rotational speed= 200 rpm, average wind speed= 7 m/sec, average noise level directly measured =57 dB(A).

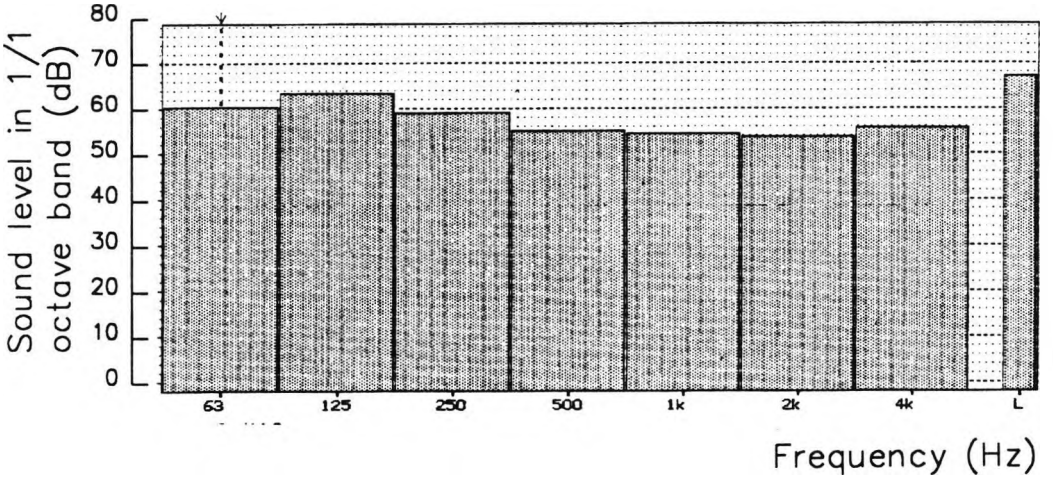

Fig 6.6 (b) Typical 1/1 octave band spectrum for the conditions corresponding to Fig 6.6 (a)

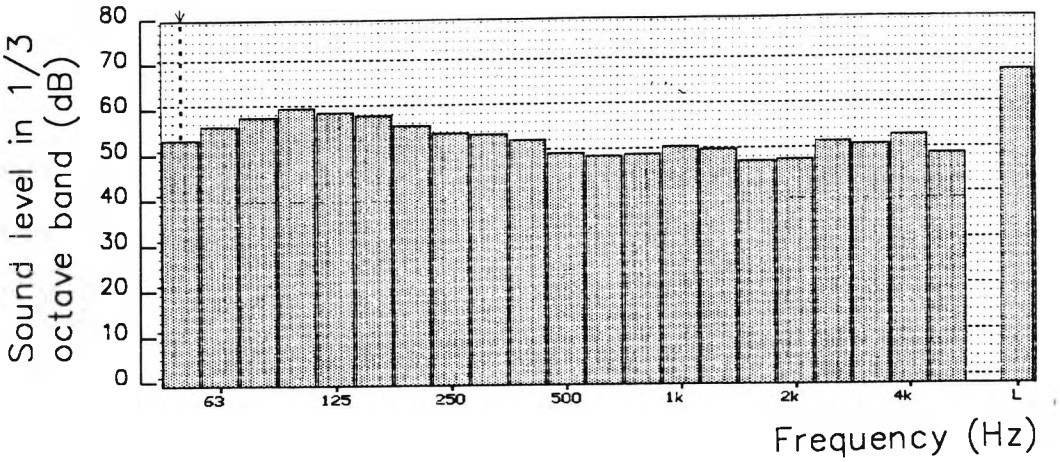

Fig 6.6 (c) Typical 1/3 octave band spectrum for the conditions corresponding to Fig 6.6 (a)

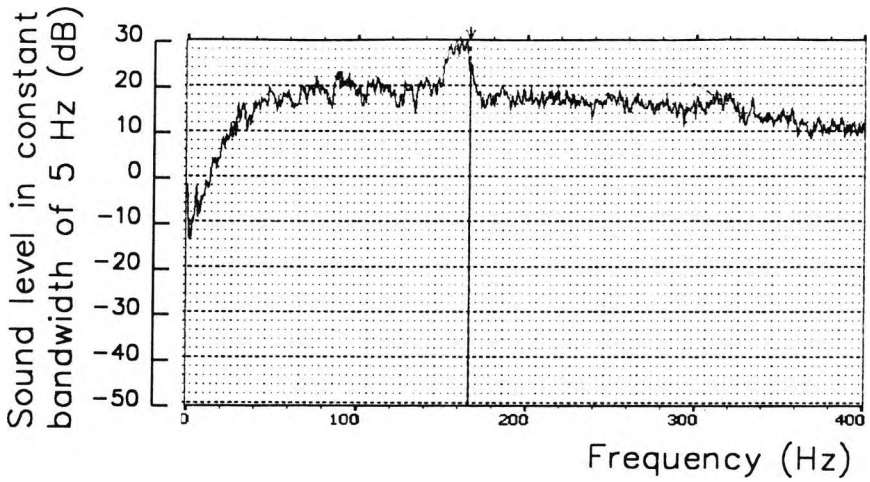

Fig 6.6 (d) Typical linear frequency spectrum for the conditions corresponding to Fig 6.6 (a)

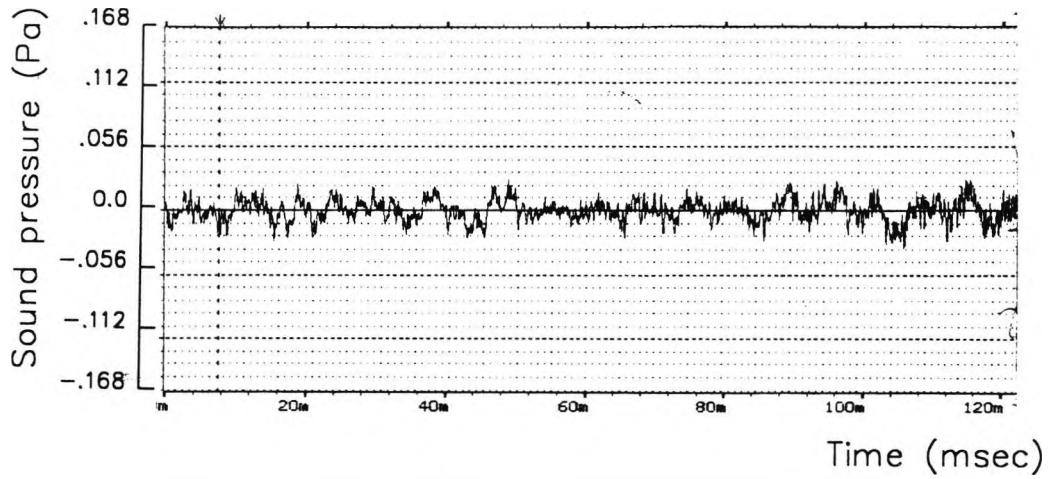

Fig 6.7 (a) Typical noise signal verses time at reference position [5], rotational speed= 150 rpm, average wind speed= 7 m/sec, average noise level directly measured =55 dB(A).

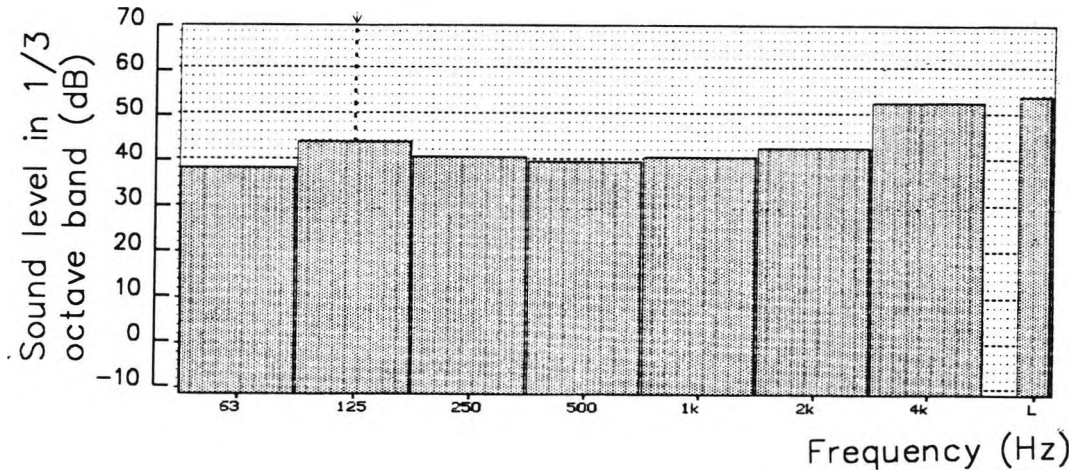

Fig 6.7 (b) Typical 1/1 octave band spectrum for the conditions corresponding to Fig 6.7 (A)

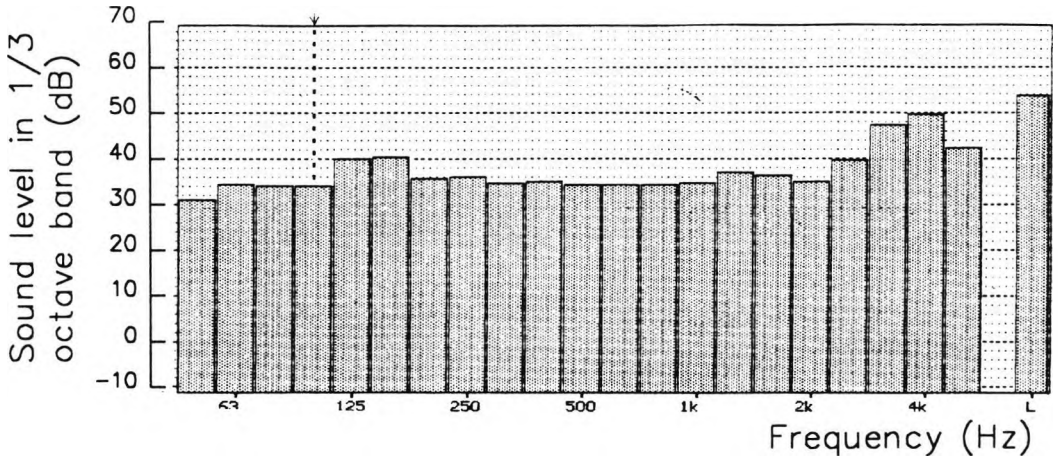

Fig 6.7 (c) Typical 1/3 octave band spectrum for the conditions corresponding to Fig 6.7 (a)

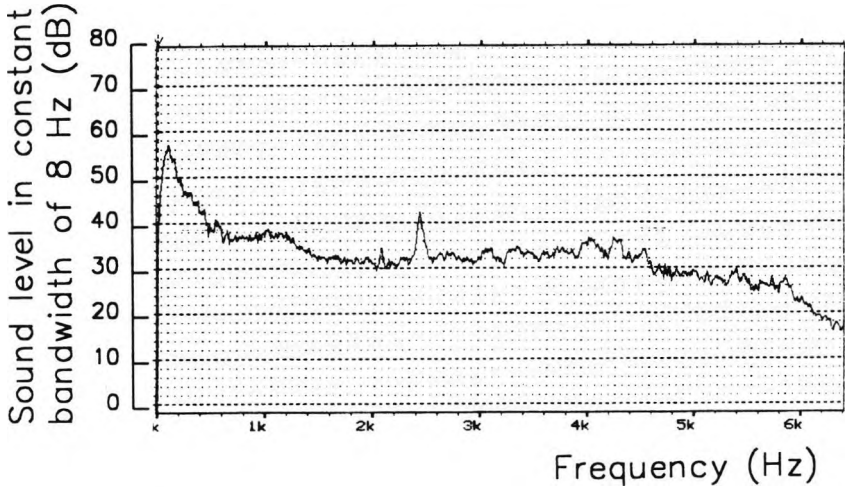

Fig 6.7 (d) Typical linear frequency spectrum for the conditions corresponding to Fig 6.7 (a)

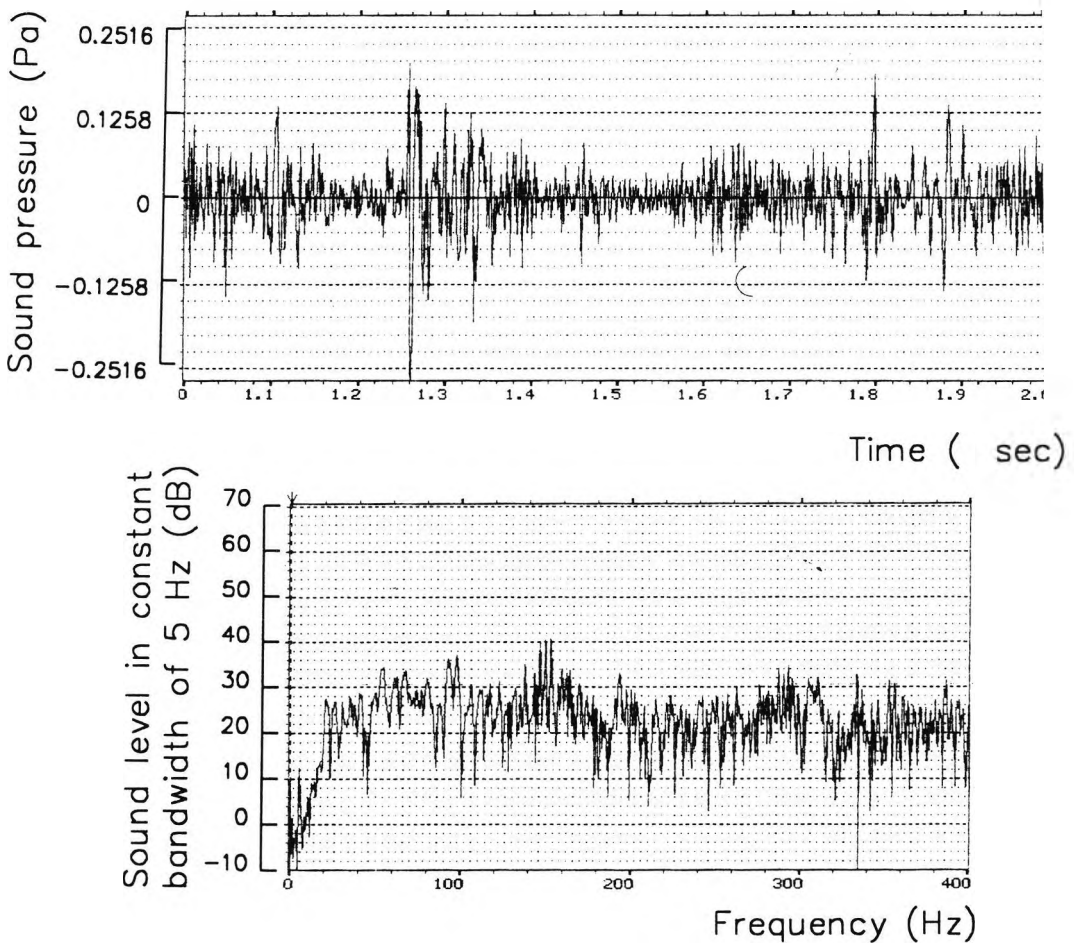

Fig 6.8(a) Typical noise signal and narrow band spectrum at reference position [1], rotational speed= 200 rpm, average wind speed= 7 m/sec, average noise level directly measured =62 dB(A).

6.8 Directivity of broad band noise

The basic shape of the spectra is dominated by broad band noise, and it can be seen from Fig 6.3 that the averaged level varies by up to 6 dB(A) around the site.

Figs 6.6 provide results for noise measurement of the machine at position [5] for a rotation speed of 200 rpm.

The most dominant part of the wind turbine noise spectra is a broad band peak centred around 2.5kHz as seen in Fig 6.9(d). From Fig 6.3 it is seen that the noise level is highest along the rotation axis of the machine, which indicates that the dominant blade source is radiating perpendicular to the blade surface. Theoretically, the wind turbine is a dipole source ; the downstream noise level is higher than in any other direction. (The directional nature of the wind turbine noise is clearly shown in the theoretical directivity pattern demonstrated in Chapter 7).

6.9 Effect of observer height

It is clear from equation (4.15) that increasing the observer height up to the level of the rotation axis will increase the noise level, due to change in the term M_r and the small reduction in the distance of the observer from the source. By applying the WTGNOISE for two different observer heights, an increase of about 2 dB(A) for a 2 m increase of height is obtained.

6.10 Effect of source height

Increasing the wind turbine height increases noise level downwind and at ground level (by about 2 dB for a 40 m to 120 m height change), as explained earlier in Chapter 2, Section 2.4.5. (see Fig 2.9.). Again, the fluctuations are expected to reduce with increasing frequency due to absorption by the atmosphere. In addition, as the height of the wind turbine increases there will be a slight decrease of the sound level at high frequency because of atmospheric absorption.

6.11 Mechanical noise

Whilst measurements were taken, mechanical noise was audible at all measurement positions and at different wind speeds. This was due mainly to the rubbing between the nacelle and the tower during relative movement.

Furthermore there was also mechanical noise resulting from binding of the friction brake in the nacelle. This noise varied significantly, even when the wind direction stayed constant for a period of time. There was also noise from small vee-belts and other parts of the transmission, but it was difficult to identify this noise on the spectra.

It should be noted that the machine was relatively old, and that a more modern machine would tend to be quieter from the mechanical point of view.

6.12 Wind induced noise

In a normal wind turbine generator operation environment the background noise level may be dominated by wind induced noise resulting from the wind buffeting the microphone diaphragm. Using a windshield at ground level makes the wind contribution insignificant.

6.13 Comparison of measured and predicted noise level

By applying the computer code WTGNOISE to predict the level of noise emitted from the Cambridge machine downwind, and comparing the predicted and measured noise levels in Figs 6.1(a) and 6.1(b) it may be seen that there is a difference between the two cases. Fig 6.1(a) indicates a difference of about 3-5 dB (A) between two noise levels at 100 rpm, which is highlighted in Fig 6.10. Likewise the difference in the case of Fig 6.1(b) is approximately 3 dB(A) at 200 rpm, as shown in Fig 6.11. It is considered that the difference in each case is due to mechanical noise which is more dominant at 100 rpm compared with 200 rpm, since the aerodynamic noise is less at the lower rotor speeds. At 200 rpm, the difference of 3 dB(A) implies that the aerodynamic and mechanical contributions to the overall noise at the measurement point are approximately equal. It is concluded therefore that the program WTGNOISE is reasonably reliable for predicting the aerodynamic part of the noise level, and can be used at the design stage of a wind turbines.

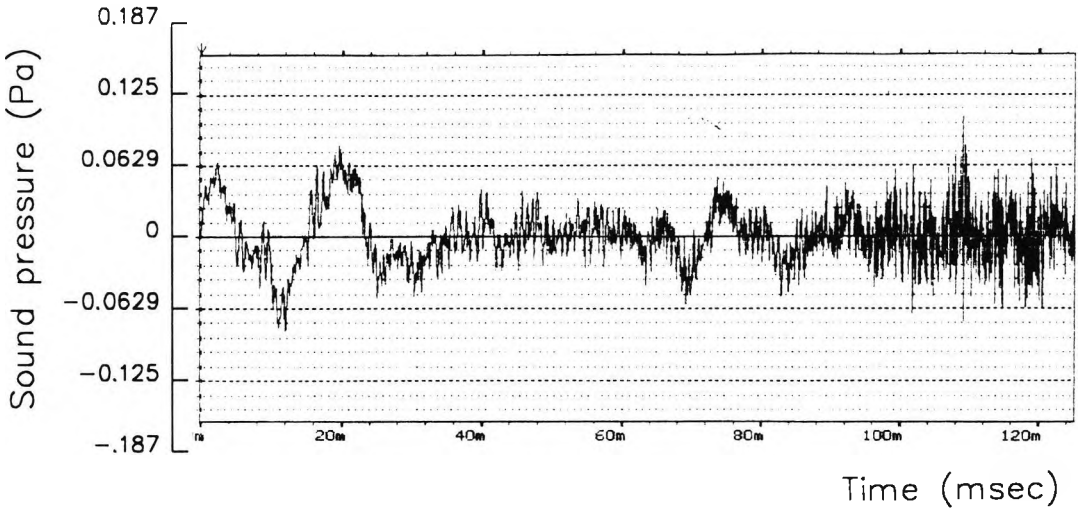

Fig 6.9 (a) Typical noise signal verses time at reference position [1], rotational speed= 200 rpm, average wind speed= 6.7 m/sec, average noise level directly measured =62 dB(A).

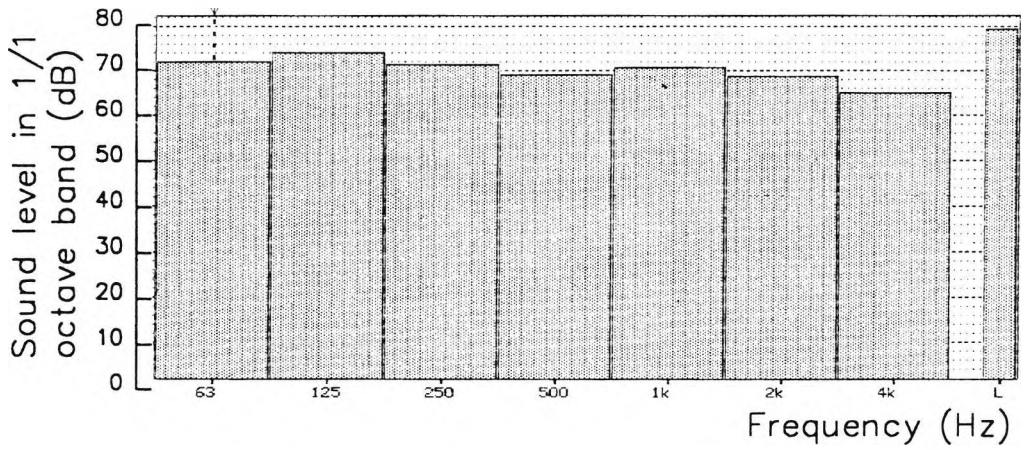

Fig 6.9 (b) Typical 1/1 octave band spectrum for the conditions corresponding to Fig 6.8 (a)

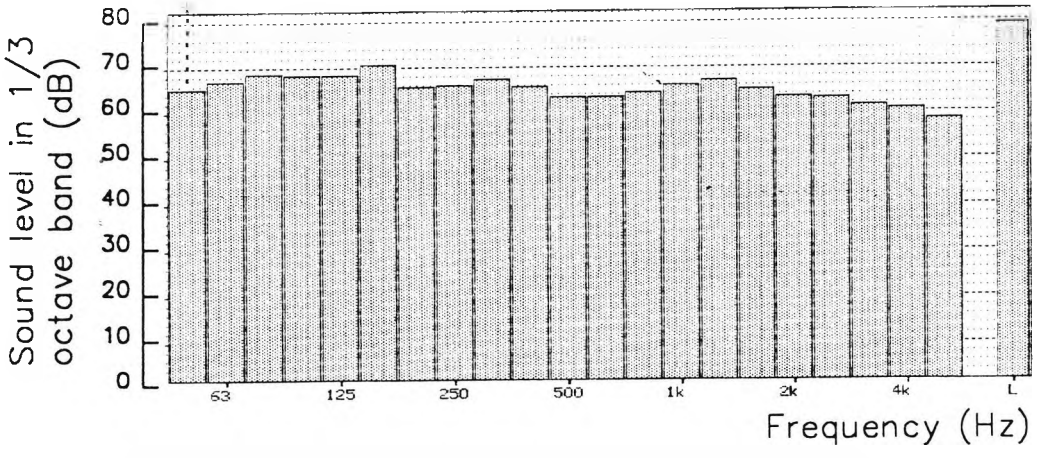

Fig 6.9 (c) Typical 1/3 octave band spectrum for the conditions corresponding to Fig 6.9 (a)

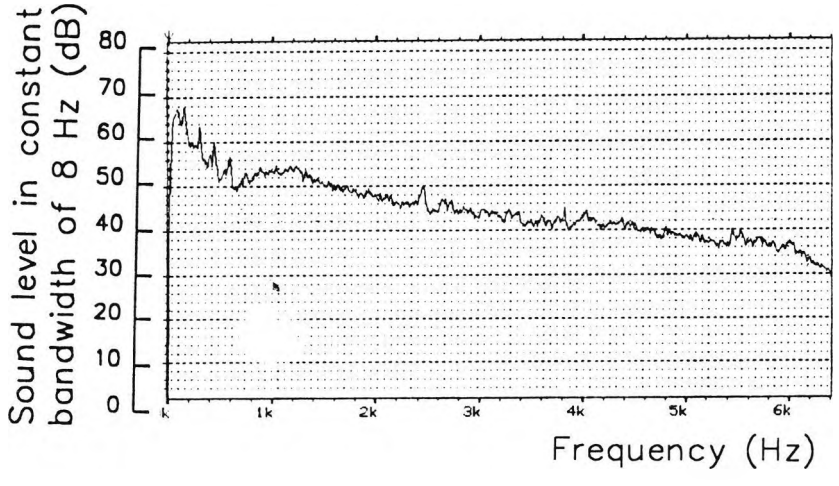

Fig 6.9 (d) Typical linear frequency spectrum for the conditions corresponding to Fig 6.9 (a)

The published results of measurements taken over past years of the acoustic emission from wind turbines has shown that the maximum acoustic energy is concentrated in the low frequency range, often below 100 Hz.

The frequency characteristics of turbine noise have been shown to be important since the wind turbine is capable of radiating both coherent and incoherent noise. The coherent sounds are usually impulsive. The source of the coherent noise appears to be the rapid unsteady blade loads encountered as the blade passes through the wake of the tower structure.

The radiation of the low-frequency and impulsive sound from horizontal-axis wind turbines is due to three main sources:

1-steady blade loads.

2-unsteady blade loads due to operation in a ground shear;

3-unsteady load experienced by the blades as they cross the tower wake.

WTGNOISE is capable of handling the three sources of noise mentioned above. This capability can be checked by examining equation (4.15) where the noise level emitted from the machine is determined as a function of the height of the wind turbine, pressure distribution on the blade, and the wind speed.

Acoustic emissions of the wind turbine machines can be categorised into those deriving from mechanical components

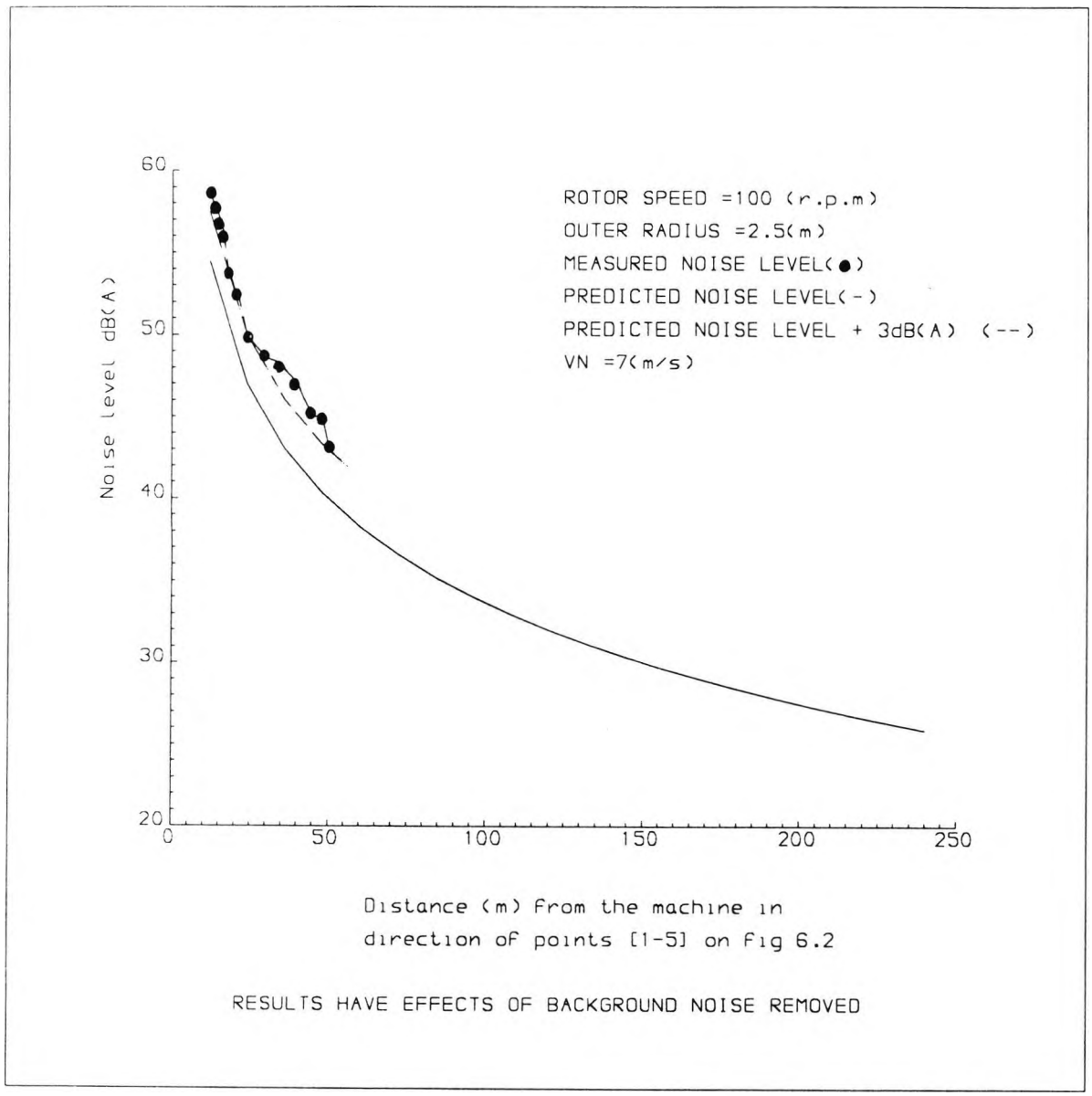

Fig 6.10 Comparison between measured and predicted noise level emitted from Cambridge test site machine, showed predicted noise + 3 dB(A).

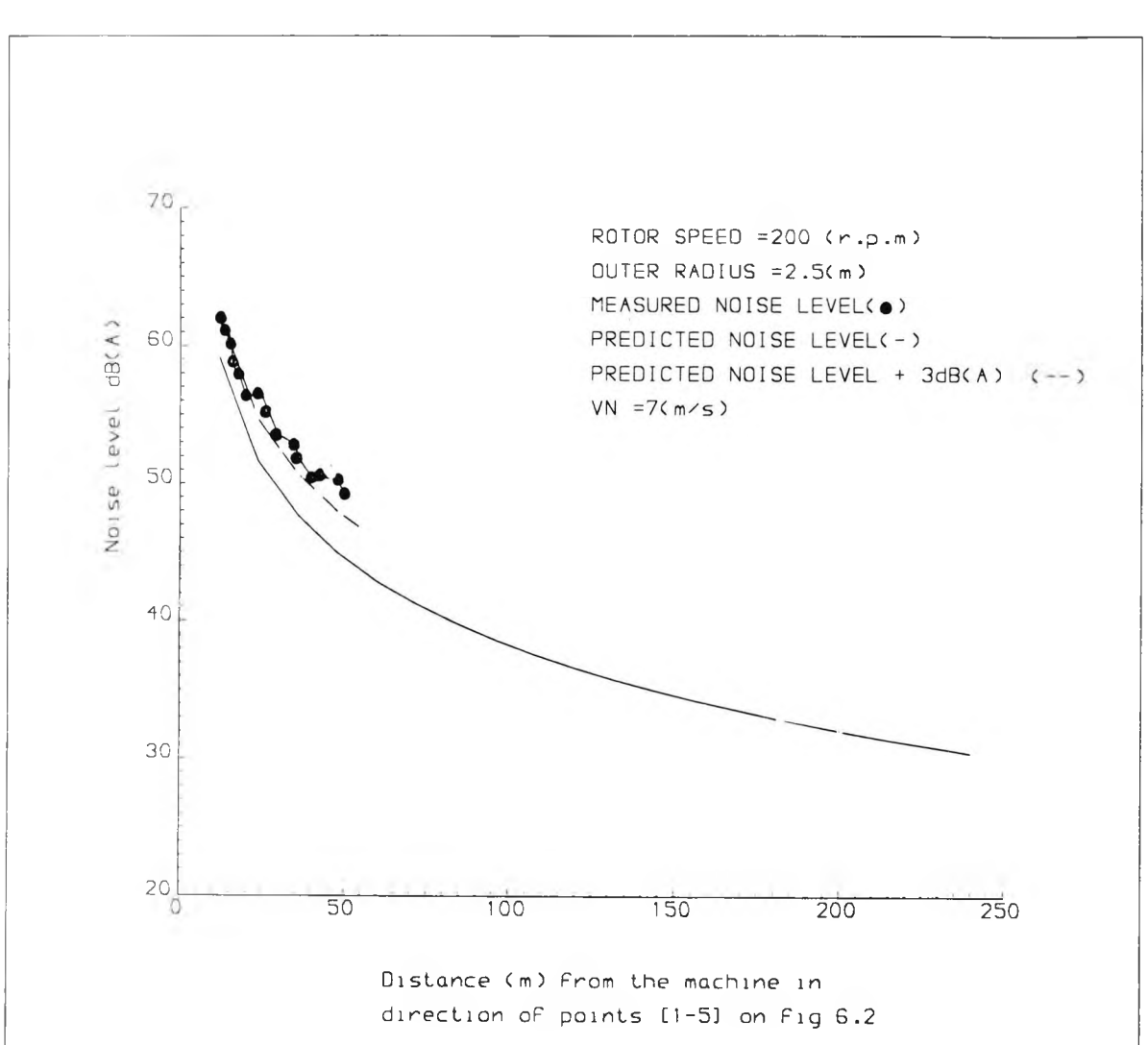

Fig 6.11 Comparison between measured and predicted noise level emitted from Cambridge test site machine, showed predicted noise + 3 dB(A).

and those deriving aerodynamically. Analysis of these sources has shown [31] that for smaller turbines, with a rotor diameter of up to 20 m, the mechanical contribution is the more important factor, whereas for larger turbines, the aerodynamic component is more dominant. The results of the emitted noise level from the Cambridge machine indicated that the mechanically derived noise on this small machine is the more important.

6.14 CONCLUSION

The overall results from this Chapter indicate that there is an acceptable agreement between the aerodynamic contribution to noise inferred from measurements taken at the Cambridge site and that provided by WTGNOISE. This is useful in the following Chapter regarding the prediction of the noise level of from new blade aerofoil designs and the effect of various parameters on the overall noise level from a machine. The difference between the overall measured and the predicted noise levels is considered to be primarily due to the fact that WTGNOISE does not include the mechanical noise contribution.

CHAPTER

7

THE DESIGN OF QUIETER WIND TURBINES

7.1 Introduction.

An aim of the current research is to provide the knowledge that will allow the redesign of a quieter wind turbine without affecting the output power. This takes into consideration the parameters that affect the level of noise emission from a machine. As an example of what can result from improved noise emission, a ten dB(A) reduction would allow a building to be three times closer to a wind turbine machine than before.

The requirement for quieter wind turbines is being stimulated through subsidy bonuses in some countries. With a growing trend towards wind farms in populated Europe, the requirement becomes more acute. It can be achieved by reducing the aerodynamic noise through blade optimum design and this can follow from establishing a new technology for the design of blades, taking into consideration the specific characteristics of the wind turbine itself. It is obviously important to understand the nature of the noise and the effect of various parameters on the noise level. Reduction of mechanical noise can be achieved using well known techniques.

7.2 Aerodynamic noise reduction.

Aerodynamic noise reduction is not necessarily easy to achieve because it depends on so many different factors such as the blade geometry and aerofoil characteristics. In this Chapter we examine, using the WTGNOISE program tested in Chapter 6, the effect of each of the important factors on the noise level to discover what can be done to make wind turbines less noisy.

7.2.1 Rotational speed, tip speed ratio and number of blades

The rotational speed is the single most important factor in determining the noise level of a wind turbine generator. Fig 7.1 clearly shows the effect of the rotational speed on the noise level as predicted by WTGNOISE.

The result is so significant that it is worth examining the theory in Chapter 4 for an explanation.

The terms l_r and M_r in equation (4.15) play a major role and, for example, the following factor has a large effect on the acoustic pressure.

$$\left\{ \frac{l_r}{r^2 |1-M_r|} \right\}$$

In this, l_r decreases for slower rotational speeds, due to the lower aerodynamic loading.

Also, M_r is a function of the rotational speed, because M_r= v × constant, where v is the magnitude of the local velocity on the blade, and thus a reduction of the rotational speed

means that denominator increases, with a consequent reduction in pressure level. This conclusion is borne out by results for different types of machines at different conditions [31], [40], [44], [46]. The level of the sound pressure variations are most directly affected by rotor speed and wind speed. By using WTGNOISE to predict the noise level of MS-1, at a rotational speed of 88 rpm, it is shown possible to reduce that noise by 5 dB if we reduce the rotational speed to 66 rpm, (see Fig 7.1) but the power will be also reduced by about 25% if all other parameters remain the same.

So the marked effect of the rotational speed on the noise level is clear but the problem is that a reduction of the rotational speed leads ultimately to an output power penalty. In Holland there is a legislation preventing wind turbine generators from operating at night if a certain level of noise is exceeded. It is recommended to use machines having two speeds, one for night time running and the other during the day thereby achieving some matching of power requirements since at night consumption is lower than by day. This idea has been discussed fully by Harrison [62]. For the same output power, an increase in the number of the blades involves a decrease of the tip speed ratio which has a beneficial effect on the noise level emitted from the machine. Therefore, for the same output, a three blade machine is less noisy than a two blade machine.

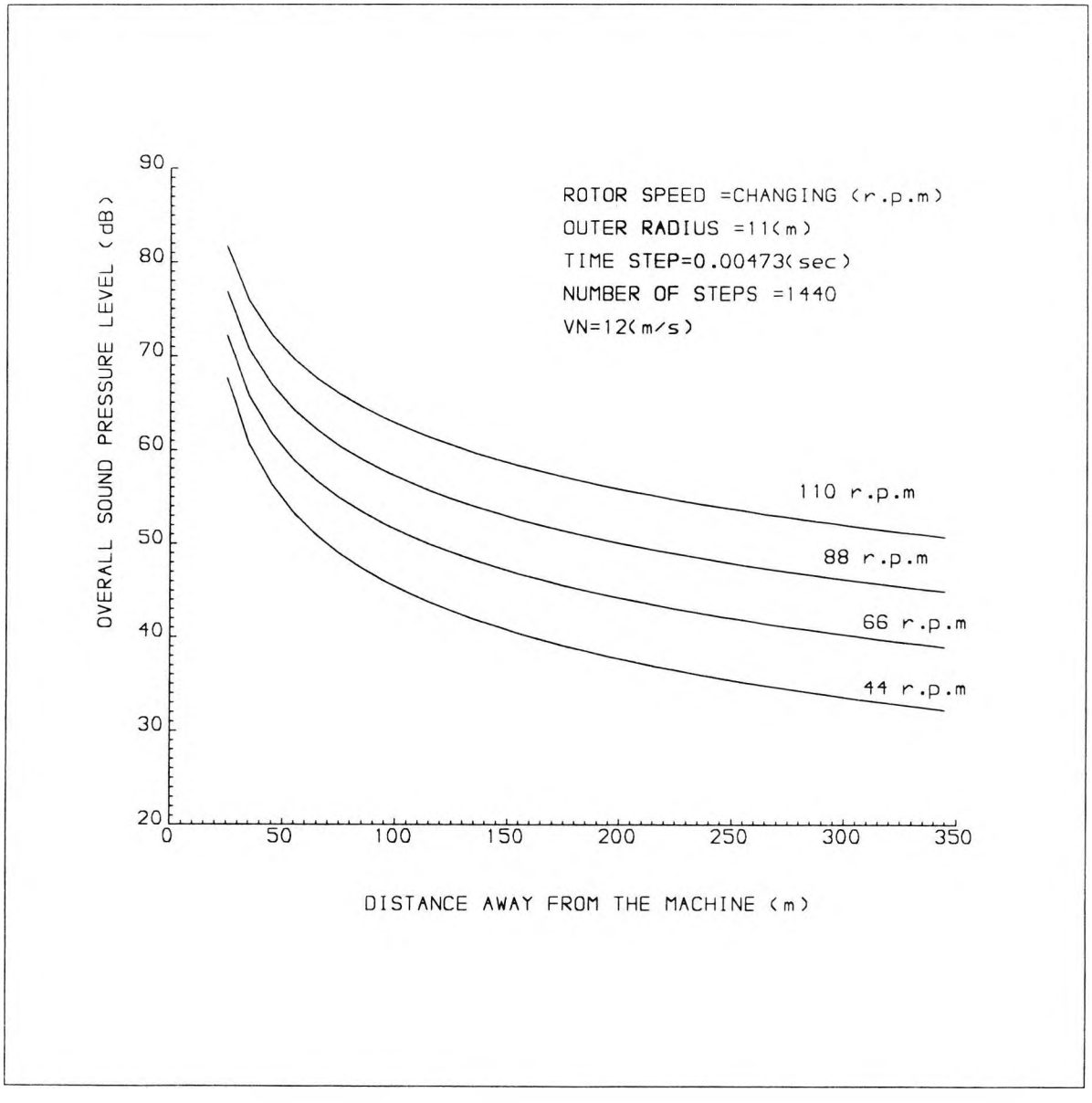

Fig 7.1 Effect of the rotational speed on the predicted noise level downstream, machine type and specification is MS-1.

As an example, WTGNOISE was used to compare the noise levels of machines of similar specifications (based on MS-1); it was found that the two blade configuration was noisier than the three blade configuration by about 5.8 dB at reference position [5], all other conditions being the same.

7.2.2 Tower wake.

(i) Downwind rotor.

Impulsive "thumping" sounds which result from blade/tower-wake interactions when the blade passes through the tower wake are believed to be the dominant source of annoyance in large downwind machines such as the MOD-1 configuration **[63]**.

Accurate noise estimation requires a detailed description of the rotor loading as it passes through the complex tower wake, and this is difficult to make with certainty. However, average noise calculations using average wake characteristics are in general agreement with average noise measurements **[40]**.

It is difficult to extrapolate model results for the downwind configuration to full scale since all the parameters which affect the wake also affect the generated noise. The inherent unsteadiness of wake flows may produce noise which is louder than would be expected from average measurements or calculations based on average wake characteristics **[40]**.

One way to reduce noise which has no energy capture penalty is by aerodynamic improvement of the tower. Guidance for beneficial changes to wind turbine support towers is contained in Figs 7.2 and 7.3.The data presented are based on a simplified analytical study of wind turbines with downwind rotors and cylindrical towers. In Fig 7.2 it can be seen that a narrow wake with a large wake deficit is the worst case for producing high-frequency noise. If the velocity deficit is minimised, then the noise at all frequencies is reduced. If, in addition, the width of the wake is increased, then the high-frequency noise is suppressed. Fig 7.3 indicates the best shape for a wake defect from a noise reduction standpoint. The shape derived by Schlichting from test data on smooth cylinders [64] is seen to cause the highest level of high-frequency noise. A wake with a cosine-squared shape produces less noise and, surprisingly, a Gaussian wake produces no high frequency noise. The implication from Fig 7.3 is that high frequency noise might be eliminated if the tower could in some way be modified to produce a Gaussian wake. However, this is not really practical since it would imply utilising a tower of a special cross-section which rotated with the nacelle when the wind changed direction. Thus, engineering considerations and the need for the wake characteristics to remain independent of wind direction imply circular or near circular cross-sections for non lattice towers.

Very small differences in the wake shape assumed for a noise calculation can have a large effect on the high frequency components of the noise predicted. The implied sensitivity of the calculation procedure to small changes in wake definition indicates the need for additional work to correctly model full-scale tower wakes[40].

An additional possibility is that cross-flows from the wind into the rotor might have significant acoustic effects. Investigation of this should also form part of future experimental and theoretical research [45].

There is evidence that small reductions in the amplitude of impulsive noise can be achieved if a "softer" blade is used [45]. This implies making use of structural flexibility to modify the aerodynamic loading such that it has a beneficial effect on the noise emitted; however, this would be a very difficult objective to achieve in practical terms using the normal design processes, and would require substantial basis of background analysis and knowledge.

(ii) Upwind rotor.

In the case of an upwind rotor, due to the fact that the flow slows down and changes direction in front of the tower an effect similar to the downwind rotor tower shadow is perceived. The thumping sound is less obvious, however, because the slowing down and changing of the flow in the vicinity of the tower is more gradual.

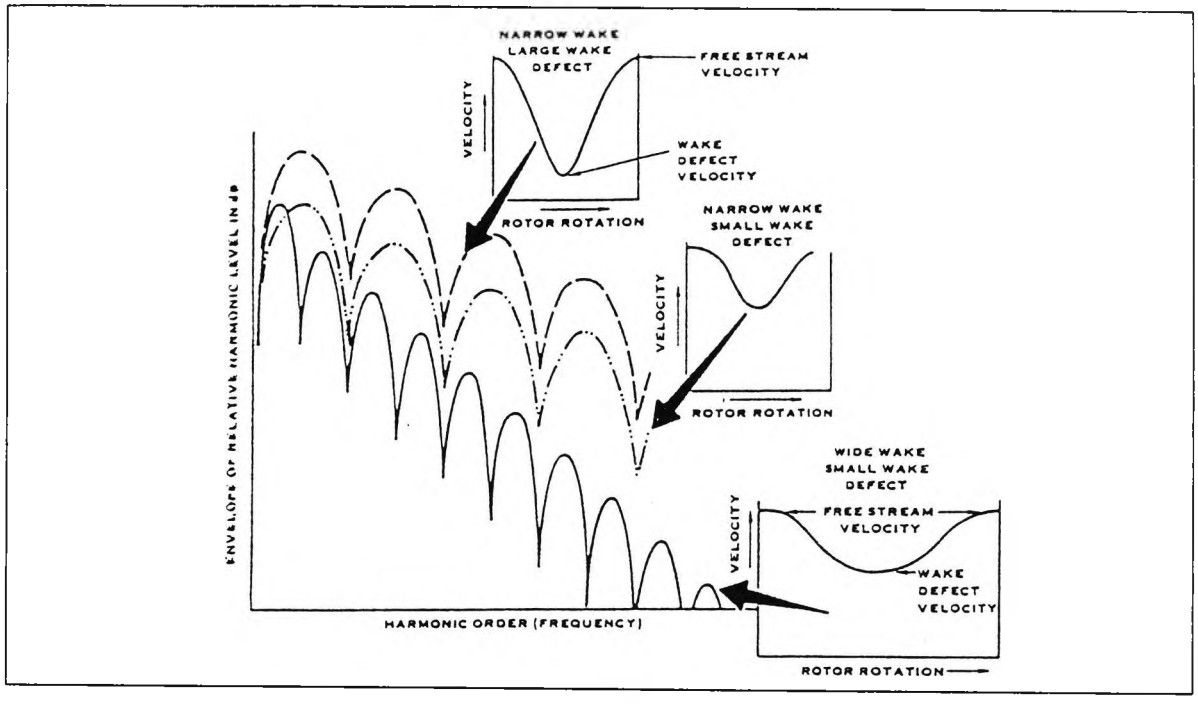

Fig 7.2 Effect of wake defect amplitude and width on noise spectrum. Extracted from Ref [40].

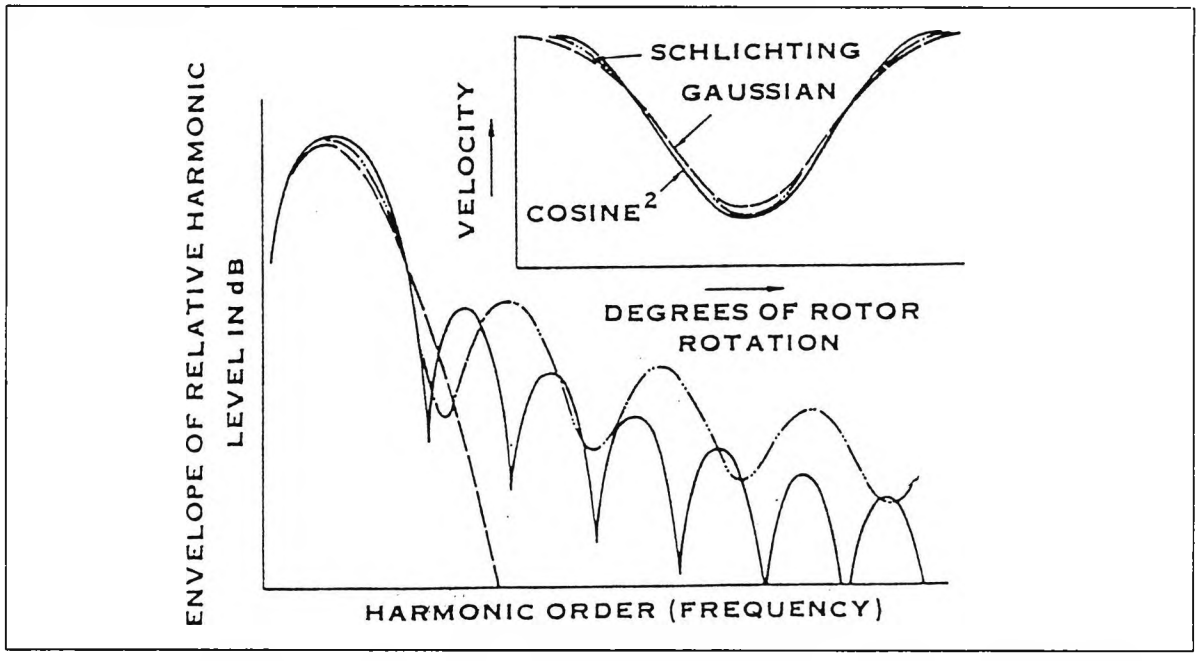

Fig 7.3 Effect of wake velocity defect shape on noise spectrum shape. Extracted from Ref [40].

7.2.3 Reduction of the peak pressure on the blade

It can be seen from equation (4.15) that the term l_r which represents the pressure on the blade in the radiation direction has a substantial effect on the noise level emitted from the wind turbine, and thus reduction of this pressures will lower the noise level. See Fig 7.4 which shows the effect of l_r on the noise level emitted from a machine with an LS-1 blade at a rotation speed of 88 rpm and outer radius 11 m. Because l_r is a function of C_L, any reduction in C_L implies a reduction in the noise level.

A higher performance aerofoils (higher $C_L$max etc..) do not, according to Garrad [65], produce any more power than a lower peak pressure section but it does generate larger pressures. It is clear, therefore, that the lifting peak pressure of the aerofoil should not exceed the design peak pressure [65] in order to reduce the noise level to its lowest possible values. A high performance aeorfoil does not necessarily produce more power then a lower lift section because, for example, on a pitch regulated machine the outer span of the blade does not approach stall and the larger lift coefficients are never used to generate power. However, the pitch control system may react too slowly to prevent high loads resulting from sudden gusts. Fig 7.5 was used in Reference [65] to illustrate this point. On a stall regulated rotor, the lower lift requirement is more obvious since it is an integral part of the design. Fig 7.6, taken

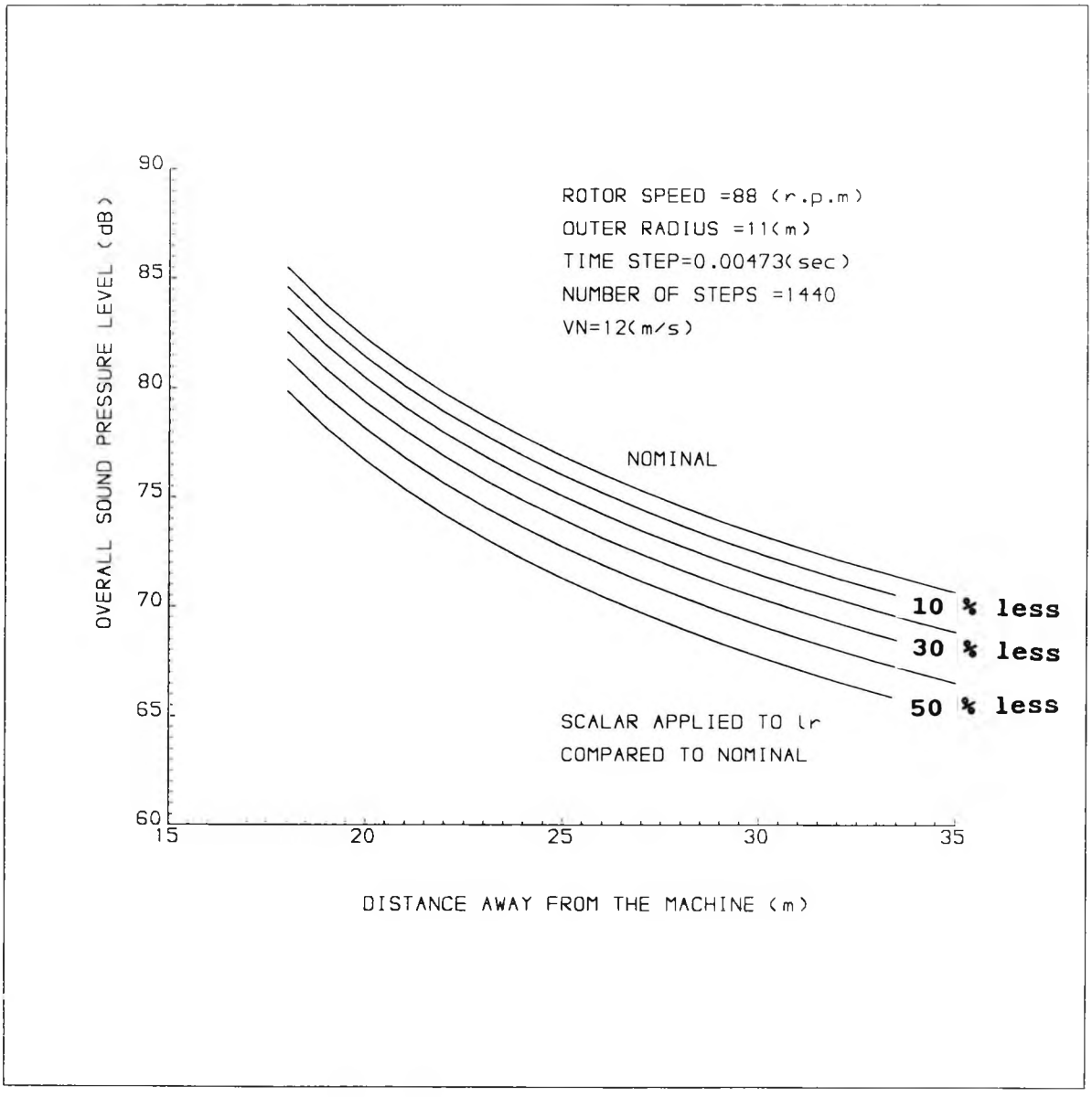

Fig 7.4 Effect of l_r on the predicted noise level downstream , data of LS-1 was used in the calculation.

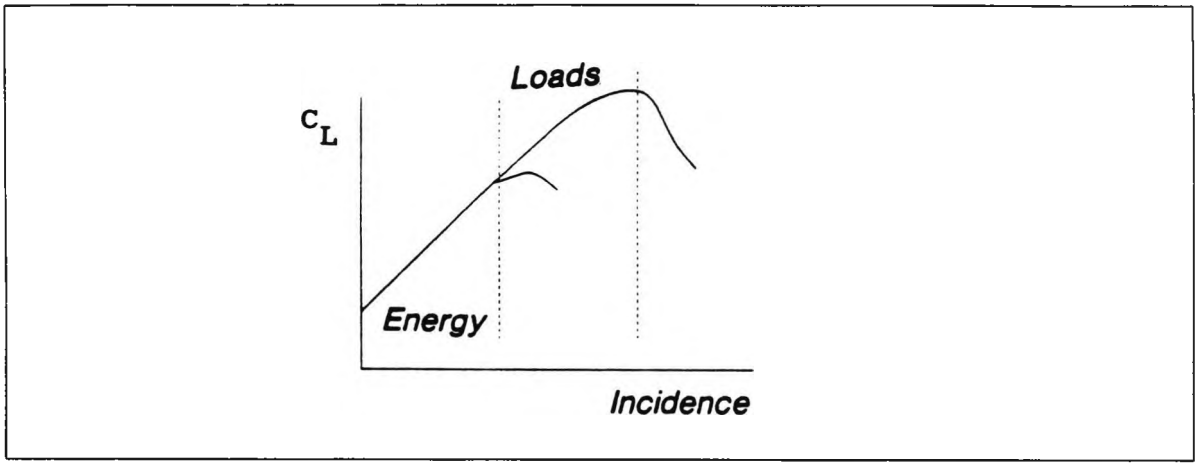

Fig 7.5 Relationship between energy and load shows that increase in C_L does generate more energy after certain level. Extracted from Ref [65].

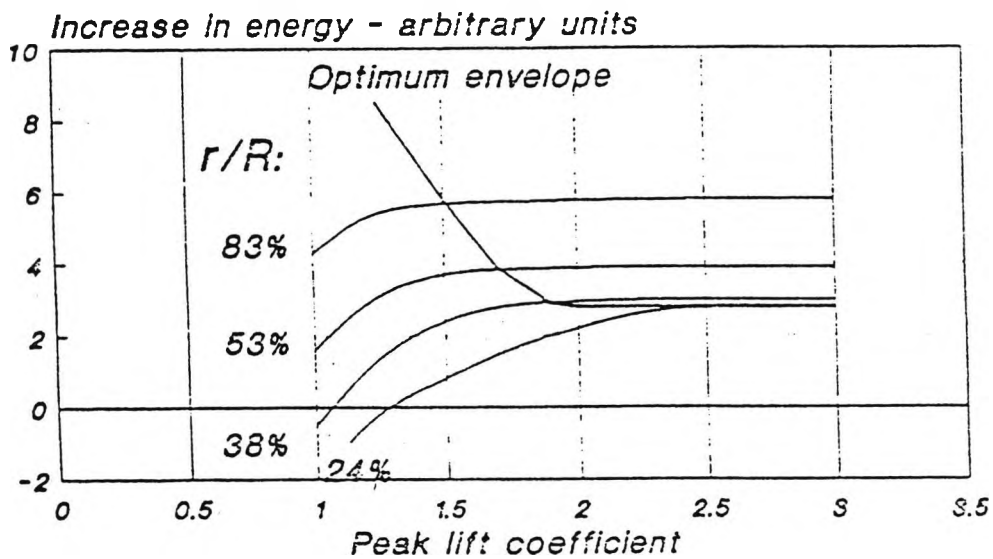

Fig 7.6 Determination of maximum useful C_L. extracted from Ref [65] (r is local raduis, R is blade raduis).

from the same Reference, shows the variation of peak c_L with radius to achieve optimum energy capture.

7.2.4 Effect of chord

The effect of the chord on the noise level is to be found through an understanding of the mathematical model. In this model, by applying the same forces on two blades having different chords, the pressure on the surface of the smaller chord blade is found to be higher, and thus more noisy; conversely, increasing the chord implies decreasing the pressure which will decrease the total noise level.

For example, using WTGNOISE applied to the LS-1 aerofoil data a 20% increase of chord results in a decrease of the noise level emitted of about 2.5 dB (see Fig 7.7) whilst a 30% increase leads to a decrease of the noise level by about 3.8 dB (see Fig 7.8), other conditions remaining the same.

7.2.5 Effect of leading edge and, trailing edge.

Prior to the stall the use of a sharp trailing edge on a blade will limit vorticity which means less noise; when the blade stalls the trailing edge thickness become less important, and the wake of the blade is dominated by separation flow, which will increase the noise level.

As for the leading edge, the larger the leading edge radius compared with the chord, the lower the peak pressure and hence the lower the noise contribution from this particular source.

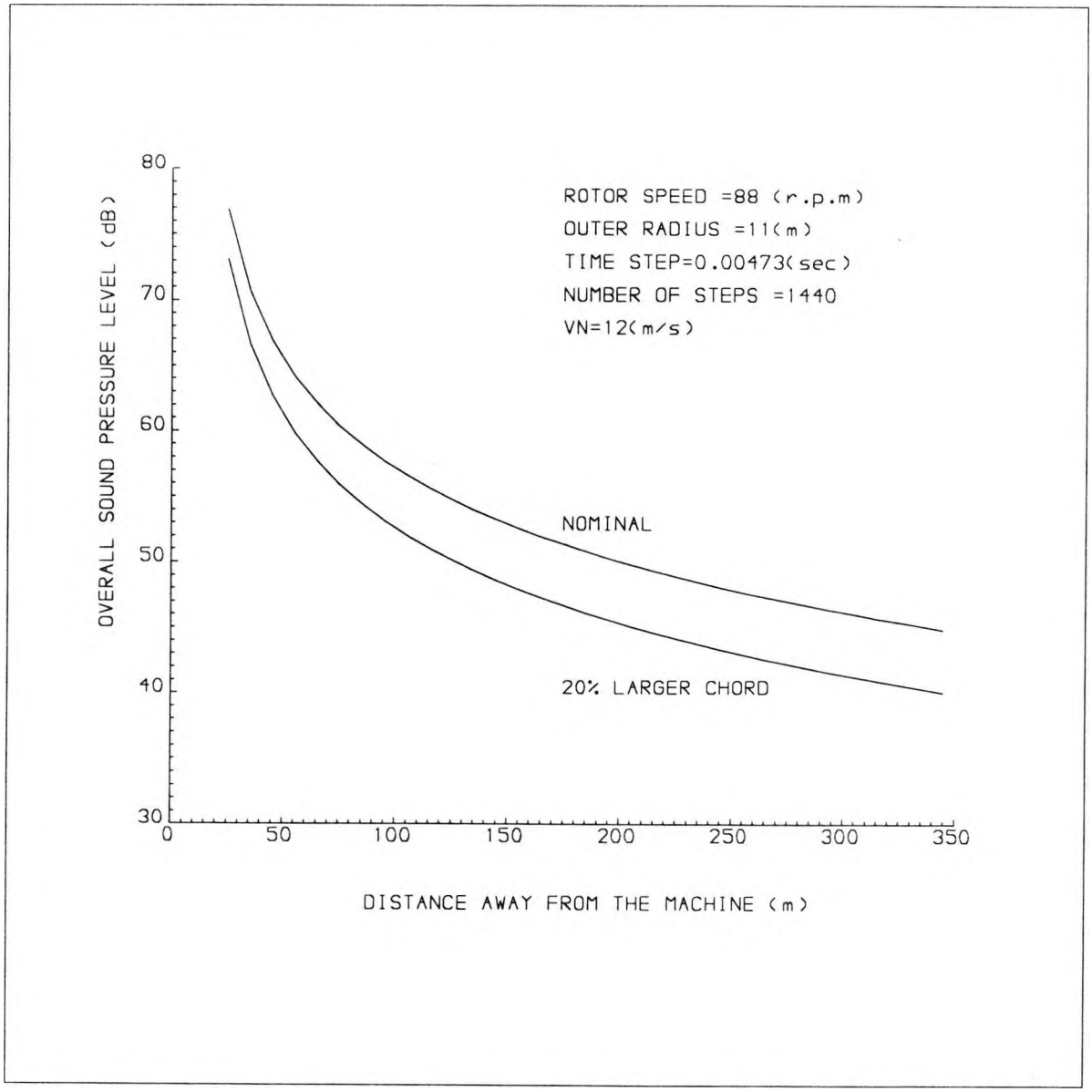

Fig 7.7 Predicted noise level downstream for aerofoil LS-1 with 20% larger chord.

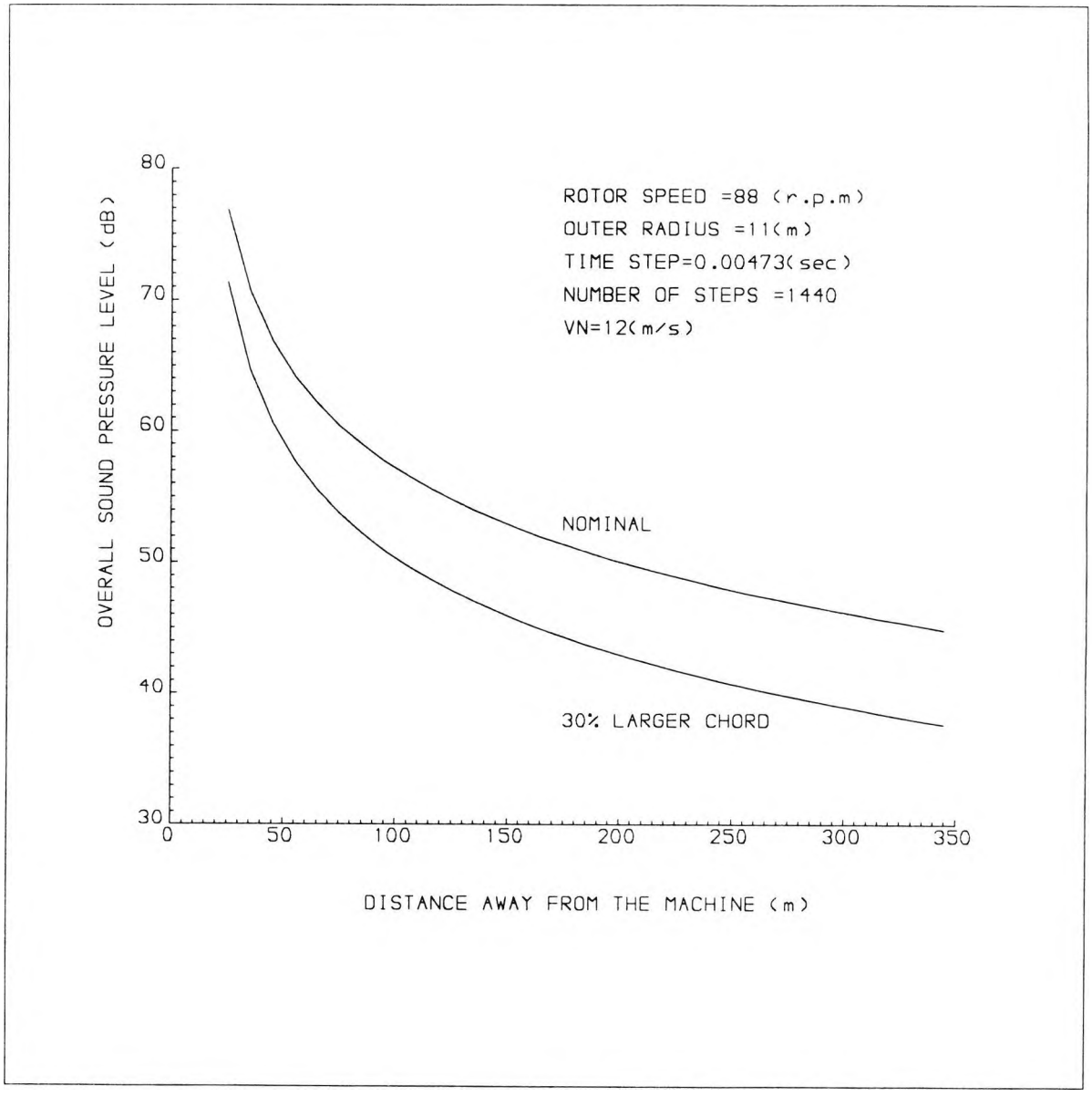

Fig 7.8 predicted noise level downstream for aerofoil LS-1 with 30% larger chord.

7.2.6 Blade design.

Blade design procedures have been developed by Wilson and Lissaman [66] who proposed a simple model for an optimum windmill. The approach used is to treat the rotor as an actuator disc, and to set up an integral for the power. The power integral is made stationary subject to an energy constraint, the result yielding the maximum power output for a given tip speed ratio.

The relationship for the maximum power coefficient is given by

$$C_p = \frac{\text{Power}}{1/2\ \rho\ V_\infty^3\ \pi\ R^2} = \frac{8}{X^2} \int_0^X (1-A)\ A' x^3\ dx \qquad (7.1)$$

where $x = \frac{rN}{V_\infty}$, $X = \frac{RN}{V_\infty}$, $A = \frac{V_\infty - u}{V_\infty}$ and $A' = \frac{\omega}{2N}$

C_p is the power coefficient, ρ is the fluid density, V_∞ is the free stream velocity, R is the rotor radius, r is the local rotor radius, X is the tip speed ratio, x is the local speed ratio, A is the axial interference factor, A' is the tangential interference factor at the rotor, ω is the fluid angular velocity downwind of the rotor , u is the axial flow velocity at the rotor, and N is the rotational speed.

Since the integral for the power involves two dependent variables, another relationship is required. This is the energy equation

$$A'(1-A')x^2 = A(1-A) \qquad (7.2)$$

After solving for the optimum, the variation of the variables A, A', $A'x^2$, x is given in Table 7.1 below

Table 7.1 Flow conditions for the optimum actuator disk

A	A'	$A'x^2$	x
.25	∞	0	0
.27	2.375	.0584	0.157
.29	0.812	.1136	0.374
.31	0.292	.1656	0.753
.33	0.031	.2144	2.630
1/3	0	.2222	∞

It is assumed that the drag component is zero, so the only force acting on the blade is the lift component. Using this assumption the incremental thrust and torque acting on an annulus containing blades B each having a chord c are

$$dT = \frac{Bc}{2}\rho W^2 C_L \cos\phi \, dr \qquad (7.3)$$

$$dQ = \frac{Bc}{2} r\rho \, W^2 C_L \sin\phi \, dr \qquad (7.4)$$

where dT is the incremental thrust, dQ is the incremental torque, W is the resultant velocity relative to the rotor element, C_L is the sectional lift coefficient, ϕ is the angle between the plane of rotation and the relative

velocity, and r is local rotor radius.

The momentum expression yields in such a case [66]

$$dT = 4\pi\rho V_\infty^2 (1-A)A\, dr \qquad (7.5)$$

$$dQ = 4\pi\rho r^3 V_\infty N(1-A)A' dr \qquad (7.6)$$

in which $b = 1 - u_{1/} V_\infty$ is the axial interference factor in the wake (u_1 being the axial flow velocity in the wake), has been assumed equal to 2A.

Since A, A' are known as a function of x the blade parameters may be determined. Table 7.2 provides the result, where ϕ is the angle between the plane of rotation and the relative velocity, and x is the local speed ratio.

Table7.2 Parameters for the optimum actuator disc [66].

ϕ	x	B c N $C_L/2\ \pi\ V_\infty$
50	0.35	.497
30	1.00	.536
20	1.73	.418
15	2.43	.328
10	3.73	.228
7	5.39	.161
5	7.60	.116

In Reference [66], the Table is used to indicate the value of x at which the chord is a maximum (about 0.7) assuming constant tip speed ratio x and C_L. If the optimum variation of chord suggested by the Table is utilised, then for a given free-stream wind velocity V_∞, the following term

$$B\ c\ N\ C_L = \text{constant} \qquad (7.7)$$

where B is the number of blades, c is now the mean chord, N is the rotational speed and C_L is a mean lift coefficient. It can be seen from equation (7.7) that increasing the number of blades or increasing the chord will result in a decrease of either N or C_L, thereby decreasing the noise level whilst maintaining output power.

The wind turbine presents a certain solidity to the airstream. This is the ratio of the total area of the blades at any one moment in the direction of the airstream to the swept area across the airstream. High solidity machines start easily with high initial torque, but soon reach maximum power at low rotational speed. Low solidity machines may require starting, but reach maximum power at high rotational speed [67], [68]. Thus increasing the number of blades and increasing the chord will result in an increase in solidity of a wind turbine machine as well as increasing the cost of the blades, which should be included in any evaluation of noise cost.

One of the most promising areas for reducing the noise level of wind turbine generators without having to pay a penalty regarding the output of the machine, or the additional cost of more or wider chord blades, is that of redesigning the blades themselves. The early blade design of wind turbines tended to follow helicopter blade design without paying a lot of attention to their specific characteristics. At present most wind turbines use conventional aircraft aerofoil sections. The most common sections are from the NACA 44xx, 230xx and 63 and 64 series. More recently the NACA general aviation aerofoils, now known as LS-1 and LS-1 MOD, have received a great deal of attention and are increasingly used on new blades. It can be seen from Fig 7.4, which is derived from WTGNOISE that the peak pressure on the blades has a great effect on the noise level emitted from the machine. The new aerofoils produce lower peak pressures on the blades, which is an advantage from the noise level point of view. In the USA work has been carried out at the Solar Energy Institute on a new series of aerofoils which had the design specification of a reduced maximum C_L. This is now at an advanced stage and full scale tests are now running on rotors using the new aerofoils in USA [65].

In the U.K, Satchwell [69], at the University of Southampton, has been looking at the design of thick aerofoils because of the apparent advantage regarding the

peak pressure on the blades for wind turbines. This work has been inconclusive to date but is continuing. Garrad [70], [71] mentions the forces on the blade of the wind turbine and the need for a new design of blade which would reduce the peak pressure on the blade; there is no need to create high peak pressures on the blade which lead to unnecessarily high noise levels. Tangler and Somers [72] have had considerable success in reducing peak lifting pressures; their aerofoil, S 805, has its point of maximum thickness almost halfway along the chord from the leading edge and is shown in Fig 7.9. Garrad [65], [71] has proposed the GHP1 and GHP2 aerofoils which he and his co-designers claim have qualities superior to the present LS-1 regarding the peak pressures. The change in the geometric shape on the upper surface is the key to the peak lift reduction. Effort has been concentrated on reducing the lift so as to produce an aerofoil with a moderate maximum lift coefficient of about 1.5. Fig 7.10 shows a comparison of the GHP1 and LS1 Mod aerofoil shapes.

The lift-drag ratio of a further new mid-span section GHP2 is compared with LS-1 Mod and root section GHP1 in Fig 7.11. This shows that the new section has a reduced peak lift over LS-1 until immediately prior to its stall [65] .

The aerofoil shapes of GHP1 and GHP2 are compared to those of LS -1 and NACA 64(3) in Fig 7.12. All aerofoils are 17 % thick and operate at a Reynolds number of 4 $\times 10^6$. The

performance of GHP-2 is promising and it has been the subject of some further experimental tests at Imperial College [65]. The results to date from these tests appear to agree with the predicted performance [73]. Fig 7.13 shows the pressure distribution of three different aerofoils, which indicates that the pressure distribution for GHP2 is flatter by comparison with that of other aerofoils [73].

Using the new GHP aerofoils, significant pressure reductions will result without any penalties in energy yield which will also reduce the noise level emitted from wind turbine. This is due to the effect of C_L max on the pressure on the blade. It has been established already in this Chapter (section 7.2.3) that reduction of C_L max implies a reduction of l_r which has a great influence on the noise level.

Using WTGNOISE to compare the noise emitted from the MS-1 rotor when the blade aerofoil sections are based on firstly the LS-1 and secondly the GHP aerofoils it was found that the latter case is less noisy by about 2.8 dB, as shown in Fig 7.14.

Twisting the blade is believed to make the pressure distribution on the blade flatter by introducing better control of the spanwise aerodynamic loading. Consequently, it provides a further means of reducing the noise level emitted from a machine. This aspect was not investigated in the current work and the author is not aware of any

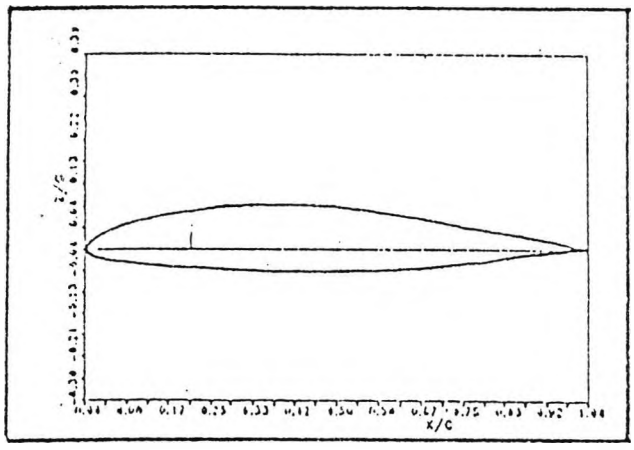

Fig 7.9 Tangler and Somers aerofoil S805.

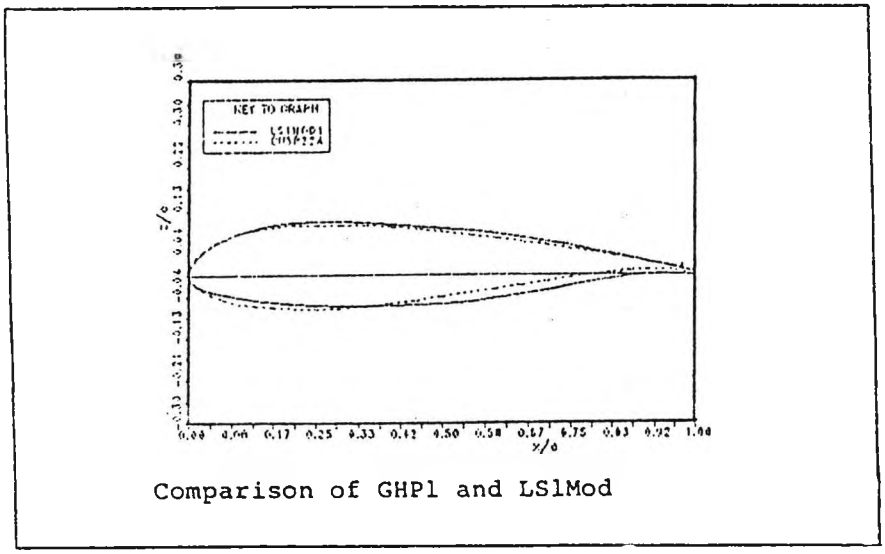

Fig 7.10 Comparison of GHP1 and LS1 Mod.

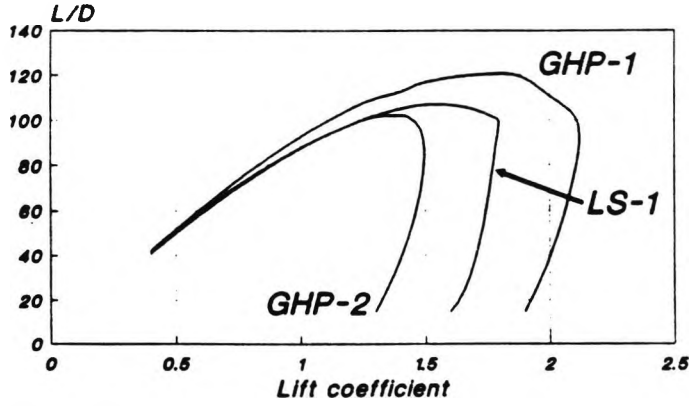

Fig 7.11 show the lift-drag ratio of the new section GHP2 compared with LS1 Mod and root section GHP1.

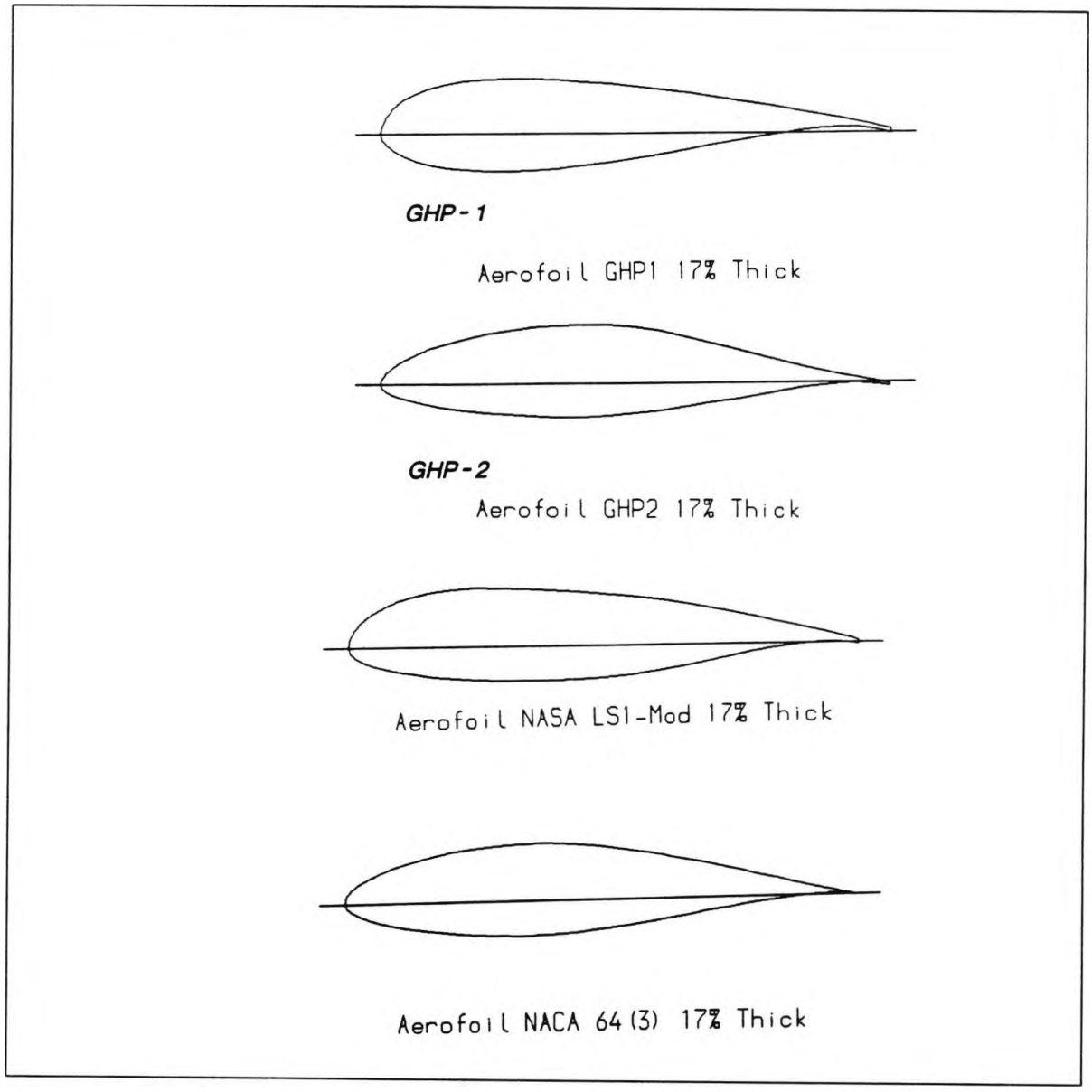

Fig 7.12 Show the aerofoil shapes of GHP1, GHP2 compared with LS1-Mod.

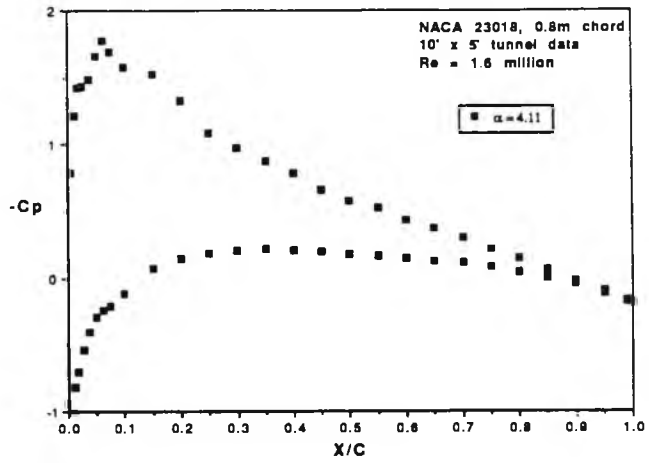

NACA 23018 aerofoil

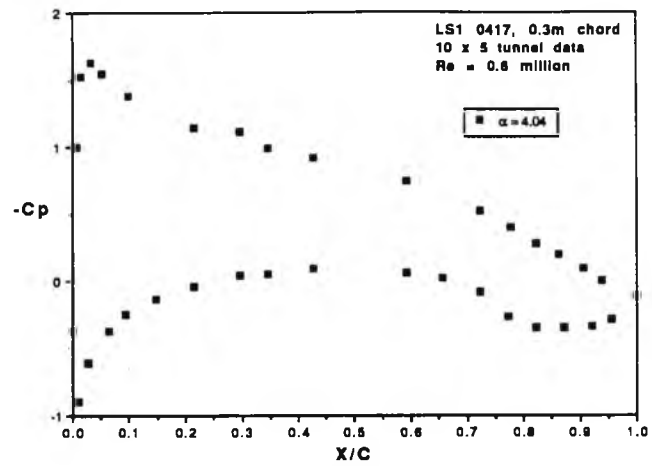

LS1 0417 Pressure distribution

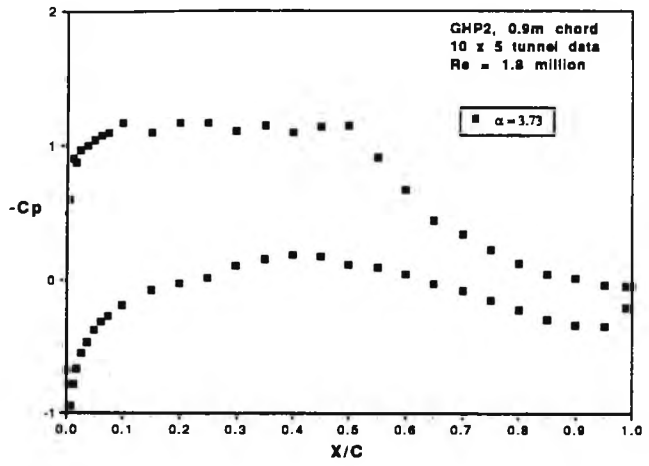

GHP2 Pressure distribution

Fig 7.13 Sample pressure distribution for three different aerofoils [71].

relevant publications. Sweeping the blade tip is also considered to reduce impulsive noise according to Metzger [40]. However it is not clear from his work how much sweep is required and how much of the blade must be swept to cause a significant reduction.

7.2.7 Optimum blade design

Research on the optimisation of horizontal axis wind turbine rotors has focussed over the last five years on minimising the direct cost of energy and obtaining maximum energy capture.

In recent years, with the growing demand for wind energy and the introduction of legislation to limit the operation of machines where the noise level is greater than that permitted, the need to take the noise characteristics into account when aiming for the optimum design has been great. However, achieving an optimum design is complicated since it involves sophisticated calculations which necessitates the use of numerical procedures [74-81]. A guideline of these calculations can be summarised by the following steps:

(i) An initial design is examined using a suitable aerofoil from the noise output point of view. This means the use of a wider chord and flatter peak pressure aerofoil. However, the power output also

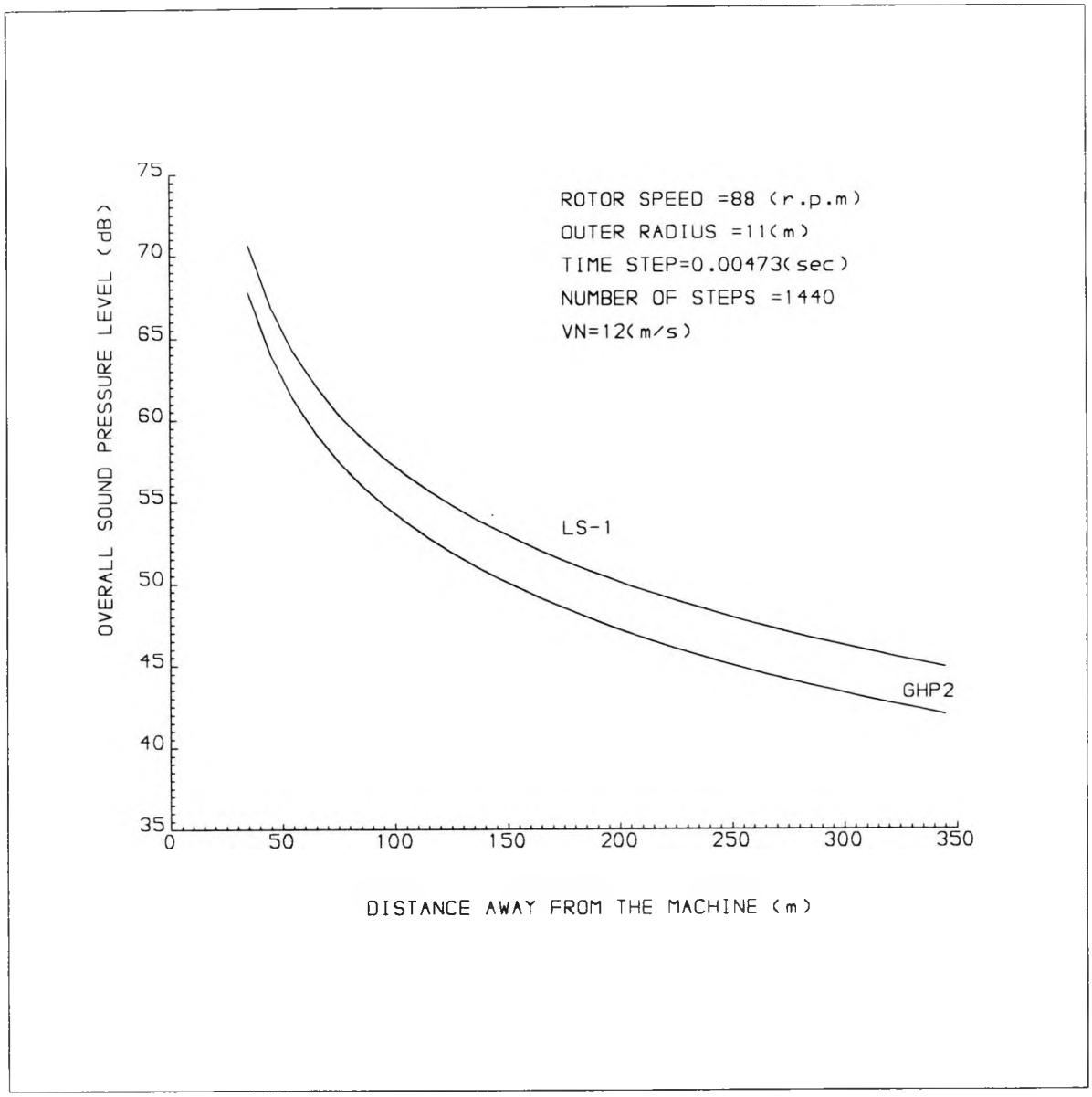

Fig 7.14 Predicted noise level downstream for aerofoils LS-1 and GHP2 applied to the MS-1 machine.

depends on other variables such as lift coefficient, rotational speed or tip speed ratio, wind speed at the site, and projected rotor area.

(ii) Normal optimum design procedures are then followed in fixing the blade parameters in addition to variables such as angle of attack and engineering data of the blade depending on a required output power. This involves determining the constant terms of equation (7.7) accordingly, which will put constraints on the types of aerofoils that can be used.

(iii) Then the rotational speed and number of blades are fixed to obtain the specified output power, varying the chord in order to adjust for the acceptable noise level.

(iv) Based on the obtained design, the noise level is predicted using WTGNOISE. If the predicted noise level is not acceptable the design should be repeated with a different wider chord.

(v) The output power of the above design is checked against the required nominal output power. It should be noted that the improvement aimed for in maximizing the output power is small, therefore this iterative calculation should be carried out accurately.

(vi) The next step involves the calculation of the costing of the design. This is a complicated process since the choice of a wider chord, for instance,

involves not only the cost of additional material but perhaps the selection of a different material altogether to maintain its durability. Moreover, it should be noted that the savings on the costs caused by the environmental sound pollution should be taken into account.

The design steps described above are illustrated in Fig 7.15 where the constraints and design goals of optimisation, taking into account the noise limitation on the machine at the design stage, are shown.

WTGNOISE helps in designing blades for minimum noise level at the ab initio stage. This blade design may serve as an ideal starting point where the required compromises, such as cost, can be made with the full knowledge of their impact on noise and energy.

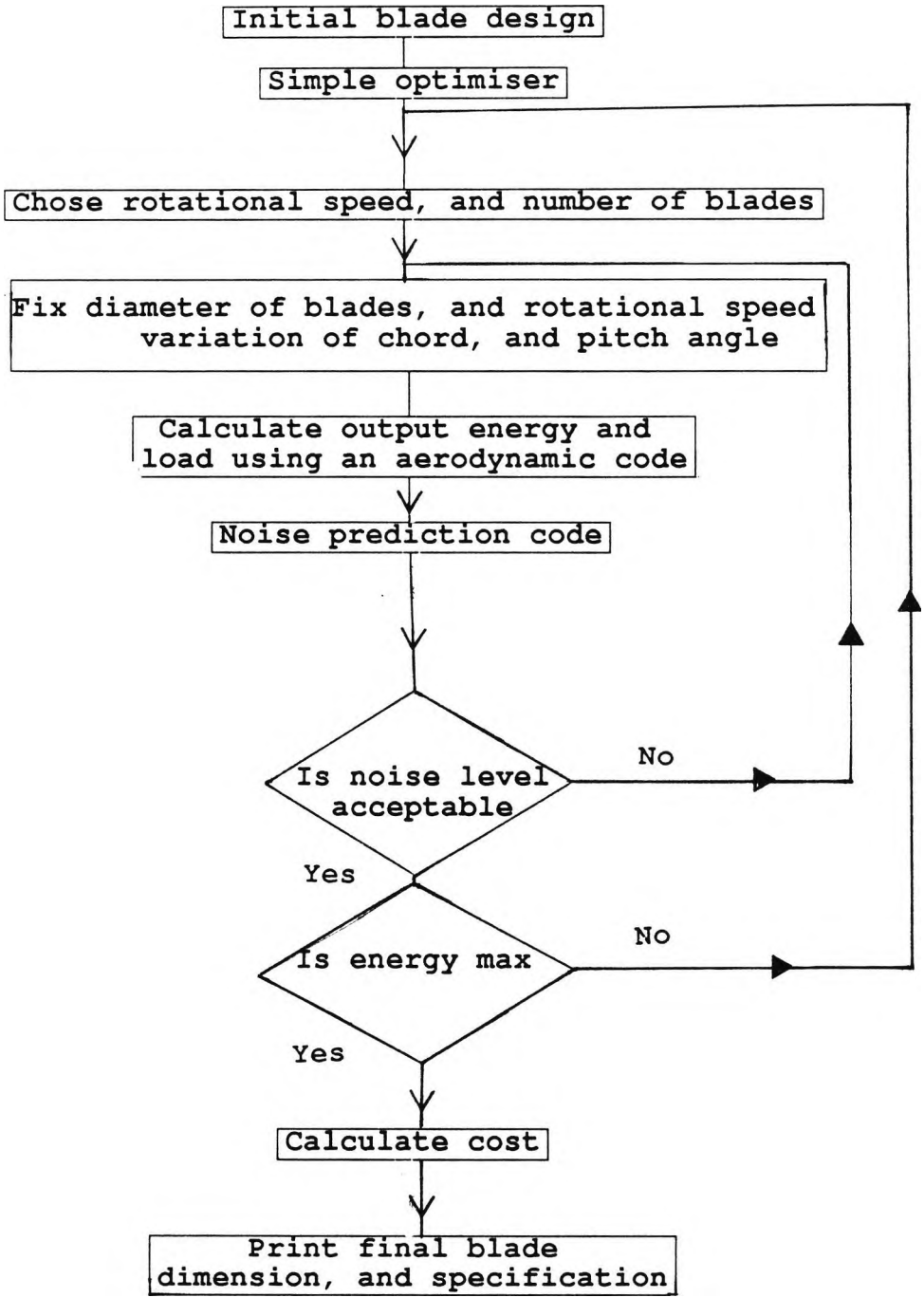

Fig 7.15 Schematic of optimisation

7.3 Mechanical noise

For the purpose of completeness, a summary of wind turbine mechanical noise follows.

Mechanical noise has been shown to be present from the measurement described in Chapter 5. It is likely that mechanical noise will be significant in most wind turbine generators. However, there are many well known techniques for alleviating mechanical noise.

Gearbox noise is a typical example of mechanical noise and it can be clearly distinguished by its characteristics [24]. It is generated by the meshing action of the gears. The vibrations produced by the gears are transmitted to the gear casing, then through the supporting structure of the casing to the panels of the power house containing the generator and controls, making the side panels a large source of noise radiation. Using modern data analysis techniques, it is possible to trace the cause of gear vibration to some of the following factors; machining, wear profile, load, speed, imbalance of the rotor and lubrication. It is also possible to identify errors in design and manufacturing by examining the spectral characteristics of the noise. After understanding the main design and operating parameters contributing to the cause of the vibrations, the problem can be alleviated by altering some of these parameters. Often noise emission from the whole unit can also be reduced by preventing

vibration transmission to the outside structural components [24]. Harmonics of the tooth mesh frequency are caused by the tooth contact even with identical tooth profiles. The noise and vibration signals are periodic at the tooth meshing rate and uniform around the circumference of the gear wheel. Helical gears are believed to generate lower noise levels than spur gears. Significant noise reductions can also be obtained by improving the alignment of the meshing gears and reducing the manufacturing tolerances. This noise can also be reduced by inserting damping material between the gear box casing and the top of the power house module, lowering the pressure angles of the gears might reduce the gear mesh frequency components.

Noise from tip brakes could be reduced through better design. Also the transmitting of torque to the generator through shafts, bearing, other mechanical parts can cause noise. It is worth making sure that the transmission causes less noise through well known techniques such as the use of appropriate lubricant, damping materials and quieter bearings.

There are also many mechanical noises deriving from simple and straight forward sources. The Cambridge wind turbine, for instance, emitted significant noise which arose from rubbing between the different parts of the machine when the nacelle rotated. It is normally easy to minimise this through careful assembly of the parts, correct tightening

of the nuts and moving parts and the use of appropriate lubricants.

Another way of reducing noise of mechanical origin emitted from the machine is to put enclosures around the noise source. The nacelle is itself a form of enclosure, and it can be properly designed; reducing the holes, gaps, and introducing damping, and absorption material on the nacelle walls will reduce the noise level emitted [80]. It is fair to say, however that each machine has its own characteristics and each should be treated individually as regards the mechanical noise. Fig 7.16 shows the mechanical components of a wind turbine machine which can generate noise.

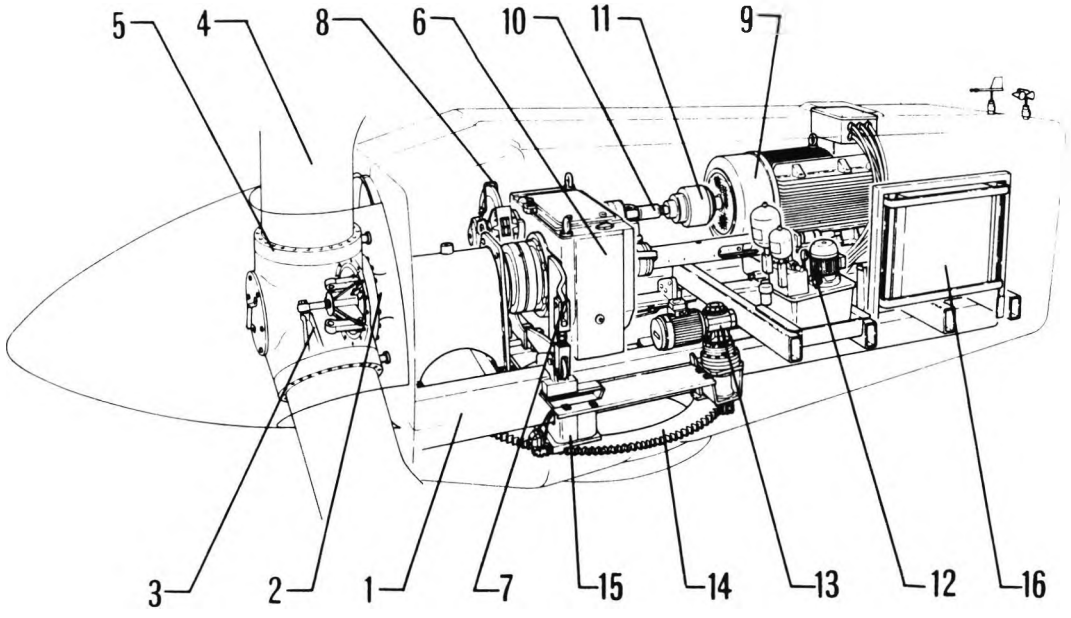

Other parts

1.Machine bed
3.Blade hub
4.Blade
5.Cast steel root
10.Cardan
15.Yaw control
16.Control unit

Parts which can generate noise

2.Main shaft
6.Gear
7.Gear tie rod
8.Disc brake
9.Generator
11.Slip clutch
12.Hydraulic unit
13.Yaw gear
14.Yaw ring

Fig 7.16 Mechanical components of a wind turbine machine which can generate noise Extracted from Ref [81].

7.4 Noise on wind farms

With the growing trend toward wind farms in the U.K, and the opening of the first wind farm in a short time, it is essential that wind farm developments are good neighbours. The rural ambient noise of 30-40 dB(A) at wind speeds coresponding to normal turbine cut-in speeds, highlights the importance of keeping generated noise to a minimum.

Using WTGNOISE to predict the noise level around one MS-1 machine, contours of equal pressure level can be drawn (see Fig 7.17.). If two machines are placed together and assuming no coherence the equi-pressure contours are as shown in Fig 7.18.

For a wind farm of 10 MS-1 machines, WTGNOISE can be used to predict the noise level around each machine, assuming as befor that there is no coherence between the machines; the distance between the machines is 7 rotor diameters i.e. 154 m in this case. The resulting equi-pressure contours are shown in Fig 7.19 which indicates that far from the wind farm a contour approximates to an oval shape.

The steps required to predict the noise level from a wind farm and relevant comments are as follows:

1- Predict the noise level for one machine by WTGNOISE, and draw the equal pressure line contours around one machine.

2- It is assumed for simplicity there is no coherence between sound pressure signals from wind

turbine machines, even though this possibility exists due to the farm consisting of identical machines running at similar speeds.

3- From the pressure contours for each machine the equi-pressure contours for a wind farm of 10 machines can be drawn, see Fig 7.19. This shows that contours sufficiently far away can be approximated to a flat-sided oval shape.

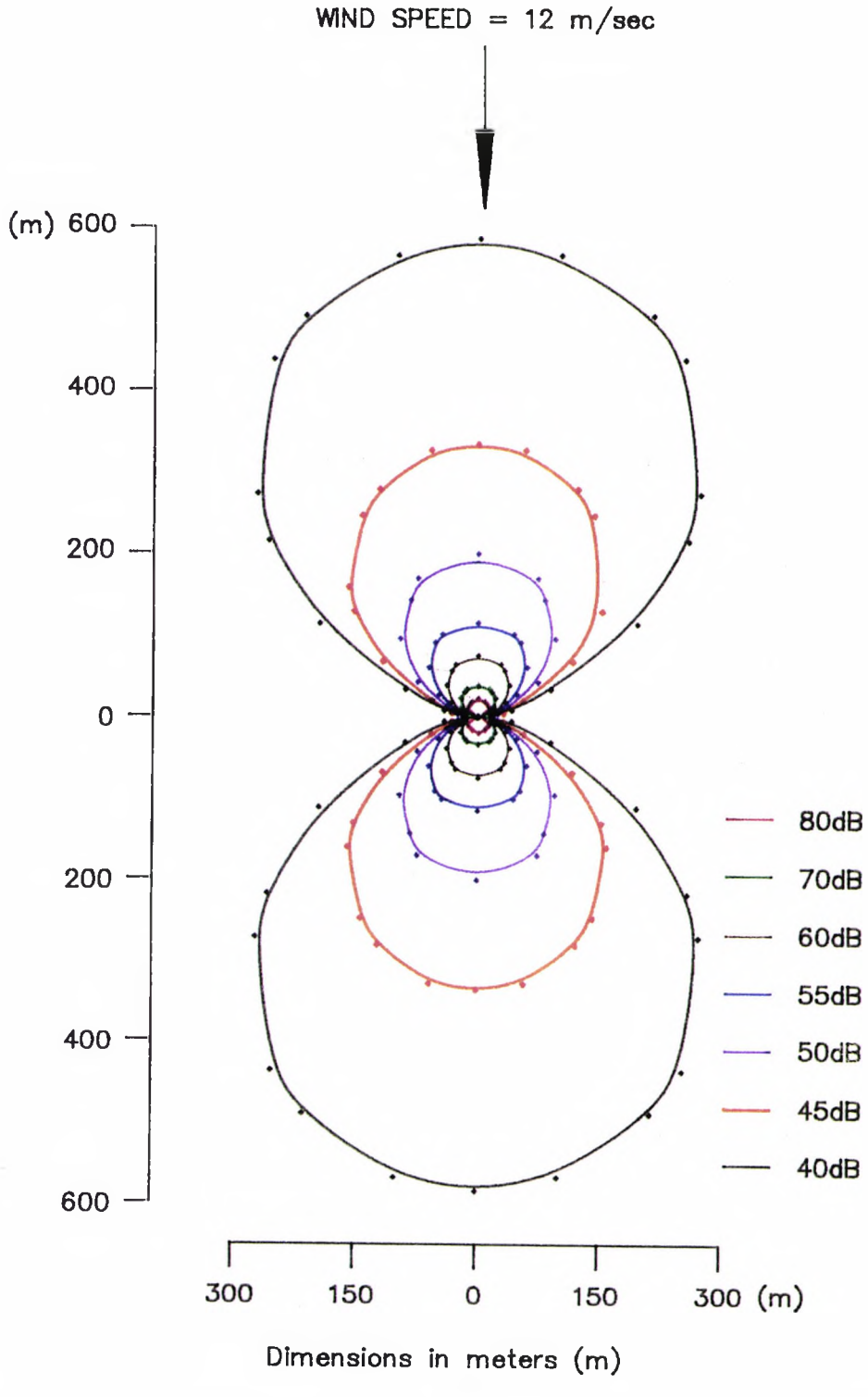

Fig 7.17 Predicted equal pressure contours for one MS-1 machine by WTGNOISE.

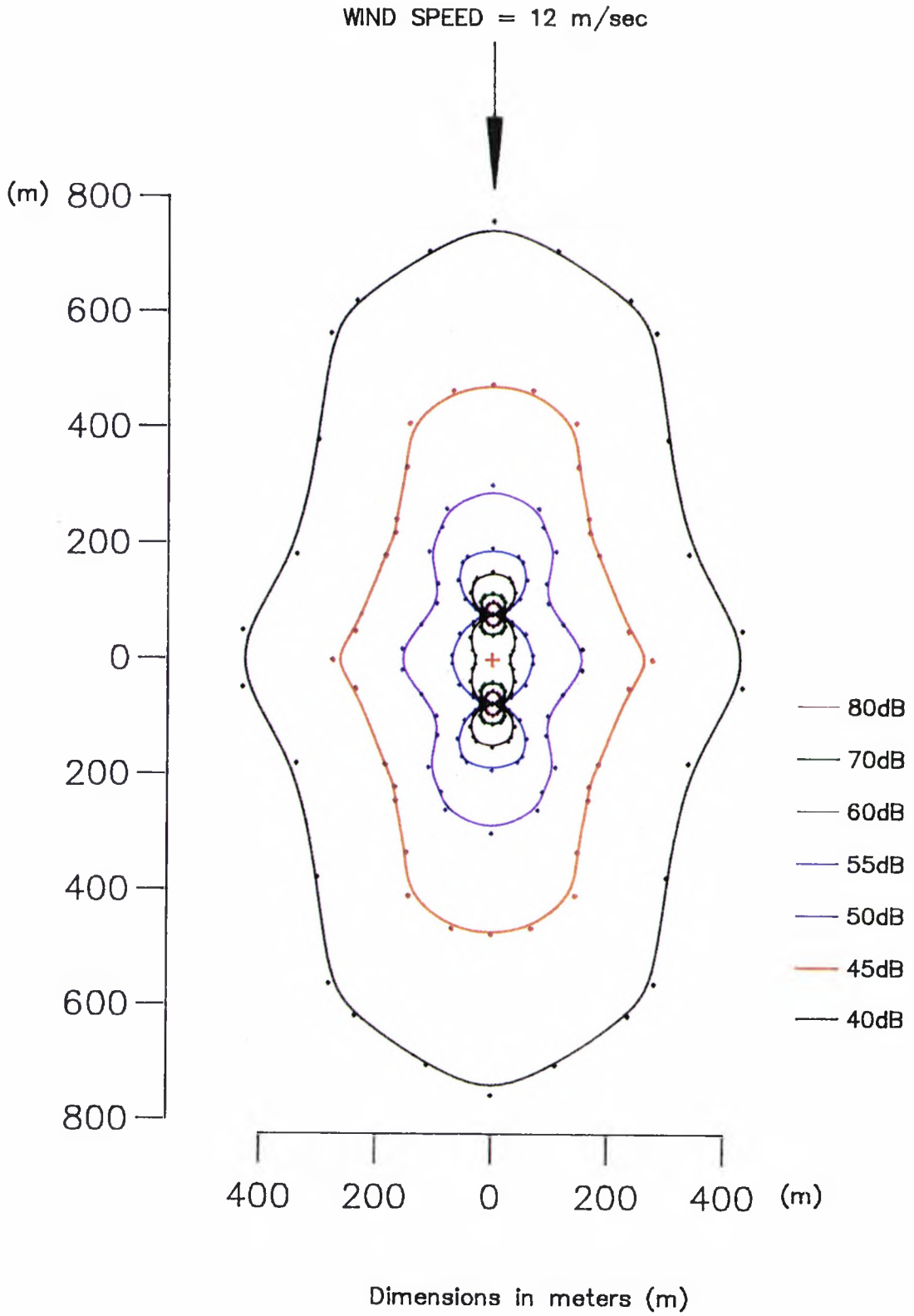

Fig 7.18 Predicted equal pressure contours for two MS-1 machine by WTGNOISE.

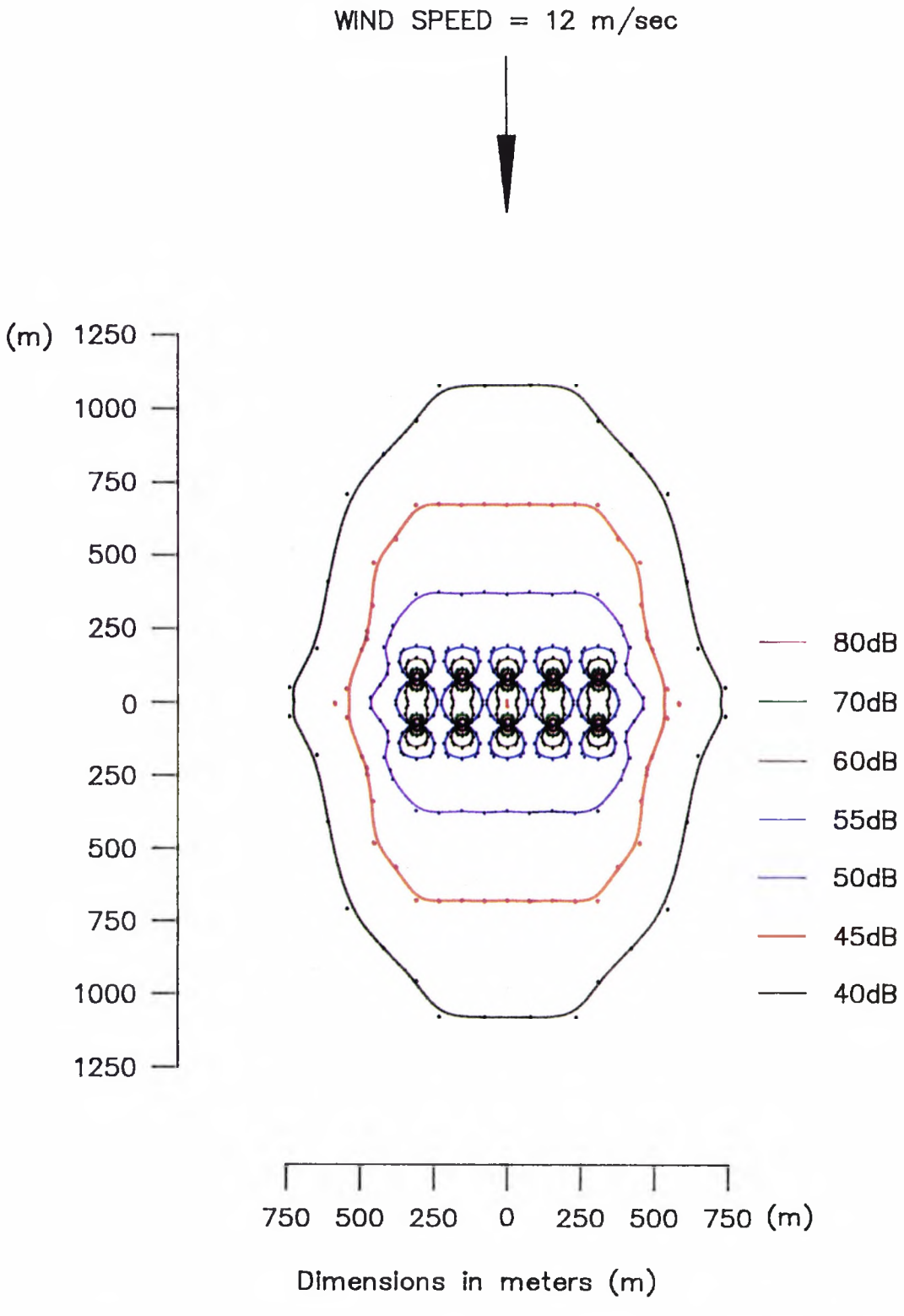

Fig 7.19 Predicted equal pressure contours for Wind Farm of 10 machines MS-1 by WTGNOISE.

7.5 Case study for wind farm

Much attention has been focussed on building wind farms in various European countries. Some wind farms are currently operating and their performance is being evaluated [84-88]. A comparison is now made of the basic noise output from two wind farms, one having a large number of small machines [83] and one having a smaller number of larger machines [89-91].

To do this, two existing machines have been chosen, namely the Vestas 25-200 for the smaller wind turbine and the machine based at Näsudden in Denmark for the larger [83], [89].

A brief description of the specifications of the two machines appears in Appendix 3

Machine Type	Vestas 25-200	Näsudden
Rated power (kW)	200	2000
Measured noise level db(A) for one machine at Ref point 1	57	69.9

A group of 10 Vestas machines is compared with a single Näsudden machine because the total nominal output power is the same in each case. The Vestas machines are placed together in two rows, as in Fig 7.20 where the distance between the machines is 7 rotor diameters.

The following assumptions are made.

1 There is no coherence in the noise spectra between the machines, and the source is a point source.

2 The position of measurements in both cases is compatible with the standard i.e at Reference point 5 (see Fig 5.11), at a distance from the machine of $2\times(h+ D/2)$.

3 Although there is an increase in turbulence level within a wind farm [84] it will have a limited effect on the noise level because of the relatively large distances between the machines (7D) . The higher frequencies, particularly, will be absorbed in to the atmosphere. Noise from this turbulence is therefore assumed negligible.

4 The wake from an upwind machine does not affect the acoustic output of a downwind machine [85].

5 For output power there will be an array efficiency normally of 95% [92] for the Vestas machine, which decreases the overall output power by about 2.5%, but it is assumed that this can be neglected, thus the output power from the group of small machines and that from the single large machine are assumed to be equal.

6 The height of the machine is quite significant in determining the noise level at a distance; increasing

the source height increases the noise level. It has been suggested in reference [19] that an increase of up to 3dB(A) is expected due to spherical spreading, for an increase in source height from 20m to 50m. This is added to the higher source i.e the Näsudden machine. See Section 2.4.5, and Fig 2.9.

7 Increase in wind speed with height for the Näsudden machine due to height of rotor will increase the noise level but it is difficult to quantify here because it depends on the direction of wind, the atmospheric conditions and the topography of the site [19], [59], [60]. The effect was assumed from Reference [19] to be around 1 dB(A) for a difference in wind speed from 10 to 15 m/s in the case of an upwind rotor.

Based on measurment of the original noise level emitted from one Vestas machine at reference point [1] of 57 dB(A) by Henningsen [83], it was found that the overall noise level of the 10 Vestas machines was 61 dB (A) at a contour passing through all the outer reference points [5] for the individual machines. This is smaller than that for the single large Näsudden machine [89] by about 7dB(A), measured at the same reference point.

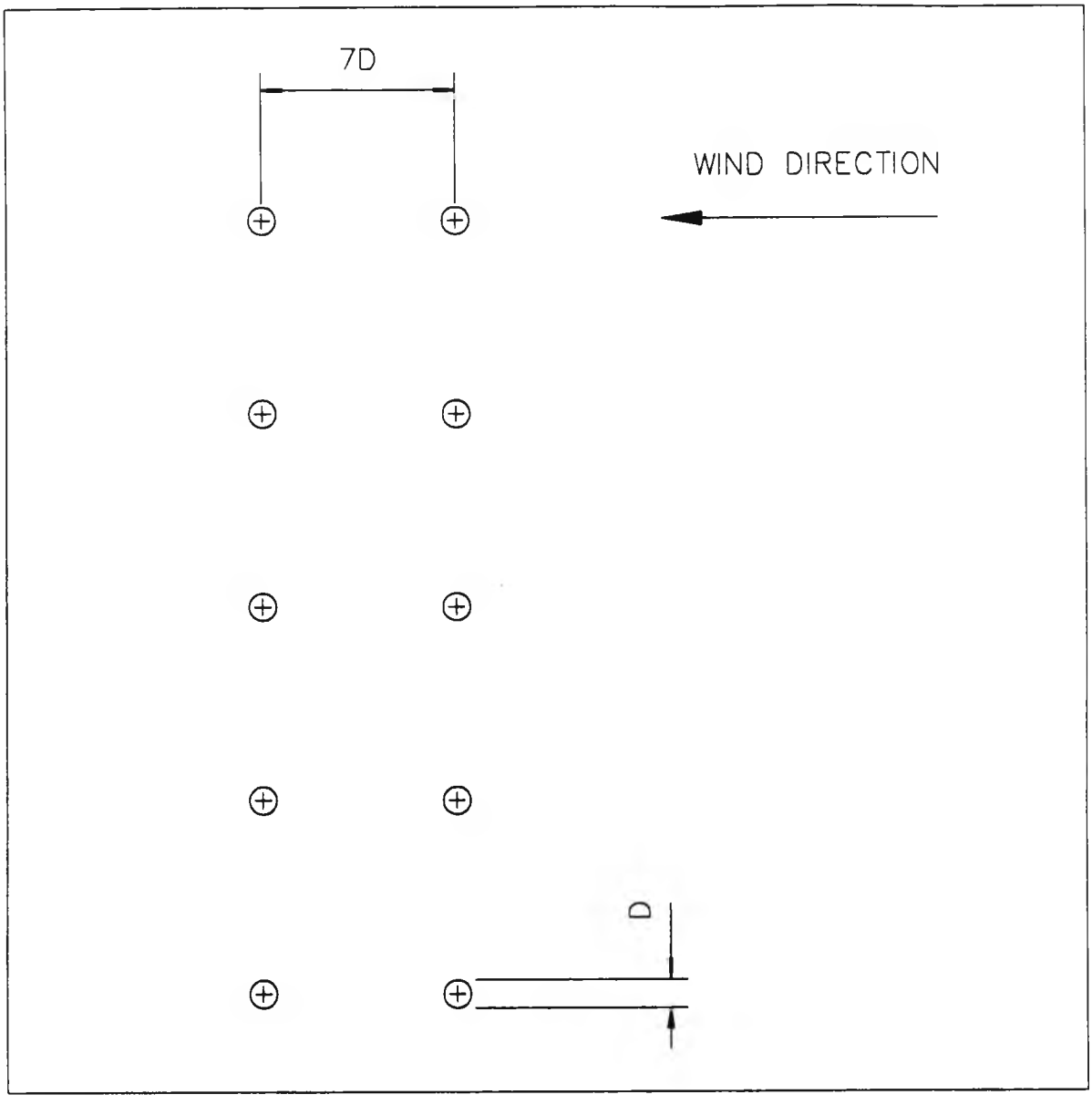

Fig 7.20 Wind farm of 10 Vestas V25-200kw 7D apart.

Fig 7.21 represents the relation between the noise level and output power in each case. Figs 7.22 and 7.23 show the expected noise level at the edges of areas surrounding the two cases, where each succeeding countour is double the distance from the source of the proceding contour. Fig 7.22 shows that for the Näsudden machine at the edge of area 1 the noise level is 67.9 dB(A) based on measurement [89]. At twice the distance from the machine, from application of basic noise theory and adjustment for the specific characteristics, i.e as regards the height of the machine and the wind speed at the higher level, the expected noise level is 65.9 dB(A) at the edge of area 2, using the same procedures, and at the edge of area 3 the noise level is found to be 63.9 dB(A).

The area of each noise level is quoted together with the noise level in table 7.3.

Table 7.3

Noise level and corresponding area for the Näsudden machine

Contour	1	2	3
Noise level dB(A)	67.9	65.9	63.9
Areas corresponding (m^2)	16.47×10^4	65.89×10^4	26.35×10^5

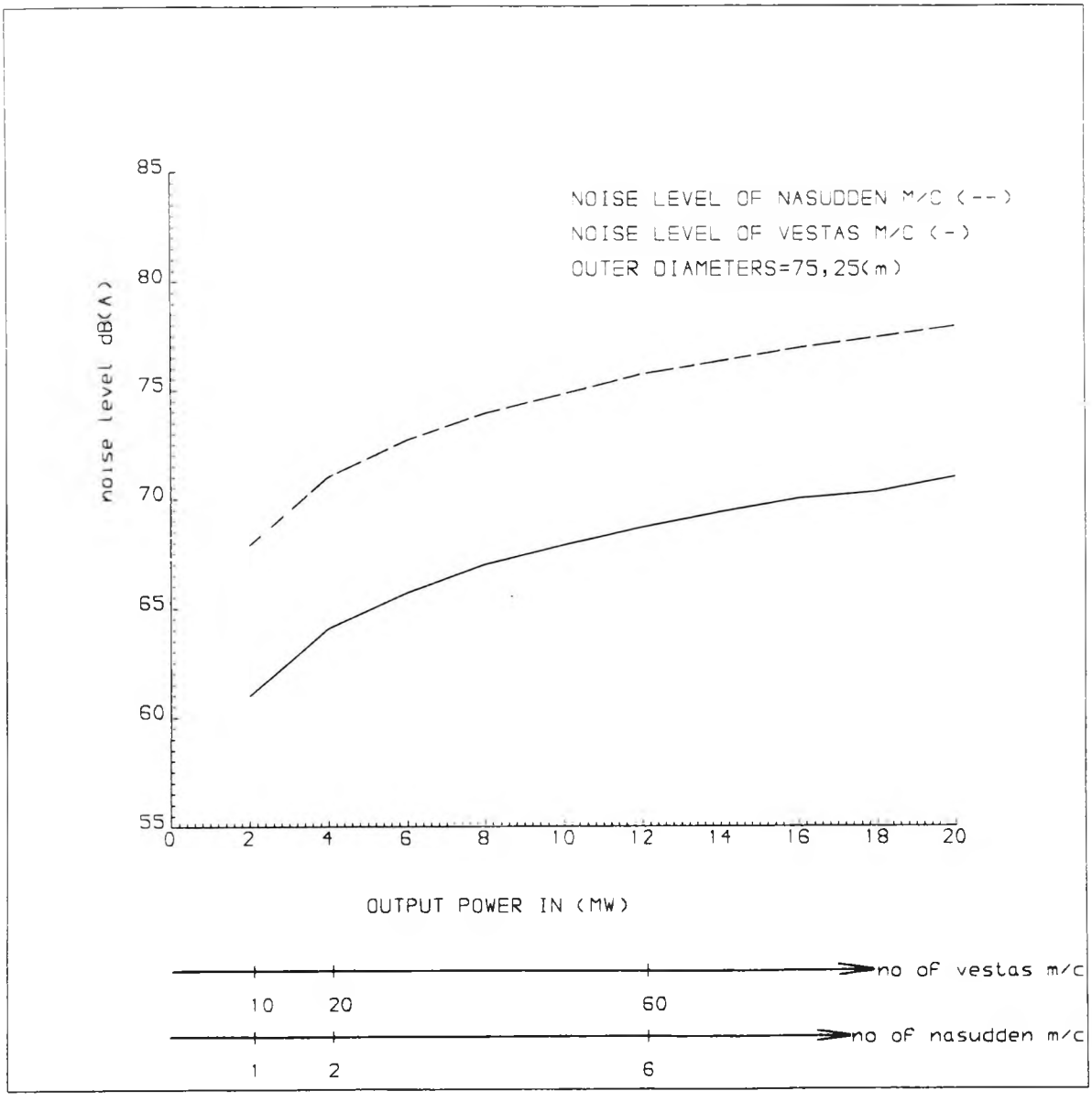

Fig 7.21 Effect of two different sizes of machine on noise level, calculated at Reference point [5], distance 2(h+D/2) from the machine where h=height of the machine and D/2=radius

point [5] =2(h+D/2) case of VESTAS=85(m)

point [5] =2(h+D/2) case of NÄSUDDEN=229 (m)

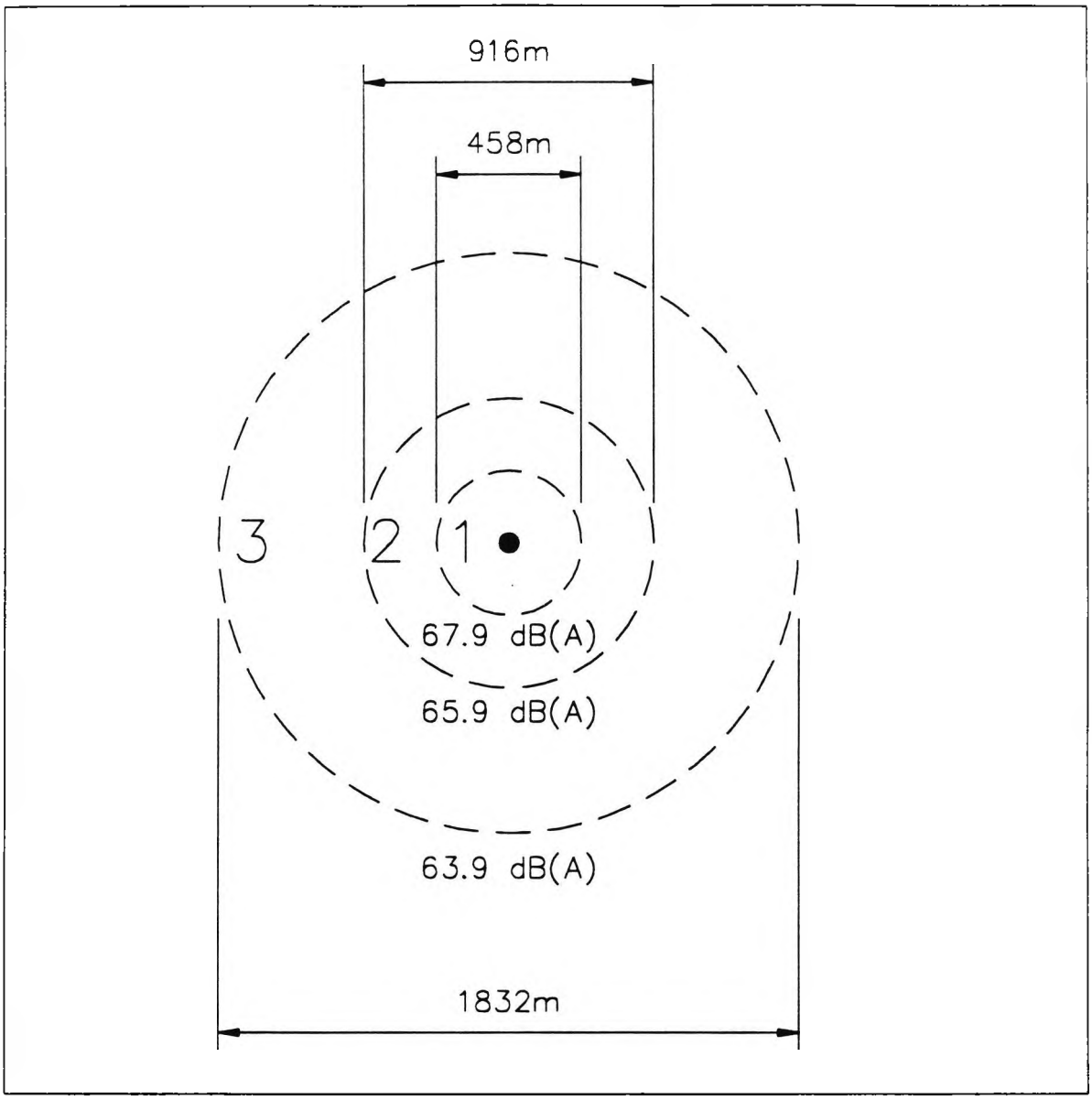

Fig 7.22 Calculated noise levels around the Näsudden machine.

Fig 7.23 shows the expected noise levels at circumferences around the Vestas machine layout. It indicates that at the edge of area 1, which was obtained by a contour passing through all the outer reference points [5] for the individual machines, the noise level is about 61 dB(A); at twice the distance the expected noise level is 55 dB(A) at edge of area 2, whilst at edge of area 3 it is 49 dB(A).
The area of each noise level is quoted togather with the noise level in Table 7.4 for the group of Vestas machines.

Table 7.4

Noise level and corresponding area for a group of Vestas machines.

Contour	1	2	3
Noise level dB(A)	61	55	49
Areas corresponding (m^2)	54.08×10^4	14.35×10^5	52.41×10^5

Fig 7.24 shows the two arrangements superimposed. The projected plots of noise levels in two orthogonal directions clearly show that the group of Vestas machines is overall quieter than a single Näsudden machine for the same power output.
It should be borne in mind, however, that the calculation for the Näsudden machine is based on the worst case scenario which is that the low frequency component is not absorbed in the atmosphere. In a real life comparison of the two configurations, the specific characteristics of

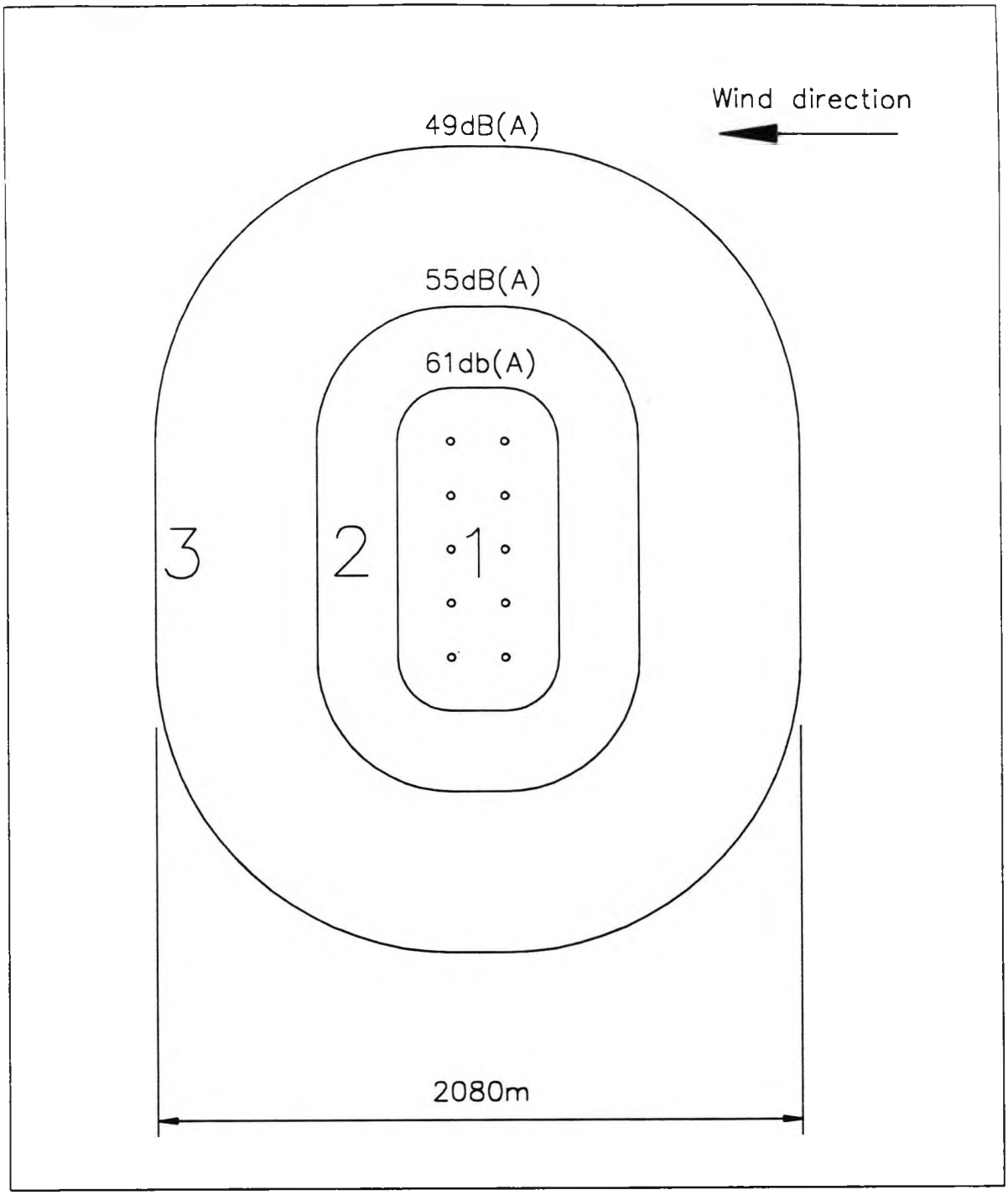

Fig 7.23 Calculated noise levels around the Vestas machine.

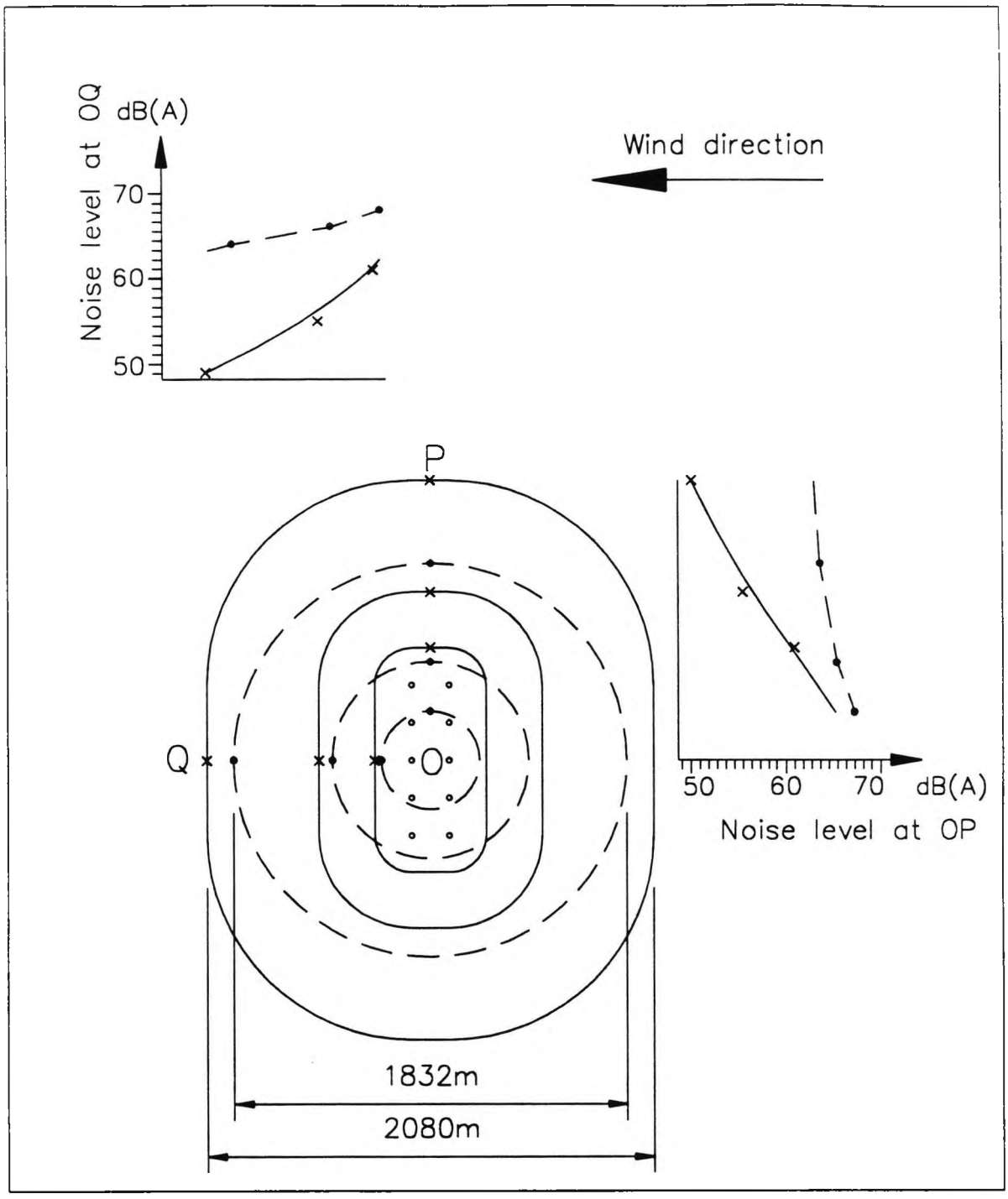

- - - - - - - **NÄSUDDEN** ——————— **VESTAS**

Fig 7.24 Diagrammatic sketch of the three areas around the machines showing that noise from the single big machine is higher everywhere.

each site (topography, ground type, landscape, average wind speed, etc..) would also have to be taken into account.

On the basis of Tables 7.3 and 7.4 a wind farm of smaller machines is less noisy than a single big machine.

A further comparison has been undertaken. In this, groups of smaller Vestas machines are compared with groups of the larger Näsudden machine having the same overall power output. The conclusion from this exercise is that a group of smaller machines is quieter then a group of larger machines having the same output power.

It is assumed that machines are placed together in two rows, and the distance between the machines is 7D (where D is the diameter of the rotor).

The expected noise level is taken at a contour passing through all the outer reference points [5], distance 2(h+D/2) from the machine, for the individual machines.

Table 7.5 Comparison of groups of machines having the same output power.

Table 7.5

Output power (kW)	2	8	12	16	20
No of Vestas m/c	10	40	60	80	100
No of Näsudden m/c	1	4	6	8	10
dB(A) for Vestas	61	67	68.7	70	71
dB(A) for Näsudden	67.9	73.9	75.7	76.9	77.9

CHAPTER

8

CONCLUSIONS AND SUGGESTIONS FOR FURTHER WORK

CONCLUSIONS

1 A study had been conducted on one of the most important environmental problems in wind turbines, namely noise. It includes a study of the parameters affecting the noise emission of wind turbines, and a review of existing computer codes. It entailed development of a computer code (WTGNOISE) for the prediction of noise from a machine at the design stage. This code was verified through detailed noise emission measurements made on the experimental machine at Lords Bridge near Cambridge under a variety of conditions.

2 The computer code WTGNOISE enables the prediction of noise levels from a wind turbine, and thus enables the differentiation between two different designs from a noise point view. It allows the prediction of noise level from different types of aerofoil sections, which is useful in the design of wind turbines. The new computer code takes into account the specific characteristics of wind turbines and the specification of the rotor blades, the accurate calculation of the dynamic forces on the blade, the observer's position and height, and also the height of the wind turbine. The program WTGNOISE was a vital tool in the current research work.

3 The overall results from WTGNOISE indicates that there is an acceptable agreement between measurements taken at the Cambridge site and the code.

4 Referring to the Cambridge machine, mechanical noise contributes significantly to the overall noise level, because it is a small wind turbine machine operating at low wind speeds. Using standard data analysis techniques, it is possible to trace the cause of mechanical noise and vibration.

5 Upwind rotor wind turbines have an advantage over downwind rotors, from the noise level emission point of view. Upwind rotors are characterized by a swishing sound, which is more acceptable than discrete tonal noise components that arise from the thumping sound emitting from a downwind rotor. Any device which reduces the disturbed wake behind the tower structure of a downwind rotor will also improve the acoustic emission of the rotor. A significant noise reduction could be achieved in downwind turbine generators without compromising performance by changing the structural configuration of towers to have a smoother wake.

6 The rotational speed is the single most important factor in determining the noise level of the wind turbine generator. By using the computer code to predict the noise level of MS-1 at a rotational speed of 88 rpm, it is shown possible to reduce that noise by 5 dB(A) by reducing rotational speed to 66 rpm. The effect of the rotational speed on the noise level is clear, but the problem is that any reduction on the rotational speed also reduces the output power. It is recommended here to use machines having two speeds, the slower for use at night when quieter operation is desired, but required power consumption is lower, and the faster for use during the day when the converse applies.

Three bladed rotors are less noisy than two bladed because of the lower tip speed ratio.

7 It can be seen that the peak aerodynamic pressures on the blades have a great effect on the noise level emitted from the machine, and thus any reduction of these peak pressures will be advantageous. Thus the type of aerofoil has been found to be important in determining the noise level emitted from a machine. Aerofoil designs GH1 and GH2 have been found to be less noisy than LS-1.

8 It has been found that increasing the chord decreases the overall noise level emitted from the machine.

9 In regard to the leading edge, a larger leading edge radius leads to lower peak pressures at the leading edge, and thus, less noise.

10 Based on the wind farm study in Chapter 7 it was found that a number of small machines are less noisy than an equivalent group of larger machines having the same overall power output.

The following areas for further work are suggested.

1 The development of WTGNOISE to include the effects of topography and landscaped effect as well as atmospheric pressure and gust conditions.

2 The development of an extension of WTGNOISE to include wind farm conditions with validation by detailed measurements on a wind farm.

3 The development of a further series of aerofoils designed especially for quietness, including appropriate experimental tests.

REFERENCES

[1] **LYNETTE, R.** "Status of the U.S. Wind Power Industry", BWEA 10th Annual Conference, London, March, 1988.

[2] **MEIR, R.A.** "The NFFO-a Department of Energy view", Thirteenth BWEA Wind Energy Conference 1991.

[3] **MOYNIHAN, C.** "The Non Fossil Fuel Obligation" Renewable Energy View issue 17 (s) Department of Energy. December 1991.

[4] **SWIFT-HOOK, D.T. and LINDLEY, D.** "Wind Energy and Environment", IEE Energy Series 4 ISBN 086341 1762 pp 1-5.

[5] **BERKHUIZEN, J.C. and SLOB, A.F.L.** "The Impact of Environmental Aspects on Wind Energy in Netherlands", IEE Energy Series 4 ISBN 086341 1762 pp 7-9.

[6] **WILLIAMS, G.J.** "Preliminary Review of the Effect of Wind Turbine Noise on the Achievable Wind Energy Resource in Cornwall". Wind power Co U.K. 1987.

[7] **MILTON KENES DEVELOPMENT CORPORATION** "Social Implication of a Wind Driven Generator Located in a

Residential Area". University of Southampton ETSU WN 5097-P1. 1989.

[8] **JOHN, W.** "Wind Energy Farm noise on nearby Residence the Citizen's View". U.S.A. 1983.

[9] **KEVIN, P.S., GROSVELD, F.W. and STEPHENS, D.G.** "Evaluation of Human Exposure to the Noise from Large Wind Turbine Generator" Noise Control Engineering Journal, July-August 1983.

[10] **DOWLING, A.P. and FFOWCS WILLIAMS, J.E.**" Sound and Sources of Sound". Ellis Horwood Limited 1983.

[11] **CHUNCHUZOV, I.P.** "Field of a Low Frequency Point Source of Sound in an Atmosphere with a nonuniform Wind-Height Distribution". American Institute of Physics, July-August 1984.

[12] **HEMPHILL, R.** "An Acoustic Ranging Technique with Application to Assessment of low Frequency Acoustic Noise of Wind Turbines" SERI/TP-215-1954 DE83009406 May 1983.

[13] **WILLIAM, W.L. and ZORUMSKI, E.W.** "Low Frequency

Acoustic Propagation in High Winds" NASA Langley Research Center, Hampton, Virginia 1990.

[14] **PIERCY, J.E. and EMBLETON, T.F.W.** "Review of Noise Propagation in the Atmosphere". Division of Physics,National Research Council Ottawa, Canada.1977 Acoustic Society of America March 1977.

[15] **RICHARDS, E.J. and MEAD, D.J.** "Noise and Acoustic Fatigue in Aeronautics" John Wiley & Sons Ltd, london.1977

[16] **BERANEK, L.L.** "Acoustics" Mc Graw-Hill Book company 1954.

[17] **SHARLAND, I.** "Woods Practical Guide to Noise Control" Woods of Colchester Limited. May 1972.

[18] **HUBBARD, H.H., GROSVELD, F.W. and KEVIN, P.** "Noise Characteristics of Large Wind Turbine Generators". Noise Control Engineering Journal, July - August 1983. pp21-29.

[19] **PINDER, J.N., PRICE, M.G. and SMITH, M.G.** "The Prediction of Noise from Wind Turbine with Regard to

Community Disturbance" Contractor Report ETSU WN 5066,U.K. 1990

[20] **EMBLETON, T.F.W, PIERCY, J.E, and DAILE, G.A.** "Effective flow Resistivity of ground Surfaces determined by acoustical measurements" J.Acoust. Soc. Am. 74 (4), October 1983.

[21] **DELANY, M.E. and BAZLEY, E.N.** "Acoustical Properties of Fibrous Absorbent Materials" Applied Acoustics pp 105 -116 (3) (1970).

[22] **ANDERSON, J.** "Noise its Measurement, Analysis,Rating and Control". Course at Department of Mechanical Engineering, City University, London U.K. 1990

[23] **SHEPHERD, K.P. and HUBBARD, H.H.** "Sound Propagation Studies for a Large Horizontal Axis Wind Turbine". NASA Contractor Report 172564 March 1985.

[24] **KRISHNAPPA, G.** "Noise and Vibration Measurement of 50 KW Vertical Axis Wind Turbine Gear Box" Noise Control Engineering Journal, January-February 1984.

[25] **LIGHTHILL, M.J.** "Sound Generated Aerodynamically". Proc

Roy Soc. London. A Vol. 267,no. 1329,may 8, 1962, pp.147-182.

[26] **KEAST, D.N.** and **POTTER, R.C.** "A Preliminary Analysis of the Audible Noise of Constant-Speed Horizontal Axis Wind Turbine Generator" U.S.Department of Energy Report No DOE/EV-0089, July 1980.

[27] **KELLEY, N.D.** "Acoustic Noise Generation by the DOE/NASA MOD-1 Wind Turbine". SERI/TR-635-1240 June 1983.

[28] **GUTIN, L.** "On the Sound of a Rotating Propeller". NACA Technical Memorandum No 1195, 1948.

[29] **ETTER, C.L., KELLEY, N.D., MCKENNA, H.E, LINN, C.** and **GARRELTS, R.** "Acoustic Measurement of DOE/NASA MOD-O Wind Turbine at Plum Brook Station Ohio" SERI/TR-635-1240, DE83011971 Golden, Colorado, June 1983.

[30] **KELLEY, N.D.** "Noise Generated by Large Wind Turbine" Paper presented at the Wind Energy Technology Conference, 16-17 March, 1981, Kansas City,U.S. 12 pp.

[31] **KELLEY, N.D., MCKENNA, H.E., JACOBS, E.W., HEMPHILL, R.R.**

Roy Soc. London. A Vol. 267,no. 1329,may 8, 1962, pp.147-182.

[26] **KEAST, D.N. and POTTER, R.C.** "A Preliminary Analysis of the Audible Noise of Constant-Speed Horizontal Axis Wind Turbine Generator" U.S.Department of Energy Report No DOE/EV-0089, July 1980.

[27] **KELLEY, N.D.** "Acoustic Noise Generation by the DOE/NASA MOD-1 Wind Turbine". SERI/TR-635-1240 June 1983.

[28] **GUTIN, L.** "On the Sound of a Rotating Propeller". NACA Technical Memorandum No 1195, 1948.

[29] **ETTER, C.L., KELLEY, N.D., MCKENNA, H.E, LINN, C. and GARRELTS, R.** "Acoustic Measurement of DOE/NASA MOD-O Wind Turbine at Plum Brook Station Ohio" SERI/TR-635-1240, DE83011971 Golden, Colorado, June 1983.

[30] **KELLEY, N.D.** "Noise Generated by Large Wind Turbine" Paper presented at the Wind Energy Technology Conference, 16-17 March, 1981, Kansas City,U.S. 12 pp.

[31] **KELLEY, N.D., MCKENNA, H.E., JACOBS, E.W., HEMPHILL, R.R. a**

BIRKENHEUER, N.J. "The MOD-2 Wind Turbine: Aeroacoustical Noise Sources, Emissions, and Potential Impact" SERI/TR-217-3036 DE88001132, January 1988

[32] **ANDERSEN, B. and JAKOBSEN, J.** "Noise Emission from Wind turbine generator a measurment method" Danish Acoustic Institute Report No 109, 1983.

[33] **GLENDINNING, A.G.** "Noise from Wind Turbine Generator" Ms c Thesis Southampton University 1983.

[34] **WELLS, R.J.** "GE MOD-1 Noise Study" General Electric Company Corporate Research and Development, Schenectady, New York 12301 U.S.A.

[35] **KELLEY, N.D.** "Acoustic Noise Generation by the DOE/NASA MOD-1 Wind Turbine" Wind Energy Branch, Solar Energy Institute Golden, Colorado 80401, SERI/TR-635-1240 June 1983.

[36] **GNEMMI, P., HAERTIG, J. and SCHAFFAR, M.** "Aerodynamic Load and Blade Vortex Interaction Noise Prediction". Vertica Vol. 14 No 2, pp 137-15.

[37] **LINDLEY, D., GARRAD, A. and GLEGG, S.A.** "Noise Prediction Programme for Wind Turbines" Report No TWC 8218, for the Department of Energy, December 1984.

[38] **FFOWCS WILLIAMS, J.E. and HAWKINGS, D.L.** "Sound Generation by Turbulence and Surface in Arbitrary Motion" Proc. Roy. Soc. London,Vol.264 A, May 8, 1969, pp 321-342.

[39] **FARASSAT, F.** "Theory of Noise Generation from Moving Bodies with an Application to Helicopter Rotor" Langley Research Center Hampton , NASA TR R-451 Washington, D.C. December 1975.

[40] **METZGER, F.B. and KlATTE, R.J.** "Downwind Rotor Horizontal Axis Wind Turbine Noise Prediction" Hamilton Standard Division Technologies Corporation, NASA Conference Publication 2185, 1981.

[41] **GREENE, G.C. and HUBBARD, H.H.** "Some Calculated Effects of Nonuniform Inflow on the Radiated Noise of a Large Wind Turbine" NASA TM 81813, Langley Research Center May, 1980.

[42] **NYSTROM, P.A. and FARASSAT, F** "A Numerical Technique for Calculation of the Noise of High Speed Propellers with Advanced Blade Geometry" NASA Technical paper 1662, 1980.

[43] **GREENE, C.G.** "Measured and Calculated Characteristics of Wind Turbine Noise" NASA Langley Research Center Virginia. NASA Conference Publication 2185, 1981.

[44] **SPENCER, R.H.** "Noise Generation of Upwind Rotor Wind Turbine Generators" The Boeing Vertol Company Philadelphia. NASA Conference Publication 2185, 1981

[45] **MARTINEZ, R., WIDNALL, S.E. and HARRIS, W.L.** "Prediction of low Frequency and Impulsive Sound Radiation from Horizontal Axis Wind Turbines" Massachusetts Institute of Technology Cambridge, U.S.A., NASA Conference Publication 2185, 1981.

[46] **VITERNA, L.A.** "The NASA-LERC Wind Turbine Sound Prediction Code". NASA Lewis Research Center Cleveland, Ohio, U.S.A., NASA Conference Publication 2185, 1981.

[47] **HOUSE, M.E.** "Wind Turbine Prediction Program" The University of Southampton, Institute of Sound and

Vibration Research, Wolfson Unit for Noise and Vibration Control, 1988.

[48] **KEISLER, H.J.** "Elementary- An infitesimal approach" PWS Publishers 1990.

[49] **JONES, D.S. and JORDAN, D.W.** "Introductory Analysis "Volume 1, Volume 2 John Wiley& Sons.

[50] **DONE, G.T.S. and KAWADRI, J.** "Dynamics and Wind Turbine Design" BWEA Conference London, March 1988.

[51] **GARRAD HASSAN. and Partners** Bristol England, U.K.

[52] **EDMUND JOHN FORDHAM, M.A.** "Atmospheric Turbulence in Relation to Horizontal Axis Wind Turbines and the Construction of two Research machines". University of Cambridge, Ph.D thesis, August 1984.

[53] **ANDERSON, M.B.** "An Experimental and Theoretical Study of Horizontal Axis Wind Turbine".University of Cambridge, Ph.D thesis, June 1981.

[54] **ABBOTT, I.H. and DOENHOFF, A.V.** "Theory of Wings Sections". Dover Publication,New York 1956 .

[55] **HENDERSON, A.R.** "Environmental Aspects of Wind Turbine Generators. Part-1 Development of a Practical Standard for the Measurement of Acoustic Noise Emission from Wind Turbine". National Wind Energy Turbine Center, Contract No 85-B-7033-11-1004-17, U.K.

[56] **LJUNGGREN, S. and GUSTAFSSON, A.** "International Energy Agency: Recommended paractices 4. Measurment of noise emission from Wind turbine" IEE Energy Series 4 ISBN 086341 1762 pp 31-58. 1989

[57] **BEEK, A.VAN.** "Wind Turbine Noise" Proceeding of the Thirteenth BWEA Wind Energy Conference PP 53-57 1991.

[58] **MARTINEZ, R., WIDNALL, S.E. and HARRIS, W.L.** "Prediction of low Frequency and Impulsive Sound Radiation from Horizontal Axis Wind Turbines" NASA Conference Publication 2185, 1981.

[59] **KELLEY, N.D., MCKENNA, H.E., HEMPHILL, R.R., ETTER, C.L., GARRELTS, R.L., and LINN, N.C.** "Acoustic Noise Associated with the MOD-1 Wind turbine: Its Source,Impact and Control, SERI/TR-635-1156, 1985.

[60] **ELLIOT, B.L.** "Noise emission from a 25 meter vertical axis Wind turbine - its measurment and assessment" IEE Energy Series 4 ISBN 086341 1762 pp 73-80. 1989

[61] **ELLIOT, B.L.** "Noise level at CEGB Wind Turbine Demonstration centre, Carmathen bay, South wales" Conference publication EWEC pp 449-451 1989.

[62] **HARRISON, L.** "Wind Power Monthly" Vol.6 No.8 August 1990. ISSN 0109-7318

[63] **STEPHENS, D.G, SHEPHERD, K.P, and FERDINAND, G.** "Wind Turbine Acoustic Standards" NASA Conference Publication 2185, 1981.

[64] **SCHLICHTING, H.** "Boundary Layer Theory", McGraw-Hill, 1968

[65] **GARRAD, A.** "New Aerofoils and Some Thoughts on Wind Turbine Aerodynamics" Garrad Hassan and Partners. BWEA Workshop on Recent Developments in Aerodynamics, Nottingham Feb 1990. (**eds : CLAYTON, B.R, DONE, G.T.S and HAINES, R**).

[66] **WILSON, R.E and LISSAMAN, P.** "Applied Aerodynamics of Wind Power Machines" July, 1974.

[67] **TWIDNELL, J and WEIR, T.** "Renewable Energy Resources" E.& F.N.Spon Ltd. London, 1986.

[68] **TAYLOR, R.H.** "Alternative Energy Sources" Adam Hilger Ltd Bristol,1983.

[69] **SATCHWELL, C and TURNOCK, S.R.**"Structurally Efficient Aerofoil Section for Use on Wind Turbines" , Proceedings of EWEC Conference in Glasgow 1989.

[70] **GARRAD, A.** Discussion with Author in 1990.

[71] **HILL, D.C and GARRAD, A.** "Design of Aerofoils for Wind Turbine use" Garrad Hassan and Partners. Bristol, EWEC Glasgow, U.K. July 1989.

[72] **TANGLER, J.L and SOMERS, D.M.** "A Low Reynolds Number Airfoil Family for Horizontal Axis Wind Turbines", Proceedings of Royal Aeronautical Society International Conference on Low Speed Aerodynamics 1986.

[73] **GRAHAM, M.R and KHOO, H.** " Stall Control of Wind Turbine Blades" ETSU WN 5095. 1990.

[74] **GARRAD, A.D.** "Dynamic of Wind Turbines" IEE

Proceedings, Vol. 130, December 1983.

[75] **GARRAD, A.D.** "An Approximation Method for the Dynamic Analysis of Two Bladed Horizontal Axis Wind Turbine Systems". 4th International Symposium, on Wind Energy Systems, September 1982.

[76] **COTON, F.N and GALBAITH, R.A.McD.** "An Aerofoil Design Mythology for low speed Aerofoil" BWEA Conference London March 1988.

[77] **MONTGOMERIE, B.** "Blade Design using Computer Aided Parameter Variation" The Aeronautical Research Institute of Sweden 1989.

[78] **INGHAM, P, ARCH, N and MOLLER, P.A.** "Aerodynamic Design of Rotor Blades for the Horizontal Axis type of Wind Turbine". BWEA Conference Publication 1987.

[79] **MILLER, R.H.** "The Aerodynamic and Dynamic Analysis of Horizontal Axis Wind Turbine" Journal of Wind Engineering and Industrial Aerodynamics,1983 pp329-340.

[80] **RENNE, D.S and BUCK, J.W.** "Studies of the Wake of a DAF 500-KW Vertical Axis Wind Turbine at Southern California Edison's Wind Energy Test Facility". Southern California Edison Company, Rosemead, California. U.S. 1990.

[81] **AMIET, R.K.** "Acoustic Radiation from an Airfoil in a Turbulent Stram". Journal of Sound and Vibration, 1975, 41(4), pp407-420.

[82] **HAMMER, J.D.G.** "100 Practical Application of Noise Reduction Methods" Her Majesty's Stationery Office.London

[83] **HENNINGSEN, P. Vestas System A/S** "Noise Emission from a Vestas V 25-200 KW (50 Hz) Wind Turbine" Report No T8.029.88, 1988.

[84] **HOJSTRUP, J.** "Turbulence Measurement in a Wind Farm" Department of meteorology, RISO National laboratory, Roskilde,Denmark BWEA 1990, PP 59-63.

[85] **HUTTING, H.K and KEMA, N.V.** "Main Results of the Research Program of the Dutch Experimental Wind Farm" The Netherlands, 1991.

[86] **HOJTRUP, J** "Turbulence Measurment in a Windfarm" Proceeding of the Twelfth BWEA Wind Energy Conference pp 59 - 63 1990.

[87] **LARKE, C and WOODBRIDGE, A.** "Toward Equitable Solution to siting and Noise problems in Windfarm" BWEA Annual Conference SWANSEA, April 1991

[88] **DUIZEND, J.** "Two new Windfarms in holland;all that had gone before" Conference publication EWEC pp 427-431 1989.

[89] **LJUNGGREN, S.** "A Preliminary Assessment of Environmental Noise from Large WECS, Based on Experiences from Swedish Prototypes", 1984.

[90] **LJUNGGREN, S.** "The Swedish Solution of the Noise Problem: Wind Turbine with Variable rpm". National Energy Administration Stockholm, Sweden, 1987.

[91] **LJUNGGREN, S.** "Analysis of the Environmental Noise Situation Around a large Swedish Prototype Wind Turbine". FFA TN 1988-16 Sweden, 1988.

[92] **GARRAD, A.** Discussion with Author in June 1991

APPENDIX [1]

WTGNOISE The computer code for calculation of noise emitted from a Wind turbine .

WTGNOISE

The Horizontal axis Wind turbine noise Code

```
c     this program is to calculate noise from Horizontal axis
c     Wind Turbine the theoretical work depend on FARASAT report
c
c       SOME TERMS USED IN PROGRAM
c      OMEGA:rotor speed
c      DENS :air density
c      SOUND:speed of sound in m-sec
c      LR   :Lr force
c      MR   :Mr mach number
c      DELSI: delta Si
c      R    :radius
c      VN   :incoming wind speed
c      PRESS:Pi the pressure
c      DELT :delta time  - time increment
c      NSTAT:No of stations
c      RO   =outer diameter
c      DELR =delta R
c      PI   =22/7
c      XMIC =distance from observer to HAWT in X direction
c      YMIC =   "      "     "      "   "    "Y    "
c      VEL  =tangential velocity at specific point
c       T   =temperature(air)
c       po  =atmospheric pressure
c       Q   =constant
c      sound=[Q*po/DENS]**.5
c        Q = 1.402
c        po=1.013*10**5 pa
c        DENS=1.293 kg/m**3   ,Q,po,DENS  at 0 temp c
       REAL  MR,LR,Y1,Y2
       DIMENSION AR(60)
       COMMON/ALLDATA/THT,RI,RO,R,DENS,SOUND,VN,DELR,PI,OMEGA,
      &DELSI,XMIC,YMIC,TEMP,VEL(1000),VELX(1000),VELY(1000),
      &RX(1000),RY(1000),RR(1000),LR(1000),MR(1000),
      &DELT,HH(1000),Y1(1000),Y2(1000),NSTEP,NSTAT
       OPEN(4,FILE='INPUT')
       REWIND(4)
       READ(4,*)RI,RO,NSTEP,THTO,SPEED,TEMP,DELT,NSTAT
       READ(4,*),DENS,VN
       OPEN(3,FILE='RESULTC')
       REWIND(3)
       OPEN(9,FILE='TTFIN')
```

```
      REWIND(9)
      OPEN(10,FILE='res')
      REWIND(10)
      WRITE(3,10)'INNER RADIUS= ',RI
      WRITE(3,10)'OUTER RADIUS= ',RO
      WRITE(3,10)'INTIAL ANGLE THT= ',THTO
      WRITE(3,10)'ROTOR SPEED     = ',SPEED
      WRITE(3,10)'TIME STEP       = ',DELT
      WRITE(3,20)'NUMBER OF STEPS = ',NSTEP
      WRITE(3,20)'NUMBER OF STAT  = ',NSTAT
      WRITE(3,10)'DENS              = ',DENS
      WRITE(3,10)'VN                = ',VN
   10 FORMAT(/3X,A,F15.5)
   20 FORMAT(/3X,A,I5)
      SOUND=(331.6+0.6*TEMP)
      WRITE(3,10)'SOUND =',SOUND
C
C                  define position of observer
C
      DO 100 I=11,220,10
      XMIC=ZMIC
      XMIC=I
      ZMIC=I
      YMIC=2
      WRITE(3,10)'XMIC        =',XMIC
      WRITE(3,10)'YMIC        =',YMIC
      WRITE(3,10)'ZMIC        =',ZMIC
      PI=4.0*atan(1.0)
      THT=THTO*0.0174532
      OMEGA=SPEED*2*PI/60.0
      DELTHT=OMEGA*DELT
*        print*,'deltht= ',deltht

*       INCRE=2*PI/DELTHT
        INCRE=1440
        print*,'incre=',incre
      DELR=(RO-RI)/NSTAT
      DELSI=DELR
      CALL LMN
      CALL INTEG1(S1)
      CALL INTEG2(S2)
       TIME=0.0
       rewind(10)
      DO  200  K=1,INCRE
C
C                  Read forces on the blade
C                   using the forces code
C
       READ(10,*)Z,Z,(AR(I0),I0=1,21)
       DO 999 i0=1,21
       DO 999 i1=1,10
       i2=10*(i0-1)+i1
       lr(i2)=ar(i0)
```

```
999     CONTINUETHIS
        THT=THT+DELTHT
        TIME=TIME+DELT
C
       CALL LMN
       CALL INTEG1(S11)
       CALL INTEG2(S22)
       PRESS1=ABS(S11-S1)
       PRESS1=PRESS1/(DELT*SOUND)
       PRESS1=PRESS1*DELSI
       PRESS2=ABS(S22-S2)
       PRESS2=PRESS2*DELSI
       PRESS=PRESS1+PRESS2
       PRESS=PRESS
       PRESS=PRESS/(4*PI)
       PRESS=20*LOG10(PRESS/(2.0*10.0**-5.0))
       WRITE(9,*) PRESS
       S1=S11
       S2=S22
  200    CONTINUE
       PRESS=PRESS
       WRITE(3,*)'PRESS IS                =',PRESS
       PRINT*,PRESS
       WRITE(3,7)XMIC,ZMIC,PRESS,PRESS
    7  FORMAT(3x,f8.3,3x,f8.3,4x,e15.5,4x,e15.5)
  100  CONTINUE
       STOP
       END
C
C                  calculation of the relative speed
C
       SUBROUTINE LMN
       REAL  MR,LR,Y1,Y2
       COMMON/ALLDATA/THT,RI,RO,R,DENS,SOUND,VN,DELR,PI,OMEGA,
      &DELSI,XMIC,YMIC,TEMP,VEL(1000),VELX(1000),VELY(1000),
      &RX(1000),RY(1000),RR(1000),LR(1000),MR(1000),
      &DELT,HH(1000),Y1(1000),Y2(1000),NSTEP,NSTAT
*       print*,'This is LMN calling .........THT = ',THT
       R=RI
       DO 300 I=1,NSTAT
          VEL(I)=OMEGA*R
          VELX(I)=VEL(I)*SIN(THT)
          VELY(I)=VEL(I)*COS(THT)
          RX(I)=R*COS(THT)
          RY(I)=R*SIN(THT)
       MR(I)=((XMIC-RX(I))*VELX(I)+(YMIC-RY(I))*VELY(I))/SOUND
*         print *,'4'
       RR(I)=ABS((XMIC-RX(I))+(YMIC-RY(I))+ZMIC)
       HH(I)=((XMIC-RX(I))**2-(YMIC-RY(I))**2)
*         print *,'5'
       MR(I)=MR(I)/RR(I)
       Y1(I)=DENS*SOUND*VN+LR(I)
       Y1(I)=Y1(I)/(RR(I)*(1-MR(I)))
```

```
      Y2(I)=(LR(I))/(RR(I)**2*ABS(1-MR(I)))
      R=R+DELR
  300 CONTINUE
*      print*,'mr=',mr
*      print*,'outlrmr'
      RETURN
      END

c-----------------------------------------


c             THIS SUB CALCULATES THE INTEGRATION OF PRESSURE
c             ALONG THE BLADE

c       calculation of integration of pressure on the blade
                              INTEG1=Y1

c         THIS SUB CALCULATE THE INTEGRATION OF NOISE PRESSURE
c          ALONG THE BLADE.
c
c       SUBROUTINE INTEG1(  SUM )
c


      REAL  MR,LR,Y1,Y2
      COMMON/ALLDATA/THT,RI,RO,R,DENS,SOUND,VN,DELR,PI,OMEGA,
     &DELSI,XMIC,YMIC,TEMP,VEL(1000),VELX(1000),VELY(1000),
     &RX(1000),RY(1000),RR(1000),LR(1000),MR(1000),
     &DELT,HH(1000),Y1(1000),Y2(1000),NSTEP,NSTAT
      SUM=Y1(1)+Y1(NSTAT)
       DO 600 I=2,NSTAT-1
       SUM=SUM+2*Y1(I)
  600 CONTINUE
      SUM=SUM/2.0
      RETURN
      END
c-----------------------------------------

       calculation of integration of pressure on the blade
                              INTEG1=Y2


c             THIS SUB CALCULATES THE INTEGRATION OF PRESSURE
c             ALONG THE BLADE TERM Y2
c
c
      SUBROUTINE INTEG2( SUM )
c
```

```
      REAL  MR,LR,Y1,Y2
      COMMON/ALLDATA/THT,RI,RO,R,DENS,SOUND,VN,DELR,PI,OMEGA,
     &DELSI,XMIC,YMIC,TEMP,VEL(1000),VELX(1000),VELY(1000),
     &RX(1000),RY(1000),RR(1000),LR(1000),MR(1000),
     &DELT,HH(1000),Y1(1000),Y2(1000),NSTEP,NSTAT
      SUM=Y2(1)+Y2(NSTAT)
       DO 600 I=2,NSTAT-1
       SUM=SUM+2*Y2(I)
600   CONTINUE
      SUM=SUM/2.0
      RETURN
      END
```

```
C     Fourier analysis for the noise signal using NAG routine
C
C
C
      INTEGER N,IFAIL
      DOUBLE PRECISION HDB(3000),WORK(3000),A(3000),B(3000)
      REAL AMP(3000),STEP(3000)
      OPEN(44,FILE='HADIL',STATUS='OLD')
      REWIND(44)
      DELT=0.1
      IFAIL=0
      N=1440
      print*,'station on'
      OPEN(4,FILE='TTFIN')
      REWIND(4)
      READ(4,*)(HDB(I),I=1,100)
      print*, 'hello'
      CALL C06FAF(HDB,N,WORK,IFAIL)
      print*,'out nag'
      IF(IFAIL.NE.0)PRINT*,'PROGRAMME FAIL'

      A(1)=HDB(1)
      B(1)=0.0
      N2=(N+1)/2
      DO 1 J=2,N2
        NJ=N-J+2
        A(J)=HDB(J)
        A(NJ)=HDB(J)
        B(J)=HDB(NJ)
        B(NJ)=-HDB(NJ)
1     CONTINUE
      IF(MOD(N,2).NE.0) GO TO 50
      A(N2+1)=HDB(N2+1)
      B(N2+1)=0.0
C     WRITING OUT THE RESULT
50    PRINT*,'COMPONENT OF DISCRETE FOURIER TRANSFORM'
      PRINT*,'     REAL          IMAGINARY   '
      DO 2 I=1,N
      WRITE(6,100) A(I),B(I)
2     CONTINUE
100   FORMAT(3X,f10.4,5X,f10.4)
      T=N*DELT/60
      DELF=1/T
      AMPMAX=0.0
      DO  3 I=1,N

      AMP(I)=(A(I)**2)+(B(I)**2)
      AMP(I)=10*LOG10(AMP(I)/(2.0*10.0**-5.0))
      IF (AMP(I).GT.AMPMAX) AMPMAX=AMP(I)
      STEP(I)=STEP(I-1)+DELF
      WRITE(44,45)I,AMP(I),STEP(I)
3     CONTINUE
      CLOSE(44)
```

```
  45    FORMAT(I3,5X,F10.3,5X,F10.3)
C       PLOTTING THE GRAPH
C
C
C
        CALL HP7550
        CALL DEVPAP(380.0,250.0,0)
        CALL WINDOW(2)
        CALL PENSEL(1,0.5,2)
        CALL AXIPOS(1,30.0,30.0,200.0,1)
        CALL AXIPOS(1,30.0,30.0,200.0,2)
        CALL AXISCA(3,20,0.0,AMPMAX,2)
        CALL AXISCA(3,N,0.0,STEP(N),1)
        CALL AXIDRA(1,1,1)
        CALL AXIDRA(-1,-1,2)
        CALL GRAPOL(STEP,AMP,N)
        CALL MOVTO2(100.0,15.0)
        CALL CHASTR('FREQUENCY')
        CALL MOVTO2(15.0,100.0)
        CALL CHAANG(90.0)
        CALL CHASTR('AMPLITUDE')
        CALL CHAANG(0.0)
        CALL CHAMOD
        CALL DEVEND
        STOP
        END
```

```
c     plotting the result and writing data using Gino software

      character*12 filein
      dimension  data (100,100,4)
      dimension t(100),y(100),xbox(5),ybox(5)
c
c**** enter data
c
      write(*,*)'enter data file name'
      read(*,10)filein
 10   format(a12)
      open(unit=8,file=filein,status='unknown')
      rewind(8)
      write(*,*)'enter no of cases and no of points'
      read(*,*)ncase,npoin
      write(*,*)'enter colum number to be plotted'
      read(*,*) kcol1,kcol2
      do 15 icase=1,ncase
      do 15 i=1,npoin
      read(8,*)(data(icase,i,j),j=1,4)
 15   continue
      close(8)
c
      call gino
      print*,'type 1 for screen 2 for hard copy'
      read*,mm
c      gould machine
      if(mm.eq.1) then
*      call t4107
      call sun
      call lincol(2)
      else if(mm.eq.2) then
*     call hp7550
      call LASERW
      endif
      call piccle
c
c**** set character size
c
      call chaswi(1)
      call chasiz(2.0,2.0)
c
c**** set the origin coordinates
c
      xo=30.00
      yo=50.0
c
c**** define the positions of the axes
c
      xleng=120.
      yleng=100.
      call axipos(1,xo,yo,xleng,1)
      call axipos(1,xo,yo,yleng,2)
```

```
c
c**** define the scale used on each axis
      xscal=1.e-10
      yscal=1.e-10
      ysc=10000000.0
      do 22 icase=1,ncase
      do 22 i=1,npoin
      fact1=data(icase,i,kcol1)
      fact2=data(icase,i,kcol2)
      fact3=data(icase,i,kcol2)
      if(fact1.gt.xscal) xscal=fact1
      if(fact2.gt.yscal) yscal=fact2
      if(fact3.lt.ysc) ysc=fact3
 22   continue
      xsc=data(1,1,kcol1)
      call axisca(1,5,0.0,xscal,1)
      call axisca(1,5,ysc-5,yscal,2)
*      call axisca(1,5,0.0,yscal,2)
c
c**** draw the axes
c
      call axidra(-2,1,1)
      call axidra(2,-1,2)
c
c**** write titles
c
      xtit1=xo+0.25*xleng
      ytit1=yo-13.
      xtit2=xo-9.
      ytit2=yo+0.5*yleng
      call movto2(xtit1,ytit1)
      call chastr('DISTANCE AWAY FROM THE MACHINE  (m)')
      call movto2(xtit2,ytit2)
      call chaang(90.)
      call chastr('noise level dB(A)')
      call chaang(0.0)
      ytitm=ytit1-10.
      xtitm=xo
      call movto2(xtitm,ytitm)
      call chastr(' FIGURE ( ) DIFFERENCE BETWEEN MEASURED AND ')
      call chastr('PREDICTED  NOISE LEVEL ')
      call movto2(xtitm,ytitm-5)
      call chastr('  FOR LORD BRIDGE  TEST SITE TAKEN AT ')
      call chastr('REFERENCE POINT [5]')
c
c**** plot the curve joining the points
c
      do 11 icase=1,ncase
c
      do 12 i=1,npoin
      t(i)=data(icase,i,kcol1)
      y(i)=data(icase,i,kcol2)
 12   continue
      call grapol(t,y,npoin)
*      call gracur(t,y,npoin)
```

```
c
 11   continue
c**** draw outer box
c
      xbox(1)=xo-25.
      ybox(1)=yo-40.0
      xbox(2)=xo+xleng+20.
      ybox(2)=ybox(1)
      xbox(3)=xbox(2)
      ybox(3)=yo+yleng+25.
      xbox(4)=xbox(1)
      ybox(4)=ybox(3)
      call movto2(xbox(1),ybox(1))
      call linto2(xbox(2),ybox(2))
      call linto2(xbox(3),ybox(3))
      call linto2(xbox(4),ybox(4))
      call linto2(xbox(1),ybox(1))
c
c**** draw legend line
c
      xleg=xo+0.5*xleng
      ytop=ybox(3)-30.
      do 333 i=1,ncase
      yleg=ytop-(i-1)*5.
      call movto2(xleg,yleg)
      if(i.eq.1) then
      call chastr('ROTOR SPEED=100 ,200 (r.p.m)')
      else if(i.eq.2) then
      call chastr('OUTER RADIUS=2.5(m)')
      else if(i.eq.3) then
      call chastr('MEASURED NOISE LEVEL(o) ')
*      call chastr('PREDICTED NOISE LEVEL(-) ')
      else if(i.eq.4)then
      call chastr('VN=7(m/s)')
*      call chastr('PREDICTED NOISE LEVEL(-) ')
      else if(i.eq.5)then
*      call chastr('VN=7(m/s)')
      endif
 333  continue
c
      call devend
      stop
      end
```

APPENDIX [2]

The computer code FORCE for calculation of pressure on wind turbine blades[50].

```
C       Computer code for pressure on wind turbine blades[50]
C
C     This program calculates the forces on wind turbine with
C     tilt, cone and yaw angles.
C
      IMPLICIT REAL*8 (A-H,O-Z)
      PARAMETER (MM=60)
      INTEGER NB,NS,II,NCTL,IT,NI
      CHARACTER*30,BLADE
      CHARACTER*4,NOTS
      DIMENSION A1K(100),CLM(MM),CDM(MM)
      COMMON/AERO/RD(MM),THT(MM),CRD(MM),
     & CY(MM),CZ(MM),FY(MM),FZ(MM),ALFAM(MM),A1(MM),
     & A2(MM),WSM(3,MM),
     & TLFM(MM),FIM(MM),HBH,ZZRF,WPRFC,
     & OMEGA,WSRF,DISHB,THT1,TWRD,AZ,TLF,WS,FI,ALFA,
     & ITM(MM),NB,NS,II,NCTL
      COMMON/AERO2/ANG(60),CL(60),CD(60)
C     **********************************
C
C....Read the blade dimensions and aerodynamic properties and
C....print the data in tables
C
C
C     **********************************
      OPEN(1,FILE='GEOM')
      REWIND(1)
      OPEN(4,FILE='INDATA1')
      REWIND(4)
      OPEN(14,FILE='res')
      REWIND(14)
C     ------------------------------------------------
      READ(4,*)BLADE
      READ(4,*)NS,OMEGA,HBH,TWRD,DISHB,ZZRF,WSRF,
     & WPRFC,ANGYA,ANGTL,ANGBT,AZ0,NI,NDATA,TOLR,
     & PITCH,NSTRT,NOTS,DENS,NCIR
      DO 5 I=1,NS
      READ(1,*) RD(I),CRD(I),THT(I)
    5 CONTINUE
C     ------------------------------------------------------
      WRITE(14,*)'  AERODYNAMIC DATA FOR BLADE : ',BLADE
      WRITE(14,*)'  ----------- ---- --- -----'
      WRITE(14,*)' '
      WRITE(14,6)'Azimuth =',AZ,'degree'
      WRITE(14,6)'Rotational speed = ',OMEGA,'rad/s'
      WRITE(14,6)'Wind speed  = ',WSRF,'m/s'
      WRITE(14,6)'Reference height for wind speed
      WRITE(14,6)'                 = ',ZZRF,'m'
```

```
      WRITE(14,6)'Hub height = ',HBH,'m'
      WRITE(14,6)'Tower radius = ',TWRD,'m'
      WRITE(14,6)'Overhang = ',DISHB,'m'
      WRITE(14,6)'Wind profile constant = ',WPRFC
      WRITE(14,6)'Angle of yaw = ',ANGYA,'degree'
      WRITE(14,6)'Angle of tilt =',ANGTL,'degree'
      WRITE(14,6)'Angle of cone =',ANGBT,'degree'
      WRITE(14,6)'Blade pitch =',PITCH,'degree'
      WRITE(14,6)'Tolerance for A and
      WRITE(14,6)' AP calculation =',TOLR
    6 FORMAT(TR3,A,F6.2,TR1,A)
C
C     ------------------------------------------
      PI=4.0*ATAN(1.0)
      H=PI/180.0
      AZ=AZ0*pi/180.0
      ANGYA=ANGYA*H
      ANGTL=ANGTL*H
      ANGBT=ANGBT*H
      ANGTW=ANGTW*H
      CAZ=COS(AZ)
      SAZ=SIN(AZ)
      CYA=COS(ANGYA)
      SYA=SIN(ANGYA)
      CTL=COS(ANGTL)
      STL=SIN(ANGTL)
      CBT=COS(ANGBT)
      SBT=SIN(ANGBT)
      NB=2
C
      DO 51 I3=1,NCIR

      DO 50 II=NSTRT,NS-1
C
      WS=WSRF
      CALL WNDSHR (RD,AZ,HBH,ZZRF,WSRF,WPRFC,WS,II)
      WSM(2,II)=WS*(-STL*SAZ+SYA*CTL*CAZ)
      WSM(3,II)=WS*(STL*SBT*CAZ+CTL*SBT*SYA+CTL*CBT*CYA)
      SOLID=NB*CRD(II)/(PI*RD(II))
      IF(NOTS.EQ.'NOTS') GOTO 38
      CALL TWRSHD (RD,WSM,AZ,DISHB,TWRD,II)
   38 CONTINUE
C
      AA1=A1(II-1)
      AA2=A2(II-1)
      AA3=0.0
      AA4=0.0
      DO 45 IT=1,NI
      IF (IT.EQ.1) GO TO 39
      IF(ABS(AA3-AA1).LE.TOLR.AND.ABS(AA4-AA2).LE.TOLR)
      & GO TO 48
C.... Applying damping
      IF(IT.GE.4) AA1=(A1K(IT-1)+A1K(IT-2)+A1K(IT-3))/3
```

```
      IF(IT.LT.4) AA1=AA3
      AA2=AA4
   39 TNFI=((1-AA1)*WSM(3,II))/((1+AA2)*(RD(II)*
      & OMEGA-WSM(2,II)))
      FI=ATAN(TNFI)
      CALL TIPLOS (RD,FI,TLF,NS,II,NB)
      TLFM(II)=TLF
      FI=FI*180/PI
      FIM(II)=FI
      ALFA=FI-THT(II)-PITCH
      ALFAM(II)=ALFA


      CALL AERCOF (IT,II,ALFA,NDATA,CLI,CDI)
      CLM(II)=CLI
      CDM(II)=CDI
      CSFI=SQRT(1/(1+TNFI**2))
      SNFI=SQRT(1-CSFI**2)
      CY(II)=(CLI*SNFI)-(CDI*CSFI)
      CZ(II)=(CLI*CSFI)+(CDI*SNFI)
      CH=(SOLID*CZ(II)*CBT/(2*SNFI*SNFI))*(1-AA1)**2
      IF(CH.GT.0.96) THEN
      AA3=(0.143+SQRT(0.0203-0.6427*(0.889-CH)))/TLF
      ELSE
      AA3=(1-SQRT(1-CH))/(2*TLF)
      ENDIF
C
      H=SOLID*CY(II)/(8*CSFI*SNFI)
      AA4=H/(TLF-H)
      A1K(IT)=AA3
   45 CONTINUE
   48 ITM(II)=AA3
      A1(II)=AA3
      A2(II)=AA4
   50 CONTINUE
C
C.... Form the aerodynamic force vectors
C
      DO 60 II=2,NS-1
      H=((1-A1(II))*WSM(3,II))**2
      H=H+((1+A2(II))*(RD(II)*OMEGA-WSM(2,II)))**2
c     H=H*0.5*DENS*CRD(II)
      h=h*0.5*dens
      FY(II)=H*CY(II)
      FZ(II)=H*CZ(II)
60    CONTINUE
      write(14,90)i3,azdeg,(FZ(I4),I4=1,NS)
      AZ=AZ+2*PI/NCIR
      AZDEG=AZ*180.0/pi
90    format(i4,f9.3,21f7.1)
51    CONTINUE
      STOP
      END
```

```
C
C
C
      SUBROUTINE AERCOF(IT,II,ALF,N,B,C)
      IMPLICIT REAL*8 (A-H,O-Z)
      INTEGER II,I,I1,I2,N
      COMMON/AERO2/ANG(60),CL(60),CD(60)
      IF(IT.GT.1) GOTO 10
      IF(II.EQ.2) OPEN(2,FILE='AERO02')
      IF(II.EQ.3) OPEN(2,FILE='AERO03')
      IF(II.EQ.4) OPEN(2,FILE='AERO04')
      IF(II.EQ.5) OPEN(2,FILE='AERO05')
      IF(II.EQ.6) OPEN(2,FILE='AERO06')
      IF(II.EQ.7) OPEN(2,FILE='AERO07')
      IF(II.EQ.8) OPEN(2,FILE='AERO08')
      IF(II.EQ.9) OPEN(2,FILE='AERO09')
      IF(II.EQ.10) OPEN(2,FILE='AERO10')
      IF(II.EQ.11) OPEN(2,FILE='AERO11')
      IF(II.EQ.12) OPEN(2,FILE='AERO12')
      IF(II.EQ.13) OPEN(2,FILE='AERO13')
      IF(II.EQ.14) OPEN(2,FILE='AERO14')
      IF(II.EQ.15) OPEN(2,FILE='AERO15')
      IF(II.EQ.16) OPEN(2,FILE='AERO16')
      IF(II.EQ.17) OPEN(2,FILE='AERO17')
      IF(II.EQ.18) OPEN(2,FILE='AERO18')
      IF(II.EQ.19) OPEN(2,FILE='AERO19')
      IF(II.EQ.20) OPEN(2,FILE='AERO20')
      IF(II.EQ.21) OPEN(2,FILE='AERO21')
      REWIND 2
      READ(2,*)
      DO 20 I=1,N
      READ(2,*) ANG(I),CL(I),CD(I)
   20 CONTINUE
      CLOSE (2)
   10 DO 30 I1=1,N
      IF (ALF.GE.ANG(I1).AND.ALF.LE.ANG(I1+1)) THEN
      I2=I1
      RATIO=(ALF-ANG(I2))/(ANG(I2+1)-ANG(I2))
      B=RATIO*(CL(I2+1)-CL(I2))+CL(I2)
      C=RATIO*(CD(I2+1)-CD(I2))+CD(I2)
      ENDIF
   30 CONTINUE
      RETURN
      END
C
C
C
      SUBROUTINE TIPLOS (RD,FI,TLF,NS,II,NB)
      IMPLICIT REAL*8 (A-H,O-Z)
      DIMENSION RD(60)
      HS=NB*(RD(NS)-RD(II))
      HS=HS/(2*RD(II)*ABS(SIN(FI)))
      HS=EXP(-HS)
      HS=ACOS(HS)
      TLF=HS*0.6366198
      RETURN
      END
```

```
C
C
C
C
      SUBROUTINE TWRSHD (RD,WSM,AZ,DISHB,TWRD,II)
      IMPLICIT REAL*8 (A-H,O-Z)
      DIMENSION RD(60),WSM(3,60)
      PI=4*ATAN(1.0)
      IF (AZ.GT.PI/2.AND.AZ.LT.3*PI/2) THEN
      H=(AZ-PI/2)**1.5
      H=-H/AZ
      FACT=1-EXP(H)


      H=RD(II)*ABS(SIN(AZ))
      THT1=ATAN(H/DISHB)
      RR=H**2+DISHB**2
      H2=TWRD**2/(4*RR)
      QR=WSM(3,II)*(1-H2)*COS(THT1)
      QT=WSM(3,II)*(1+H2)*SIN(THT1)
      QY=QT*COS(THT1)-QR*SIN(THT1)
      WSM(2,II)=WSM(2,II)+QY
      QZ=QR*COS(THT1)+QT*SIN(THT1)
      WSM(3,II)=QZ
      ENDIF
      RETURN
      END
C
C
C
C
      SUBROUTINE WNDSHR (RD,AZ,HBH,ZZRF,WSRF,WPRFC,WS,II)
      IMPLICIT REAL*8 (A-H,O-Z)
      DIMENSION RD(60)
      ZZ=HBH+RD(II)*COS(AZ)
      H1=ZZ/ZZRF
      H1=H1**WPRFC
      WS=WSRF*H1
      RETURN
      END
```

APPENDIX [3]

The specification of the two machines used in the wind farm comparison in Chapter 7

Table 3A.1

Description of the Näsudden wind turbine

Rotor diameter	75 m
Number of blades	2
Hub height	77 m
Rated power output	2 MW
Cut in wind speed	6 m/s
Design wind speed	12.5 m/s
Cut out wind speed	21 m/s
Rotor rotational speed	25 rpm
Blade chord at the tip	0.5 m
Blade chord at the root	4.0 m
Mean chord	2.36 m

Table 3A.2

Description of the Vestas V 25-200 kW wind turbine

Rotor diameter	25 m
Number of blades	3
Hub height	30 m
Rated power output	200 W
Cut in wind speed	3.5 m/s
Design wind speed	13.8 m/s
Cut out wind speed	25.0 m/s
Rotor rotational speed	33 rpm

APPENDIX [4]

Measurement results and spectrum analyses at the Cambridge site showing the effect of rubbing [Ref point [1] rotational speed 200 rpm, wind speed 7.0 m/s].

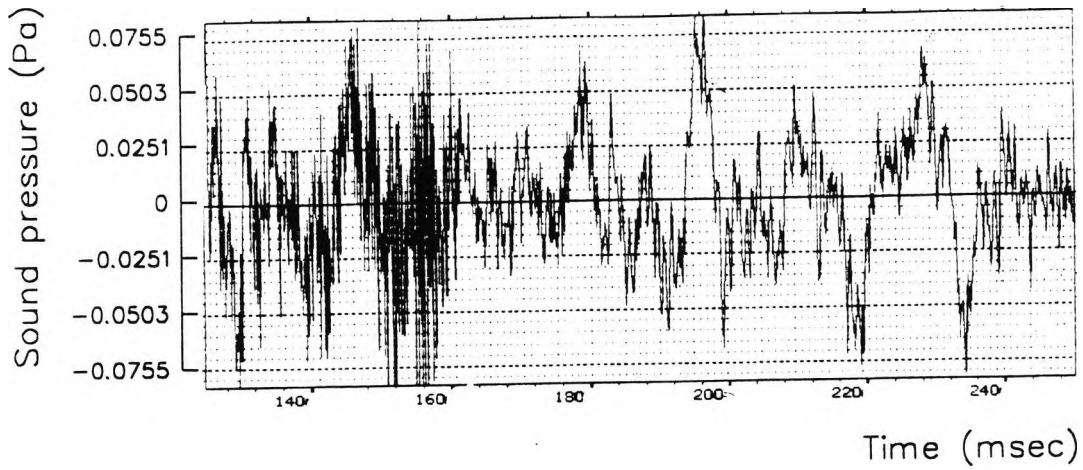

Fig 4A.1(a) Typical noise signal versus time at reference position(1), rotational speed= 200 r.p.m, average wind speed= 7 m/sec, average noise level directly measured =62 dB(A). It shows the effect of rubbing when the wind changes its direction

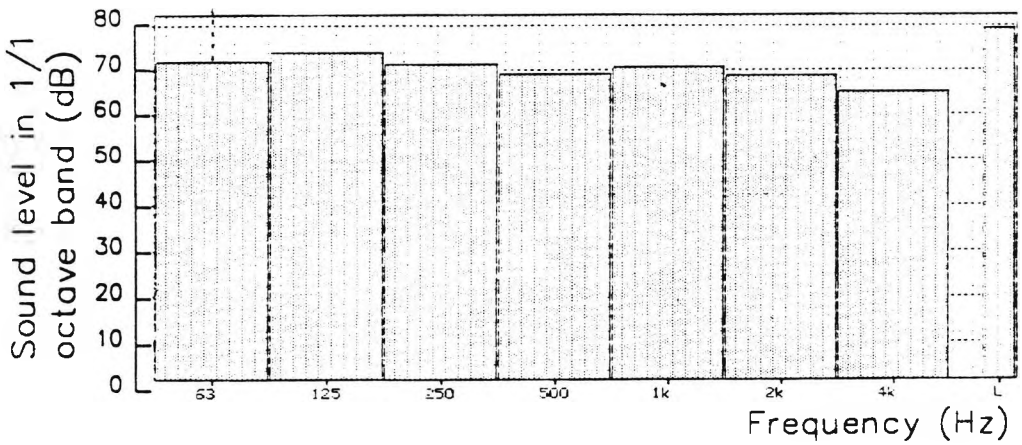

Fig 4A.1(b) Typical 1/1 octave band spectrum of the noise signal for the conditions corresponding to Fig 4A.1(a).

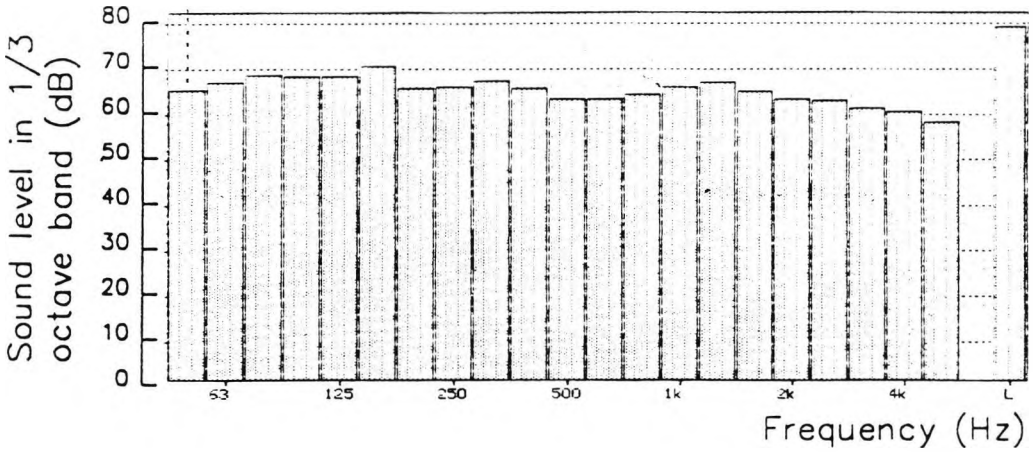

Fig 4A.1(c) Typical 1/3 octave band spectrum for the conditions corresponding to Fig 4A.1(a)

APPENDIX [5]

Reference calibration signal, generated by the sound level calibrator for calibration of sound level meter(B&K type 4230).

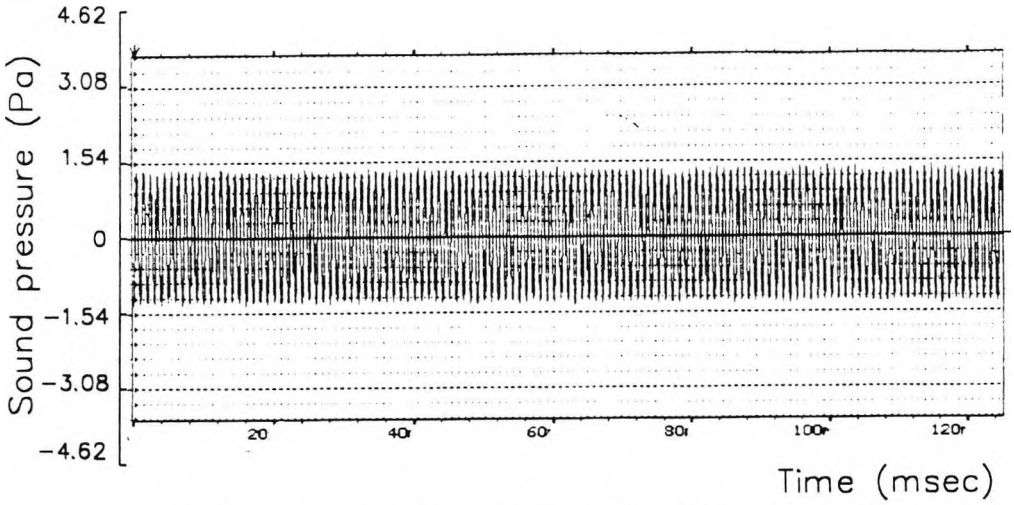

Fig 5A.1(a) Reference signal versus time providing 94dB(A), generated by the sound level calibrator (B&K type 4230).

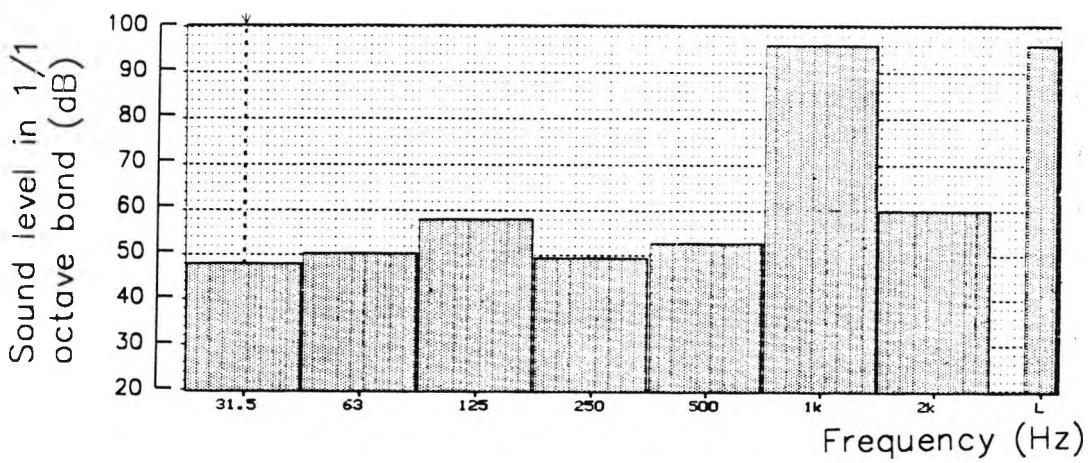

Fig 5A.1(b) 1/1 octave band spectrum for the standard signal.

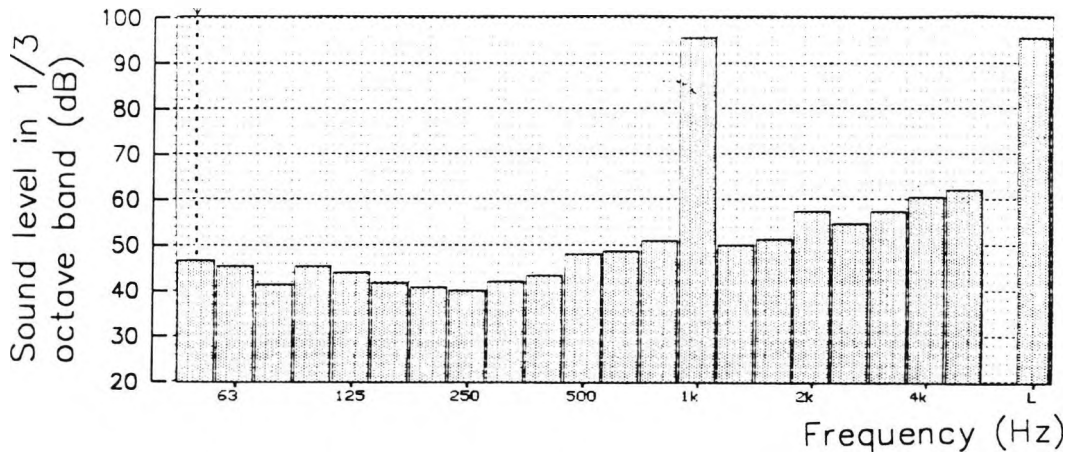

Fig 5A.1(c) Typical 1/3 octave band spectrum for the standard signal.

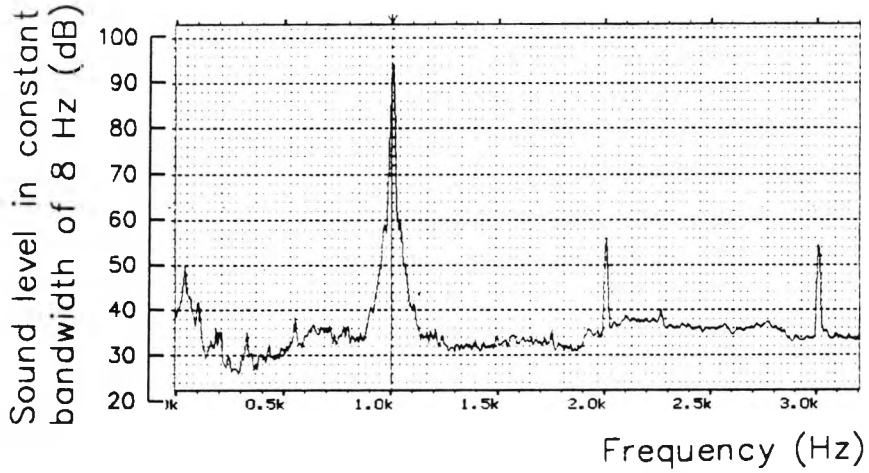

Fig 5A.1(d) Typical linear frequency spectrum for the standard signal.